Universidade de Aveiro
2021

BRUNO MIGUEL FERNANDES LADEIRA

Desenvolvimento de *scaffolds* com base em lisado de plaquetas a partir de microcápsulas para regeneração pós-enfarte do miocárdio

Development of platelet lysate based scaffolds from microcapsules for regeneration post-myocardial infarction

Universidade de Aveiro
2021

BRUNO MIGUEL FERNANDES LADEIRA

Desenvolvimento de *scaffolds* com base em lisado de plaquetas a partir de microcápsulas para regeneração pós-enfarte do miocárdio

Development of platelet lysate based scaffolds from microcapsules for regeneration post-myocardial infarction

Dissertação apresentada à Universidade de Aveiro para cumprimento dos requisitos necessários à obtenção do grau de Mestre em Biotecnologia Molecular realizada sob a orientação científica da Doutora Catarina de Almeida Custódio, Investigadora Auxiliar do Departamento de Química da Universidade de Aveiro e do Professor João Filipe Colardelle da Luz Mano, Professor Catedrático do Departamento de Química da Universidade de Aveiro.

Este trabalho recebeu apoio financeiro da Fundação para a Ciência e Tecnologia (FCT) no âmbito do projeto BEAT (PTDC/BTM-MAT/30869/2017), e do European Research Council (ERC) no âmbito do projeto ATLAS (ERC-2014-ADG-669858). O trabalho foi também parcialmente financiado pelo Horizonte 2020 da União Europeia (UE) no âmbito do projeto InterLynk, Grant agreement: H2020-NMBP-TR-IND-2020, Project ID: 953169.
Este trabalho foi desenvolvido no âmbito do projeto CICECO-Aveiro Institute of Materials, FCT Ref. UIDB/50011/2020 & UIDP/50011/2020, financiado por fundos nacionais através do FCT/MCTES.

Aos meus pais.

o júri

Presidente	Professor Doutor Manuel António Coimbra Rodrigues da Silva Professor Associado c/Agregação do Departamento de Química da Universidade de Aveiro
Vogal – Arguente principal	Doutora Maria Clara Rosa da Silva Correia Diretora de Unidade de Investigação na empresa Tech4MED
Vogal – Orientador	Doutora Catarina de Almeida Custódio Investigadora Auxiliar do Departamento de Química da Universidade de Aveiro

Agradecimentos

E assim, uma longa jornada chega ao fim.

Em primeiro lugar, preciso de agradecer à Doutora Catarina Custódio e ao Professor João Mano, pela oportunidade de fazer parte deste projeto e pelos bem como os conselhos inestimáveis que ofereceram.

Queria agradecer aos meus colegas no grupo COMPASS, que me receberam de braços abertos e ofereceram apoio e orientações sempre que foi necessário.

Queria agradecer aos meus amigos, que me acompanharam nesta jornada para que pudéssemos partilhar sugestões e sorrisos.

E queria agradecer aos meus pais e avós, pelo apoio, amor e paciência incondicionais que me ofereceram.

Obrigado!

palavras-chave

Enfarte do miocárdio, microesponjas, cápsulas de *core* líquido, lisados de plaquetas, *core-shell*.

resumo

Como principal causa de morte em todo o mundo, o enfarte do miocárdio (EM) gera custos socioeconómicos consideráveis. Os danos e complicações clínicas provocadas por EM não são adequadamente abordados pelas estratégias terapêuticas atuais. Com o advento da engenharia de tecidos e da medicina regenerativa, novas estratégias para promover a regeneração do músculo cardíaco são possíveis.

Esta dissertação foca-se na aplicação de sistemas baseados em microcápsulas para promover a recuperação de tecidos danificados. A biofabricação de microcápsulas *core-shell* para o encapsulamento de células e moléculas bioativas foi revista, juntamente com as contribuições destas plataformas no campo da medicina regenerativa.

Neste trabalho, a tecnologia de *eletrospray* coaxial foi usada para encapsular lisado de plaquetas metacrilado (PLMA) em microcápsulas de alginato, produzindo moldes sacrificiais para a preparação de *microcarriers* porosos. Ao expor as cápsulas à luz ultravioleta, foi possível induzir a fotopolimerização do PLMA. A *shell* de alginato foi removida e as partículas resultantes foram submetidas a um procedimento de liofilização, produzindo microesponjas de PLMA.

Ajustando os parâmetros de produção, o sistema proposto foi capaz de produzir microcápsulas com *cores* de diâmetro compreendido no intervalo de 300 a 600 μm, bem como microcápsulas com *shells* possuindo espessuras abaixo de 100 μm. As microesponjas preparadas a partir deste sistema permitiram a adesão de células e promoveram a agregação em microtecidos cardíacos, indicando possíveis aplicações na engenharia de tecidos.

keywords

Myocardial Infarction, microsponges, liquid core capsules, platelet lysate, core-shell.

abstract

As the leading cause of death worldwide, myocardial infarction (MI) carries considerable socioeconomic costs. The damage and clinical complications caused by MI remain unaddressed by current therapeutic strategies. With the advent of tissue engineering and regenerative medicine, novel strategies to promote regeneration of heart muscle are possible.

This dissertation focuses on the application of microcapsule-based systems to promote the recovery of damaged tissue. The biofabrication of core-shell microcapsules for the encapsulation of cells and bioactive molecules has been reviewed, along with the contributions of these platforms to the field of regenerative medicine.

In this work, coaxial electrospray technology has been used to encapsulate methacryloyl platelet lysate (PLMA) within alginate microcapsules, producing sacrificial templates for the preparation of porous microcarriers. By exposing the capsules to UV light, it was possible to induce the photopolymerization of PLMA. The alginate shell was removed and the resulting particles were subjected to a freeze-drying procedure, producing PLMA microsponges.

By adjusting production parameters, the proposed system was able to produce microcapsules with core diameter ranging from 300 to 600 μm, as well as microcapsules with shell thickness below 100 μm. The microsponges prepared with this system were shown to allow cell attachment and promote the assembly of cardiac microtissues, indicating potential applications in tissue engineering.

Table of Contents

List of Figures

List of Tables

Abbreviations

2D – Two-dimensional

3D – Three-dimensional

APA – Alginate–poly-*L*-lysine–alginate

ASCs – Adipose-derived stem cells

BMP-2 – Bone morphogenic protein 2

BMP-4 – Bone morphogenic protein 4

CHO – Chinese hamster ovary

CSCs – Cancer stem-like cells

DAPI – 4',6-Diamino-2-phenylindole

DEAE – Diethylaminoethyl

DMEM – Dulbecco's Modified Eagle Medium

DMSO – Dimethyl sulfoxide

ECM – Extracellular matrix

EDTA – Ethylenediaminetetraacetic acid

ES – Electrospray

ESCs – Embryonic stem cells

FBS – Fetal bovine serum

FGF – Fibroblast growth factor

GelMA – Gelatin methacrylate

HA – Hyaluronic acid

hASCs – Human adipose-derived stem cells

hPL – Human platelet lysate

HUVECs – Human umbilical vein endothelial cells

iPSCs – Induced pluripotent stem cells

LbL – Layer-by-layer

MI – Myocardial infarction

mRNA – Messenger ribonucleic acids

MSCs – Mesenchymal stem cells

PCL – poly(ε-caprolactone)

PDGF – Platelet-derived growth factor

PEI - Polyethyleneimine

PEG – Poly (ethylene glycol)

PEG4m – 4-arm maleimide-modified PEG

PEGDA – PEG-diacrylate

PGA – Poly (glycolic acid)

PGlA – Poly (*L*-glutamic acid)

PLA – Poly (lactic acid)

PLGA – Poly (lactic-*co*-glycolic acid)

PLL – Poly-*L*-lysine

PLMA – Methacrylated platelet lysates

PLO – Poly-*L*-ornithine

PNIPAAm – Poly (*N*-isopropylacrylamide)

PS – Polystyrene

RGD – Arginine-glycine-aspartate

SDS – Sodium dodecyl sulphate

SEM – Scanning electron microscopy

TE – Tissue engineering

TERM – Tissue engineering and regenerative medicine

TGF-β – Transforming growth factor β

UV – Ultraviolet

VEGF – Vascular endothelial growth factor

CHAPTER 1

Motivation

Chapter 1 – Motivation

1.1. General Introduction

Ischemic heart disease is the number one cause of death among adults at a global scale. It is characterized by a reduction in blood flow to cardiac tissue caused by a blockage in the arteries responsible for the heart's blood supply[1]. This is followed by a decrease in the supply of oxygen to cells. As the oxygen levels become insufficient to meet cells' demand, cell death occurs, eventually resulting in a heart attack, also known as a myocardial infarction (MI)[2]. It is estimated that someone is afflicted by MI every 40 seconds in the United States, resulting in a total of 805,000 cases per year[3]. In Portugal, MI is responsible for over 12,000 hospital admissions on an annual basis[4].

After MI, a complex inflammatory process is triggered, which determines the extent of the damage sustained by the cardiac muscle. In an initial stage, tissue necrosis leads to the release of chemical signals that are be recognized by nearby macrophages and monocytes[5]. These cells then produce and secrete chemokines and cytokines, recruiting other immune cells that migrate toward the heart, whereupon they initiate inflammation by removing the remains of dead cells, degrading the surrounding extracellular matrix (ECM) and releasing reactive oxygen species, which result in further cardiomyocyte death[6].

Cardiomyocytes and ECM components lost in this process must then be replaced, and as such, the initial inflammatory phase is followed by a proliferative phase. However, the low intrinsic renewability of cardiomyocytes prevents the generation of enough cells to fully replace the billions of cardiomyocytes lost due to MI[7,8]. As an alternative, cardiac fibroblasts migrate into the infarct zone, differentiate into myofibroblasts, and begin depositing large quantities of collagen and other ECM components, generating a fibrous scar that prevents expansion of the infarct, thus limiting changes to the architecture of the heart and allowing the recovery process to begin[9]. However, the scar tissue also interferes with the transmission of electrical signals between the cells, potentially leading to arrhythmia and cardiac dysfunction[10]. The generation of this scar is also accompanied by extensive remodeling in the structure of the left ventricle. The infarcted region suffers dilation, which causes a loss in ventricular pump function and an increase in wall stress, which in turn promotes changes in the structure of the surrounding tissues as a compensatory mechanism, thus expanding dilation of the tissue to non-infarcted regions of the heart[11]. These changes in the architecture of the heart heavily increase the risk of rupture and subsequent heart failure[10,12].

Currently, the only available approach that can achieve full recovery in the aftermath of MI is heart transplantation, a process which is heavily restricted by the limited availability of compatible donors. As an alternative, the implantation of left ventricular assist devices has also been shown to promote quality of life and reduce mortality in MI patients, however, these devices are prone to mechanical failure, they do not allow full recovery of the heart muscle, and they increase both the risk of infection and the risk of failure of the right ventricle[13–17].

New approaches are urgently required to tackle the damage caused by MI. Advances in the field of myocardial tissue engineering have contributed toward the development of new therapeutic strategies, through the design of robust models of cardiac tissue to test new drugs; the development of cell culture platforms for the production of large quantities of cells to replenish lost cardiomyocytes; and the production of cardiac patches to promote tissue regeneration[18,19].

The goal of this project was the encapsulation of a photopolymerizable biomaterial of human origin derived from platelet lysate (PLMA)[20] in core-shell microcapsules, as a means to produce platforms for the development of cardiac microtissues. These microtissues could eventually be used as a model for myocardial disease and in the preparation of transplantable cardiac patches. The production of core-shell microcapsules was investigated and optimized, as a first step toward the development of these platforms. Herein, the resulting core-shell capsules were used as a template structure in the production of porous microcarriers for the bottom-up assembly of cardiac microtissues.

Chapter 2 of this dissertation will review the state-of-the-art regarding the microfabrication of core-shell microcapsules and their application in tissue engineering and regenerative medicine, as these structures constitute the basis of this work. In Chapter 3, the materials and experimental procedures used throughout this project have been highlighted. The experimental results have been displayed and discussed in Chapter 4. Finally, Chapter 5 summarizes the main conclusions of this project while also exploring potential future directions for this research.

1.2. References

1. Finegold JA, Asaria P, Francis DP. Mortality from ischaemic heart disease by country, region, and age: Statistics from World Health Organisation and United Nations. *Int J Cardiol*. 2013;168(2):934-945. doi:10.1016/j.ijcard.2012.10.046

2. Moran AE, Forouzanfar MH, Roth GA, et al. The Global Burden of Ischemic Heart Disease in 1990 and 2010: The Global Burden of Disease 2010 Study. *Circulation*. 2014;129(14):1493-1501. doi:10.1161/CIRCULATIONAHA.113.004046

3. Virani SS, Alonso A, Benjamin EJ, et al. Heart Disease and Stroke Statistics—2020 Update: A Report From the American Heart Association. *Circulation*. 2020;141(9). doi:10.1161/CIR.0000000000000757

4. *Portugal - Doenças Cerebro-Cardiovasculares Em Números -2015*. Direção Geral de Saúde; 2017.

5. Latet SC, Hoymans VY, Van Herck PL, Vrints CJ. The cellular immune system in the post-myocardial infarction repair process. *Int J Cardiol*. 2015;179:240-247. doi:10.1016/j.ijcard.2014.11.006

6. Frangogiannis NG. The inflammatory response in myocardial injury, repair, and remodelling. *Nat Rev Cardiol*. 2014;11(5):255-265. doi:10.1038/nrcardio.2014.28

7. Zlatanova I, Pinto C, Silvestre J-S. Immune Modulation of Cardiac Repair and Regeneration: The Art of Mending Broken Hearts. *Front Cardiovasc Med*. 2016;3. doi:10.3389/fcvm.2016.00040

8. Ma Y, Halade GV, Lindsey ML. Extracellular Matrix and Fibroblast Communication Following Myocardial Infarction. *J of Cardiovasc Trans Res*. 2012;5(6):848-857. doi:10.1007/s12265-012-9398-z

9. Carlson S, Trial J, Soeller C, Entman ML. Cardiac mesenchymal stem cells contribute to scar formation after myocardial infarction. *Cardiovasc Res*. 2011;91(1):99-107. doi:10.1093/cvr/cvr061

10. Richardson WJ, Clarke SA, Quinn TA, Holmes JW. Physiological Implications of Myocardial Scar Structure. Terjung R, ed. *Compr Physiol*. 2015;5(4):1877-1909. doi:10.1002/cphy.c140067

11. Pfeffer MA, Braunwald E. Ventricular remodeling after myocardial infarction. Experimental observations and clinical implications. *Circulation*. 1990;81(4):1161-1172. doi:10.1161/01.CIR.81.4.1161

12. Baig MK, Mahon N, McKenna WJ, et al. The pathophysiology of advanced heart failure. *Am Heart J*. 1998;135(6):S216-S230. doi:10.1016/S0002-8703(98)70252-2

13. Gopinathannair R, Cornwell WK, Dukes JW, et al. Device Therapy and Arrhythmia Management in Left Ventricular Assist Device Recipients: A Scientific Statement From the American Heart Association. *Circulation*. 2019;139(20). doi:10.1161/CIR.0000000000000673

14. Kilic A, Acker MA, Atluri P. Dealing with surgical left ventricular assist device complications. *J Thorac Dis*. 2015;7(12):2158-2164.

15. MacIver J, Ross HJ. Quality of Life and Left Ventricular Assist Device Support. *Circulation*. 2012;126(7):866-874. doi:10.1161/CIRCULATIONAHA.111.040279

16. Rose EA, Gelijns AC, Moskowitz AJ, et al. Long-Term Use of a Left Ventricular Assist Device for End-Stage Heart Failure. *N Engl J Med*. 2001;345(20):1435-1443. doi:10.1056/NEJMoa012175

17. Slaughter MS, Rogers JG, Milano CA, et al. Advanced Heart Failure Treated with Continuous-Flow Left Ventricular Assist Device. *N Engl J Med*. 2009;361(23):2241-2251. doi:10.1056/NEJMoa0909938

18. Dwyer KD, Coulombe KLK. Cardiac mechanostructure: Using mechanics and anisotropy as inspiration for developing epicardial therapies in treating myocardial infarction. *Bioact Mater*. 2021;6(7):2198-2220. doi:10.1016/j.bioactmat.2020.12.015

19. Archer CR, Sargeant R, Basak J, Pilling J, Barnes JR, Pointon A. Characterization and Validation of a Human 3D Cardiac Microtissue for the Assessment of Changes in Cardiac Pathology. *Sci Rep*. 2018;8(1):10160. doi:10.1038/s41598-018-28393-y

20. Santos SC, Custódio CA, Mano JF. Photopolymerizable Platelet Lysate Hydrogels for Customizable 3D Cell Culture Platforms. *Adv Healthcare Mater*. 2018;7(23):1800849. doi:10.1002/adhm.201800849

CHAPTER 2

Biofabrication of core-shell microcapsules and potential applications in tissue engineering and regenerative medicine

Chapter 2 – Biofabrication of core-shell microcapsules and potential applications in tissue engineering and regenerative medicine

Abstract

The construction of biomaterial scaffolds that accurately recreate the architecture of living tissues *in vitro* is a major challenge in the field of tissue engineering and regenerative medicine. Core-shell microcapsules hold great potential in this regard, as they can resemble the hierarchical structure present in most biological systems. The independent modulation of the composition of both core and shell layers allows the design of compartmentalized platforms tailored to the recreation of specific cell niches. Techniques such as electrospray, microfluidics and layer-by-layer assembly have been successful in producing core-shell microcapsules for the encapsulation of cells and bioactive factors. This review provides an overview of available materials and techniques used in the generation of core-shell microcapsules, while also highlighting some of their potential applications in the design of innovative and effective therapeutic strategies.

Keywords: Microencapsulation, microcapsules, core-shell structures, tissue engineering, regenerative medicine.

2.1. Introduction

Organ transplantation is, in many cases, the only viable option for the treatment of damaged organs, however, it is heavily limited by factors such as the reduced availability of donors and the rejection of transplants due to the body's immune response[1]. The search for alternative therapeutic options for these patients has led to an increased interest in the field of tissue engineering and regenerative medicine (TERM). TERM approaches seek to combine the use of cells, biomaterial scaffolds and bioactive molecules to promote tissue repair *in situ* and possibly replace damaged tissue[2–4]. These approaches can include the development of bioengineered cells[5], microtissues[6], organoids[7] and potentially even whole organs[8], in order to produce biological structures for transplantation, as well as robust *in vitro* models of disease that can be implemented in the study of potential drug candidates.

The culture, assembly and delivery of these structures can take advantage of microencapsulation strategies in order to produce closed scaffolds that maintain the viability

of cells while isolating them from the surrounding environment. Microencapsulation is a process used in a wide range of industries to preserve products of interest, such as essential oils[9], growth factors[10], drugs[11], proteins[12], bacterial cells[13] or mammalian cells[14] by enveloping them in a polymer coating. Originally proposed in 1964[15], microencapsulation has been used to preserve the stability of sensitive molecules during delivery and shield cells from the immune system, preventing their recognition and rejection, and forgoing the need for immunosupressants, which carry dangerous side effects[16–18].

Core-shell microcapsules consist of discrete multilayered particles containing one or more cores enveloped by a polymer shell. The shell is responsible for mass transfer and conferring mechanical stability to the microcapsules, while the core should ensure the stability and viability of encapsulated molecules, structures and cells. The core of the capsules can consist of a hydrogel, a liquid or gas. Due to the independent nature of both the shell and the core, their properties can be adjusted separately, resulting in highly tunable microencapsulation platforms that better reproduce the hierarchical and compartmentalized 3D architecture of natural systems[19].

In this review, advances in the development of core-shell microcapsules for application in biomedical applications will be examined. An overview of commonly used biomaterials in the construction of core-shell microcapsules will be presented, followed by an exploration of the most relevant biofabrication techniques. Subsequently, some current applications of microcapsules in the study and treatment of relevant disorders will be reviewed.

2.2. Architecture of core-shell microcapsules

2.2.1. Biomaterials used in the generation of the shell

The shell is a semipermeable coating that regulates mass transfer between the interior of a microcapsule and the surrounding environment. As such, it should allow the diffusion of small molecules, including the entry of nutrients and oxygen required for cell growth and the release of metabolic waste products or encapsulated drugs and bioactive factors. By adjusting the characteristics of the polymer shell, such as its thickness and porosity, it is possible to control the release rate of these molecules, which is useful in the design of platforms for the sustained release of drugs, proteins and paracrine factors[20]. The shell also functions as a protective barrier, maintaining the structure of the capsules while shielding its

contents from the outer environment and promoting immunoprotection of encapsulated materials.

Biomaterials used in the generation of the shell must be biocompatible, non-immunogenic and provide mechanical stability to the microcapsules. One of the most prominently used polymers in the biofabrication of microparticulate materials is alginate, a family of negatively charged polysaccharides that can be obtained from brown algae, consisting of linear copolymers of (1,4)-linked β-D-mannuronate and α-L-guluronate[21]. These materials are generally non-thrombogenic, non-immunogenic, biocompatible and can be acquired for a low cost[22,23]. Alginates are optimal for the production of scaffolds in mild conditions, due to their ability to form hydrogels when placed in contact with a solution of divalent cations such as Ca^{2+}, Ba^{2+} or Sr^{2+}, through a process known as ionotropic gelation[21,24–26].

Alginate shell microcapsules have been frequently prepared through electrospray and microfluidics by coating the core material with an alginate solution and introducing a solution containing calcium ions, which crosslinks the alginate[27]. Reversely, it is also possible to introduce droplets of a solution containing Ca^{2+} into an alginate solution, producing capsules with a thin membrane and a liquid core[28,29]. The addition of surfactants to the alginate solution has also been reported to allow the encapsulation of a wide variety of liquids within microcapsules with thin shells[27]. Alginate has also frequently been combined with different polycations in layer-by-layer (LbL) assembly to produce microcapsules with multilayered shells[30–32].

Despite its beneficial properties and widespread application, alginate also presents significant drawbacks. The relative content of each alginate in mannuronic acid and glucuronic acid influences its mechanical properties, stability and permeability, which impacts the reproducibility of biofabrication methods. It has also been suggested that alginates with a high content in mannuronic acid may increase the likelihood of triggering an inflammatory response[33–35]. Due to its natural source, alginates used in biomedical applications must undergo an extensive purification procedure, in order to fully remove contaminants that will reduce their biocompatibility, such as polyphenols, proteins or endotoxins, which increases its cost[21,34]. Furthermore, alginate does not naturally possess domains for cell adhesion, which results in low cellular attachment to the resulting hydrogels[22,36], however, it has been shown that cell adhesion can be improved by introducing

ECM-derived peptide moieties in the polymer backbone, such as RGD[22,37], YIGSR[38] or DGEA[37].

While the ionotropic gelation of alginate is a commonly pursued strategy to produce both the shell and core of the microcapsules, another commonly employed method is the use of polymers containing methacryloyl moieties. These functional groups allow the production of hydrogels through photopolymerization, a process that can also be performed in mild conditions. This strategy has been employed to produce microcapsules for cell encapsulation and drug delivery using microfluidic platforms[39,40] as well as superhydrophobic surfaces[41]. One of the most prominently used photocrosslinkable polymers is gelatin methacrylate (GelMA), a chemically modified form of gelatin[42]. Gelatin is a natural, non-immunogenic, biocompatible and biodegradable polymer with relatively high solubility, which possesses bioactive motifs that promote cell adhesion[43,44]. While gelatin solutions can be thermally crosslinked, the introduction of methacryloyl moieties can be used to produce hydrogels with improved mechanical properties, which can be modulated by adjusting the substitution rate of methacryloyl groups or the polymer density[45]. Recently, the modification of gelatin with catechol-like moieties has also been reported[46]. This strategy allows the production of entirely protein-derived systems through coordination with iron, producing a robust shell with adhesive properties that promotes cell attachment to the inner shell wall, producing a cell monolayer along its curvature.

Microcapsule shells have also been prepared using inorganic molecules. Cha et al. reported the formation of a silica hydrogel to coat cells grown on GelMA microcarriers[47]. Cardiac cells were cultured on the surface of spherical GelMA microgels produced in a microfluidic platform. The silica shell was then introduced by a sol-gel procedure to protect the cells from mechanical stress, oxidative pressure and exposure to immune cells. The shell was shown to protect the encapsulated shells from highly oxidative agents without compromising cell migration or proliferation. Furthermore, the silica shell was shown to be biodegradable, producing metabolites that are safely excreted from the body. Alginate core silicate shell microcapsules have also been developed for bone TERM applications[48]. The capsules were shown to induce the formation of apatite *in vitro* when placed in simulated body fluid. Additionally, they were also shown to be an efficient carrier for the sustained release of proteins, achieving high protein loading efficiency.

Synthetic polymers have also been proposed as substitutes for alginate and other natural materials, as they are highly tunable materials that can be produced in a reproducible manner while also possessing improved mechanical properties[49]. One such polymer is poly(ethylene glycol) (PEG), which has been prominently used in cell encapsulation[5,50,51]. It is a biocompatible material that can be easily functionalized to introduce hydrolysable segments, bind growth factors and introduce chemical groups that promote cell adhesion and modulate the immune response[52,53]. As such, PEG is a compound of great interest in the generation of core-shell capsules for cell encapsulation and delivery of bioactive factors. For example, dithiothreitol-modified PEG-diacrylate has been used to encapsulate heparin microparticles, producing core-shell structures with biodegradable shells and multiple cores for the sequestration, isolation and delivery of proteins. These capsules provide a system that preserves the structure and activity of growth factors while also offering tight control over the timeframe of their release[54]. PEG has also been explored in the design of aqueous biphasic systems for generation of microcapsules in oil-free microfluidic platforms[55], which will be discussed in greater detail in a later section of this review.

2.2.2. Core structure

Core-shell microcapsules can be fabricated with a wide variety of core architectures, including solid, liquid and hollow cores. Microcapsules with hollow cores are used in the encapsulation of proteins, drugs, DNA, growth factors and other bioactive molecules. These microcapsules can then be delivered into the body to promote cell proliferation and guide tissue repair.[56]. They are produced through the deposition of a multilayer membrane over a sacrificial core, through LbL technology, followed by dissolution of the core. Possible materials that have been used to generate the initial sacrificial core include poly-*DL*-lactic acid and poly (*DL*-lactic-*co*-glycolic acid) (PLGA)[57], silica[58] and $CaCO_3$[59], the latter of which has been prominently used due to its low production cost, high loading capacity and biocompatibility[56].

For the purposes of cell encapsulation, the role of the shell is to isolate cells from the immune system, while the role of the core is to provide appropriate conditions for continued cell survival and proliferation[60]. In order to guarantee a suitable microenvironment for the growth of encapsulated cells, the cores of the microcapsules should be able to mimic the properties of native tissues. Hydrogels have been prominently used in the production of microcapsules

and other biomaterial scaffolds, as they consist of highly hydrated materials organized in porous structures possessing mechanical properties that mimic those of soft tissues and the native extracellular matrix (ECM)[61,62]. Microcapsule cores have often incorporated components derived from natural tissues, such as Matrigel®[63], collagen I[64], GelMA[47], or decellularized ECM[65] to act as support systems for the proliferation of cells, tissues and organoids[63].

While these porous hydrogel scaffolds have been prominently used in the encapsulation of cells and proteins, the polymer matrix heavily restricts the movement of cells as well as the diffusion of nutrients and oxygen required for their survival. As such, a possible alternative has emerged. By taking inspiration from biological structures such as fish-eggs[27] and embryo[66], liquid core capsules, in which the internal core is in the liquid state, can achieve enhanced mass transfer, as well as greater stability, while also allowing the free movement of cells in the aqueous environment of the core, which improves cell-cell interactions and allows them to self-organize in structures more favorable to their proliferation, such as cell spheroids[67–69]. Liquid core microcapsules with alginate shells have been proposed as aqueous bioinspired 3D platforms for the culture of embryonic stem cells (ESCs), which can be differentiated into different cell lines for cell replacement therapy[27,66,70].

Current fabrication techniques are able to encapsulate a wide variety of liquids in microcapsules, producing versatile platforms with multiple applications, even beyond the field of tissue engineering. Microcapsules with oil cores have been generated as vehicles for drug delivery[71]. Microcapsules have also been used to encapsulate ionic liquids, which could have applications in areas such as chemical catalysis, production of pharmaceuticals and environmental remediation[72]. In order to allow the encapsulation of cells, the core solutions often consist of cell suspensions in culture medium, buffer solutions, saline or a mannitol solution[70,73]. These capsule-based systems have been shown to improve the stability of long-term *in vitro* cell culture when compared to cell culture in solid beads[74]. The encapsulation of cells suspended in polymer solutions is also a possibility. For example, Park et al. utilized hyaluronic acid/alginate core-shell capsules to produce MSC spheroids with the purpose of promoting angiogenesis *in vivo*[75].

Commonly, liquid core capsules for cell encapsulation are obtained by entrapping cells in a polymer particle, which is then used as a template for the deposition of a multilayer membrane, which will constitute the shell. The template core is then liquefied. This was the

basis of the first cell microencapsulation procedure, performed by Lim and Sun[32], who encapsulated pancreatic islets in a core-shell capsule with a liquefied core of alginate. This process involves the use of chelating agents, such as EDTA or sodium citrate[76], which sequester the divalent cations responsible for the ionic crosslinks in the alginate hydrogels. Gelatin can also be used in the formation of liquefied core capsules due to its mechanism of thermal gelation. Gelatin solutions produce hydrogels when cooled at low temperatures, while higher temperatures result in the liquefaction of the hydrogels[77]. As such, it is possible to produce gelatin microparticles by cooling droplets of a gelatin solution at 4°C, which can then be coated with an outer membrane[77,78]. The gelatin cores return to the liquid state at physiological temperature, resulting in liquefied cores after implantation.

A considerable limitation of liquid core microcapsules in cell encapsulation is the inability of cells to survive in suspension. In the absence of a suitable substrate for cell adhesion, most mammalian cell lines initiate a form of programmed cell death known as anoikis. In living tissues, this guarantees that only cells that are successfully integrated into the tissue can survive[79–81]. The anchorage-dependent character of these cells thus requires the addition of other structures that permit cell attachment. The most commonly used strategy to overcome the anchorage-dependence of mammalian cell lines is the co-encapsulation of cells with microcarriers[82,83]. These microcarriers consist of polymeric microparticles that provide cells with a surface for attachment, and which can be tailored to present cells with mechanical and structural cues to guide their proliferation, differentiation, orientation and aggregation. A more in-depth look into these structures will be provided in the following section.

2.2.2.1. Microcarriers

The use of microcarriers as attachment sites in suspension culture was originally proposed by van Wezel in 1967, providing a 3D platform that allows the culture of cells in bioreactors[84]. Microcarriers have since been studied as platforms for cell therapy and tissue engineering[85–87] and the production of recombinant factors[88], viral vaccines[89–91] and more recently, synthetic meat[92].

2.2.2.2.1. Considerations on the structure of microcarriers

Microcarriers used in cell culture have displayed spherical, cylindrical, hexagonal, disk-like and lens-shaped geometries[93–95]. The geometry of the microcarriers, combined with the

topographical features of their surface, influences the organization and orientation of attached cells, as well as the available surface area for cell proliferation.

With regards to their surface topography, microcarriers are generally categorized by their pore structure. In smooth microcarriers, which lack porosity, cells grow on the surface of the carrier as a monolayer. This also applies to microporous microcarriers, in which the dimensions of the pores do not allow the entry of cells into the internal structure of the microcarriers. However, the small pores allow the penetration of proteins and biochemical signals produced by cultured cells. The secretion of bioactive molecules and their infiltration into the internal structure of microporous microcarriers thus create a unique biochemical microenvironment within the carriers, which influences the growth and behavior of the cells[85,96,97]. The main disadvantage of both smooth and microporous microcarriers is the low available surface area for cell attachment, which limits cell proliferation. In order to increase the available surface area for cell proliferation, it is possible to produce sponge-like microcarriers that allow the infiltration of cells inside their inner structure, which also protects the cells from mechanical stress[98]. These microcarriers are known as "macroporous" microcarriers, despite possessing pores with typical diameters in the 20–40 μm range, in order to distinguish them from microporous microcarriers, which do not allow the entry of cells[96,99]. Macroporous microcarriers possess a complex 3D internal architecture consisting of an interconnected pore network, which greatly increases the available surface area for cell attachment, enhancing the cell densities that can be achieved. The porosity, pore dimensions and pore connectivity of these microcarriers can be adjusted to regulate cell proliferation, cell-cell interactions and mass transfer, in order to ensure proper diffusion of nutrients, oxygen, and waste products while also improving the regenerative potential of the cell-laden microcarriers[96,100–102].

Microcarriers with specific topographical features can also be fabricated in order to present cells with cues that activate mechanotransduction pathways, modulating cell differentiation, proliferation and interactions between cells. Recently, disk-like microcarriers with nano-grooved surface patterns have been used as cell carriers with high surface area to induce differentiation of stem cells into an osteogenic lineage[103]. These topodisks were successfully able to promote cell adhesion and control cell orientation, while directing cells toward an osteogenic lineage, even without the addition of paracrine signals that promote differentiation. By adjusting the topographical and biophysical cues displayed by the

microcarriers in the core of the microcapsules, it should be possible to tailor the properties of capsule-based systems toward different biomedical applications, by modulating cell behavior.

2.2.2.2.2. Considerations on the composition of microcarriers

A wide variety of biomaterials have been used in the generation of microcarriers, including natural and synthetic polymers, bioactive glass[104] and bioceramics such as hydroxyapatite[105]. Natural polymers used to prepare microcarriers include dextran, gelatin, cellulose and alginate [84,106–109]. Another polymer that has been increasingly used is chitosan, a positively charged polysaccharide obtained through the alkaline hydrolysis of chitin, which can be readily obtained from the exoskeletons of invertebrates such as crustaceans and insects, as well as the cell walls of fungi[110]. Polystyrene (PS) is the most commonly used synthetic polymer in commercially available microcarriers[93,111]. Biodegradable synthetic microcarriers have also been thoroughly researched for the fabrication of microcarriers, including polymers such as poly(*L*-lactic acid) (PLLA), poly(glycolic acid) (PGA), PLGA and poly(ε-caprolactone) (PCL)[97,112].

Both PLLA[30,82,83,113,114] and PCL[115–117] microparticles have previously been co-encapsulated with cells within microcapsules. This approach has been successfully used to create platforms that promote osteogenesis[30,114,117]. Due to a lack of cell recognition sites in these polymers, the surface of the microcarriers was coated with collagen to improve cell adhesion. Attachment of cells to microcarriers is dependent on non-covalent interactions between the surface of the microcarriers and proteins on the surface of cells, encompassing electrostatic forces, hydrogen bonds, dipole-dipole interactions and van der Waals forces[118]. Parameters such as the polarity and density of the surface charge, as well as the topography, mechanical properties and wettability of the surface all influence the effectiveness of cell-microcarrier interactions, as reviewed elsewhere[96,119,120]. As such, functionalization of the surface of the microcarriers is often pursued as a strategy to improve cell attachment. This can be accomplished by introducing positive charges on the surface of the microcarriers, through functionalization with PLL or small charged chemical groups[93,112,121]. Improving the wettability of the microcarrier surface has also been pursued as a strategy to achieve greater cell adhesion. This can be accomplished by modifying the surface of microcarriers using methods such as UV-ozone treatment[122]. It is also possible to improve cell attachment by

coating the surface of the microcarriers with bioactive molecules, which often includes components of the ECM, such as laminin, collagen, fibronectin, Matrigel®, vitronectin or small peptides that possess peptide sequences that promote cell recognition and adhesion, most commonly the RGD sequence[123–126]. Surface functionalization is a versatile strategy that can also be used to produce microcarriers with specialized applications. For example, microcarriers with cell-selective properties can be produced by attaching antibodies to their surface[127]. The immobilization of growth factors on the surface of the microcarriers can also be used to guide cell differentiation. This approach has been employed to produce microcapsules that promote chondrogenesis[113].

2.3. Biofabrication techniques used in the generation of microcapsules

The development of core-shell capsules with defined characteristics for biomedical applications requires a careful consideration of the methods used in their production. While a wide variety of strategies has been used to produce core-shell structures, including sol-gel methods[47], emulsion polymerization[128], superhydrophobic surfaces[41,46] and superamphiphobic surfaces[129], this section will focus on overviewing the most commonly used biofabrication methods for microcapsule production, including microfluidic platforms, electrospray and layer-by-layer (LbL) assembly.

2.3.1. Microfluidics

Microfluidic platforms are miniaturized devices that can be used to manipulate fluids at a micrometer scale, allowing precise control over the flow of multiple solutions[130]. These platforms have increasingly been used in the fields of drug screening, cell culture and disease modeling, as they allow the imposition of specific conditions, achieving a precise reenactment of specific cell niches, providing accurate simulations of *in vivo* conditions and even allowing the recreation of entire biological systems through organ-on-a-chip and system-on-a-chip platforms[131].

The ability to rigorously adjust flow rates in these platforms can be harnessed to produce highly monodisperse microcapsules, while also offering precise control over the porosity, dimensions, anisotropy and morphology of the capsules[132,133]. The production of microcapsules in microfluidic platforms is based on the flow of a polymer solution, known as the dispersed phase, which intersects the flow of another, immiscible fluid, known as the

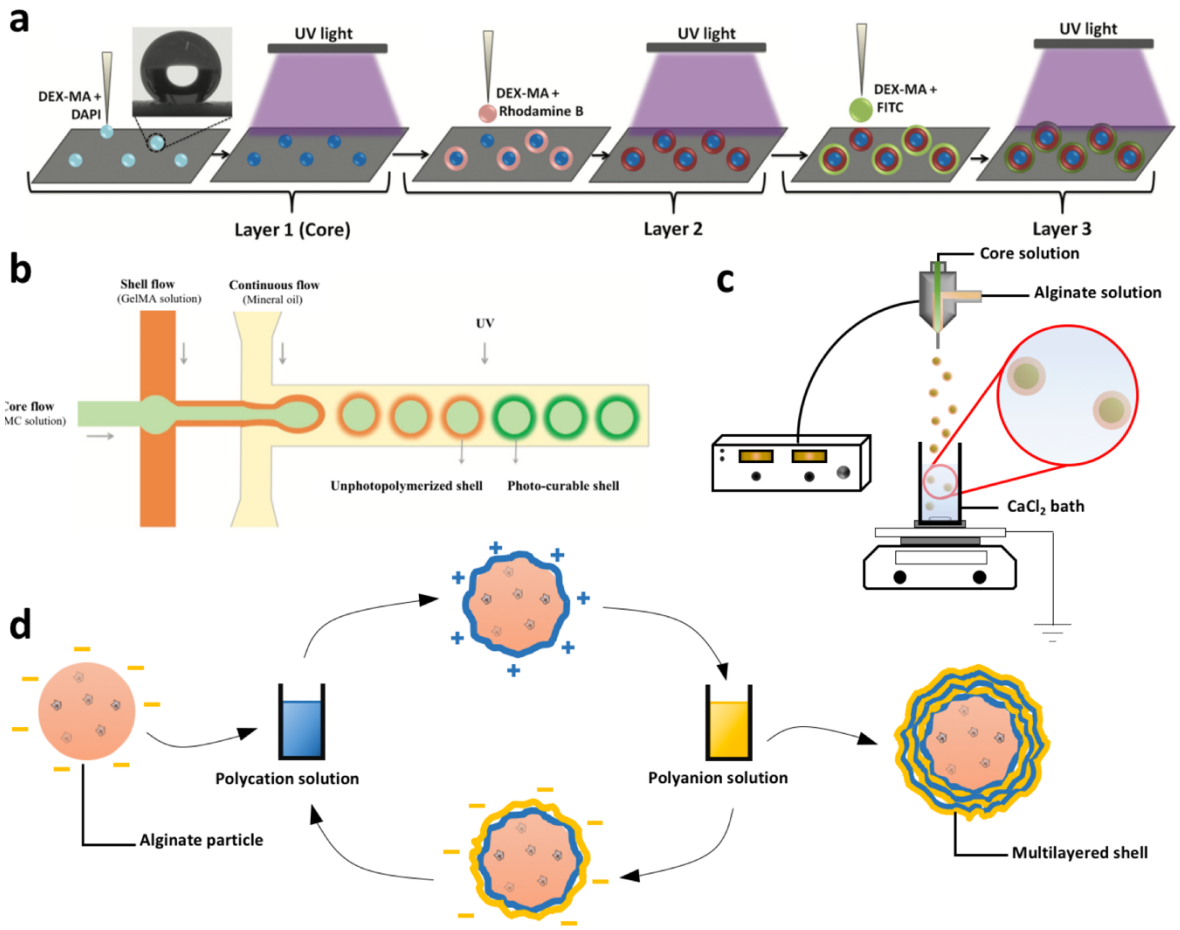

Fig. 2.1. Schematic representation of biofabrication techniques used in the preparation of core-shell capsules. (a) Superhydrophobic surfaces[41]. (b) Microfluidic devices[39]. (c) Coaxial electrospray. (d) Layer-by-layer assembly.

continuous phase, resulting in the break-up of the dispersed phase, which produces droplets through oil-in-water or water-in-oil emulsions[131,134].

The encapsulation of cells has been accomplished using different configurations, including T-junctions, flow focusing and coaxial flow units[133,135,136]. By combining two droplet forming units, it is possible to generate core-shell microcapsules through double emulsion systems[130,132]. By increasing the number of inner flows, or simply by adjusting the solution flow rates, it is possible to produce microparticles with multiple cores, and by increasing the number of droplet forming units, multilayered shells can be obtained[132,134].

A simple procedure to produce core-shell capsules consists of coating the core components with an alginate solution and adding a calcium salt, such as $CaCl_2$, to the continuous phase, producing the shell. This strategy has been employed in the production of capsule-based systems for the formation of spherical embryoid bodies[136]. Alternatively, capsules with

alginate shells have also been obtained by mixing insoluble $CaCO_3$ particles into the alginate shell solution and employing a continuous phase containing an acidic solution, which reacts with the $CaCO_3$, releasing Ca^{2+} ions that introduce crosslinks in the alginate[137].

The incorporation of crosslinking agents in the continuous phase is also a possible procedure used in the generation of the shell. For example, 4-arm maleimide functionalized PEG (PEG4m) has been used to develop a capsule-based platform through chemical crosslinking[138]. A coaxial flow system consisting of an inert PEG core solution enveloped in a sheath of PEG4m is broken up into core-shell emulsions and the outer PEG4m solution is then crosslinked using an oil phase containing dithiothreitol. By adjusting the core and shell solution flow rates, it is possible to achieve precise control over the dimensions of both the core and shell, producing a system with highly tunable shell thickness. Polymers functionalized with methacryloyl groups can also be used to produce the outer shell of the droplets, by coupling the microfluidic device with an UV lamp[39,40,139].

The use of microfluidic biofabrication platforms for biomedical applications has been hindered by the need to use organic solvents and oils, which are toxic to cells, denature proteins and are harmful to the environment[140]. A possible alternative is the use of mineral oils, which possess better biocompatibility[141]. Another alternative is the use of aqueous biphasic systems, which are obtained by producing solutions of two incompatible solutes, such as PEG and dextran, at appropriate concentrations[55,142]. These systems can be used to minimize contact between the oil phase and the encapsulated material, while also facilitating removal of the oil. Recently, a PEG-diacrylate/dextran system has been harnessed to produce microcapsules for the dual-delivery of vascular endothelial growth factor (VEGF) and platelet-derived growth factor (PDGF)[143]. This setup employed a continuous phase containing fluorocarbon oil, which was easily washed out without compromising the stability of the encapsulated growth factors. The generated capsules were shown to improve cardiac function after *in vivo* implantation, while also providing a promising platform for the delivery of drugs, signaling molecules and mRNA.

Additionally, aqueous biphasic systems can also be used to develop oil-free biofabrication procedures that eschew the need for organic solvents altogether[144]. A limitation of all-aqueous systems, however, is that it is more difficult to control the properties of the final microcapsules, although this limitation can be circumvented by using an oscillating valve,

which can be used to produce microcapsules with specific properties by adjusting oscillation frequencies and solution flow rates[140,144].

2.3.2. Electrospray

Electrohydrodynamic atomization, also known as electrospray (ES), is a versatile technique used in the generation of both micro and nano scale particulate materials, allowing a high degree of control of the production procedure and generating highly monodisperse particles[145]. The basic principle of ES is the extrusion of a conductive polymer solution through an electrified metal nozzle, which breaks up the liquid, generating droplets that are deposited on a grounded collector[145,146].

The dimensions, morphology and polydispersity of the obtained particles are heavily dependent on operational parameters such as the applied voltage, flow rate, nozzle diameter, tip to collector distance and chosen collector; environmental factors such as temperature and humidity; and the properties of the polymer solution, such as viscosity, surface tension, polymer concentration, solvent conductivity, volatility and permittivity[145,147–149]. The effect of processing parameters on the properties of microparticles has been well documented elsewhere[149–153]. In summary, higher flow rates will generally increase the electric force required to overcome the surface tension, resulting in an increase in particle diameter, however, they may also lead to an unstable jetting process, decreasing the uniformity of the particles. The applied electric field heavily influences both the jetting mode and the dimensions of the particles. Higher applied voltages will lead to a more thorough break-up of the polymer solution, resulting in smaller particles, while increasing the tip to collector distance will weaken the electrical field, increasing the capsule diameter. Lastly, the selection of an appropriate nozzle is required, as nozzles with higher diameter will introduce instability in the jetting process, while lower nozzle diameters will produce smaller particles.

Many different ES configurations are possible, further contributing to the versatility of the technique. Monoaxial setups are able to produce particles in a diverse range of morphologies and shapes[154], including core-shell capsules, which can be obtained through the incorporation of water-in-oil emulsions[146]. Additionally, liquefied capsules coated in thin membranes can also be obtained using aqueous biphasic systems. Vilabril et al. developed an encapsulation procedure based on the extrusion of a dextran solution containing alginate into a collector bath consisting of a PEG solution containing poly-*L*-lysine (PLL)[155].

Alginate and PLL are two polyelectrolytes of opposing charge, which suffer complexation at the interface of the two phases, leading to the generation of a robust and permeable membrane that envelops a liquid core. These capsules were shown to support the proliferation of MSCs and the formation of cellular aggregates.

Core-shell capsules are also commonly obtained by employing coaxial nozzles[67,152]. The formation of capsules with multiple shells is also possible by using a triple coaxial setup[156]. In coaxial ES, the properties of both core and shell solutions will influence the resulting core-shell structures. As such, the surface tension, conductivity, viscosity, permittivity and flow rate of both solutions must be selected appropriately[151,152].

The application of a high voltage electric current during microcapsule generation could hinder the survival of cells, however, it has been shown that cell proliferation is not affected by the electrospraying process when the strength of the applied electrical field is below 3 V/cm[157]. When compared to microfluidics, coaxial electrospray presents numerous advantages, as it is a one-step process that requires a single solvent, eschewing the need for the use of organic solvents or complex solvent systems. This also facilitates recovery of the microcapsules after production and reduces the amount of waste produced. Furthermore, ES provides greater control over the properties of the microcapsules, as it relies on a greater amount of parameters that can be modulated and optimized[145]. As the implementation of microcapsule based strategies advances to the clinical stage, coaxial ES could provide an avenue toward the large scale production of microcapsules, as it can be performed in sterile conditions, it is easy to use, and it can achieve high production and encapsulation rates, with further potential for application at industrial scales by employing multiple nozzles[70,158–160].

2.3.3. Layer-by-layer assembly

LbL assembly has been explored as a simple, versatile, low-cost and environmentally safe approach for the generation of ultrathin films using a vast range of starting materials, including enzymes, polymers, ceramics or metals[161] As a cell encapsulation method, it can be used to generate microcapsules enveloped in thin multilayered membranes with tunable structure, permeability and composition[162,163]. Despite being a time-consuming process with reduced scalability, LbL assembly can be performed in mild conditions while using aqueous solvents, which is advantageous for the generation of suitable platforms for TERM

applications. The encapsulation of pancreatic islets through LbL assembly was a pioneering approach in cell encapsulation[32].

Core-shell systems can be obtained through the sequential adsorption of polymers on the surface of a sacrificial core, which acts as a template. The assembly of the multilayered shell can rely on multiple forces acting between the chosen materials, including hydrogen bonds, hydrophobic interactions, covalent bonds and electrostatic interactions[56]. The generation of microcapsules for cell encapsulation has often relied on the electrostatic forces between polyelectrolytes with opposing charges. Appropriate polycations and polyanions are selected and sequentially deposited to produce a polymer shell. In this process, the template cores are coated in a dilute solution of polyelectrolyte in order to produce the first layer of the membrane. The capsules are then washed, and placed in a solution of a second polyelectrolyte, with opposing charge. This process is repeated until the shell has reached the desired thickness[164].

The inner core of the capsule can then be liquefied, dissolved or eliminated, allowing the generation of microcapsules with solid, liquefied or hollow cores[58,68]. By adjusting the morphology of the initial sacrificial core, it is possible to construct capsules with a wide diversity of geometries[116].

Alginate–poly-*L*-lysine–alginate (APA) capsules are one of the most prominently used systems in cell encapsulation. These capsules contain an alginate core surrounded by a multilayered shell of PLL and alginate. Cells are mixed in an alginate solution, which is used to create solid microparticles through ionic crosslinking in a $CaCl_2$ solution, often through ES[165]. The microparticles are then coated with a first layer of PLL and a second layer of alginate, through LbL. Further layers can be added, and it is also possible to liquefy the alginate core. These systems have been used to deliver stem cells[31,166], pancreatic islets[167], hepatocytes[168] and Chinese hamster ovary (CHO) cells[169]. While PLL is commonly selected as a polycation in LbL assembly, it has been shown to be toxic to cells at higher concentrations and if it is not properly bound to the capsules, it can potentially be immunogenic, resulting in fibrosis[170–172]. As such, other polycations have been researched as possible alternatives, such as chitosan[173], poly-*L*-ornithine (PLO)[174], poly(allylamine)[175] or copolymers of PLL and PEG[176], which have allowed the production of capsules with reduced immunogenicity, enhanced biocompatibility and improved mechanical properties.

2.4. Biomedical applications of core-shell microcapsules

In recent decades, core-shell capsule-based platforms have been prominently explored in different fields of medicine, tissue engineering and cell culture with the purpose of designing effective encapsulation systems for the delivery of cells, tissues, drugs and proteins. Possible applications have included the delivery of pancreatic islets to individuals suffering from type I diabetes, as well as the development of TERM approaches to bone and heart disorders. They have also been suggested as bioinspired scaffolds for 3D cell culture and disease modeling. In this section, the contributions of core-shell microcapsules to each of these fields will be explored.

2.4.1. Type I Diabetes

Research efforts into the potential biomedical application of microcapsules were pioneered by Lim and Sun, in their attempts to develop therapeutic approaches to type I diabetes mellitus[32]. Type I diabetes is a metabolic disorder caused by an autoimmune response to β-cells, located in pancreatic islets. These cells are responsible for the production of the hormone insulin, which regulates the cellular intake of sugar. As such, type I diabetes causes insulin deficiency, which results in increased blood sugar levels[177]. It is estimated that type I diabetes comprises 5 to 10% of all diabetes cases, with a global incidence of 15 cases per 100000 people, and it is projected that both the incidence and prevalence of this disease will continue to increase globally[178,179].

The transplantation of pancreatic islets has been proposed as a therapeutic strategy to restore β-cells in the pancreas and reduce the need for insulin injections, however, this process has been hindered by rejection of the transplanted islets[177]. Initially, it was shown that encapsulation in microcapsules prolonged the survivability of transplanted islets in rats from 8 days to 3 weeks[32]. The results obtained by Lim and Sun were later confirmed by O'Shea et al.[167], who also extended the survival period of islets to a full year, in rats, through encapsulation in APA microcapsules. Early clinical studies regarding the transplantation of encapsulated islets in a human patient showed that this approach was capable of granting insulin independence for a period of 9 months[33]. As previously mentioned, PLL presents several limitations, which has prompted its replacement with other polymers, such as chitosan[180] or PLO[181]. Wang et al.[182] explored over one thousand polyelectrolyte combinations and produced multicomponent capsules with highly tunable dimensions and

mechanical properties using sodium alginate, cellulose sulphate, poly-methylate-co-guanidine, calcium chloride and sodium chloride.

The co-encapsulation of pancreatic islets with other cell types, such as mesenchymal stem cells (MSCs)[183,184] or Sertoli's cells[174], is a strategy that has been shown to extend islet survival, while also improving the regenerative potential of the microcapsules. Recently, it has also been shown that inclusion of hyaluronic acid in the matrix of the alginate core enhances survival of insulin-producing cells[185]. One of the major obstacles to the long-term viability of encapsulated islets is the development of hypoxic conditions in the capsules, due to the high oxygen demand of pancreatic islets.[181,186]. The inclusion of oxygen carrier materials has been explored as a strategy to reduce damage caused by hypoxia in the short-term[187]. A review of these materials has been provided elsewhere[188].

Table 2.1. Summary of core-shell microcapsule platforms developed for the treatment of type I Diabetes. This summary covers the materials used to produce both the core and shell of the capsule, the technique used to generate the capsules and the biological materials encapsulated in each structure.

Shell material	Core structure	Production technique	Encapsulated material	Ref.
PEI/PLL	Alginate	LbL	Pancreatic islets	32
Alginate/PLL	Alginate	LbL	Pancreatic islets	167
Alginate/PLL	Alginate-HA	Ionotropic gelation, LbL	Rat Ins1E cells	185
Alginate/PLO	Alginate	LbL	Pancreatic islets, Sertoli's cells	174
Alginate/PLO	Alginate	Ionotropic gelation, LbL	Pancreatic islets (core) FGF-1 (Alginate shell)	181,189, 192
PLL	Pancreatic dECM	Ionotropic and thermal gelation	Insulin producing cells derived from adult human liver cells or MSCs	65
Alginate/PLL	Alginate	Ionotropic gelation, LbL	Adult porcine islets	186

A more long-term approach would be the promotion of vascularization at the site of implantation, in order to increase blood flow and oxygen supply in the affected area. This can be accomplished through the delivery of pro-angiogenic factors such as fibroblast growth factor 1 (FGF)[189], PDGF[190] and VEGF[191]. A possible application of this strategy was studied by Opara and coworkers, who attempted the co-delivery of cells and pro-angiogenic

growth factors in a compartmentalized platform. Pancreatic islets were encapsulated in the core of an alginate-PLO-alginate microcapsule and FGF-1 was incorporated in the shell[181,189,192]. Long-term viability of the capsules was achieved, particularly when microcapsules were delivered to the omentum, a highly vascularized tissue, highlighting the importance of proper vascularization in islet survival[189].

2.4.2. Bone defects

In 2015, an estimated 8.5% of the global population was aged 65 and older. By 2030, this proportion is expected to increase to 12.0% and by 2060, it is estimated that it will reach 16.7%[193]. The aging of the global population is expected to increase the incidence of bone defects. Bone grafting is already the second most common tissue transplantation procedure, after blood transfusion[194]. However, this procedure holds many limitations. Autologous bone grafts require two surgical procedures, may damage the donor site and yield a limited amount of tissue. Allogeneic bone grafts, on the other hand, display inferior healing capabilities, while also carrying the risk of immune rejection and of transmitting pathogens from donor to patient[195–197]. The implantation of metals, ceramics or biomaterial scaffolds has also been explored, however, these materials often display inadequate mechanical properties, poor integration with the native tissue or reduced cell attachment. Applying TERM approaches to the treatment of bone defects could provide new options for enhanced graft incorporation, formation of bone tissue and development of engineered bone constructs[198]. Core-shell structures are optimal for the delivery of both cells and proteins in bone TE strategies, as they can better mimic the hierarchical structure of bone when compared to other microencapsulation platforms[199].

Multilayered hollow-core microcapsules for the delivery of osteogenic growth factors were designed by Facca et al. using LbL[58]. Bone morphogenic protein 2 (BMP-2) and transforming growth factor β1 (TGF-β1) were incorporated in a PLL/poly-*L*-glutamic acid (PLL-PGlA) multilayered shell. The capsules were shown to increase the stability of the growth factors and induce the formation of bone *in vitro*, in the presence of ESCs. The hollow core microcapsules were then embedded in an alginate gel along with ESC derived embryoid bodies and implanted *in vivo*. The resulting gel was shown to induce bone formation and vascularization. Microtissues with enhanced mechanical properties were produced by Luo and coworkers by combining an open porous gelatin shell with a core

generated from demineralized bone matrix loaded with BMP-2[6]. The core-shell structures exhibited high cell seeding efficiency, sustained release of BMP-2, higher viability of seeded bone marrow mesenchymal stem cells, and enhanced calcium deposition and mineralization when compared to gelatin derived microtissues. When implanted *in vivo*, the core-shell microtissues were shown to promote the formation of bone.

Liquefied core microcapsules have also been proposed as a platform for the fabrication of bone tissue for TE applications. In 2011, Mano and coworkers showed that SaOs-2 cells encapsulated in liquefied alginate core microcapsules coated with a multilayered membrane of chitosan and alginate retained viability after encapsulation[68]. Further studies showed that co-encapsulation of adipose-derived stem cells (ASCs) and endothelial cells in liquefied microcapsules can induce osteogenic differentiation of the ASCs even in the absence of osteogenic growth factors, providing an effective strategy for the development of bone tissue[30,114]. Furthermore, the differentiated ASCs were shown to produce and secrete paracrine factors such as BMP-2 and VEGF, which travel from within the capsules to the surrounding environment through diffusion, thus revealing the possibility of using the encapsulated cells as biofactories for the production and sustained release of biochemical signaling molecules.

Table 2.2. Summary of core-shell microcapsule platforms for application in bone TE. This summary covers the materials used to produce both the core and shell of the capsule, the technique used to generate the capsules and the biological materials encapsulated in each structure.

Shell material	Core structure	Production technique	Encapsulated material	Ref.
PLL/PGlA	Hollow core	LbL (sacrificial PS template)	BMP-2, TGF-β1 (incorporated in shell)	58
Calcium silicate	Alginate	Ionotropic gelation	Proteins	48
PLL/Alginate/Chitosan	Alginate	LbL	ASCs, endothelial cells, PLLA microparticles	30,114
Gelatin	Demineralized bone matrix	Micro-stencil array chip	BMP-2 (core) BMSCs (shell)	6
PLL/Alginate/Chitosan	Alginate	Electrospray, LbL	ASCs, osteoblasts, PCL microparticles	117

When these capsules were implanted *in vivo*[114], not only was the formation of mineralized tissue observed, but it could be observed even in capsules that were not subjected to *in vitro*

pre-differentiation procedures, indicating that the microcapsules could be readily implanted after preparation. Liquefied microcapsule platforms have also been used to develop bone microtissues through the co-encapsulation of osteoblasts, adipose-derived stem cells and PCL microparticles[117]. In dynamic culture conditions, the hydrodynamic shear improved cell-cell interactions, generated larger cell aggregates and induced the osteogenic differentiation of ASCs even in the absence of osteogenic growth factors and osteoblasts. Furthermore, microcapsules co-encapsulating ASCs and osteoblasts in a dynamic environment displayed clear signs of mineralization, such as the growth of apatite-like minerals, similar to those found in native bone tissue.

2.4.3. Cardiovascular diseases

In the last decades, the development of numerous therapeutic and preventive measures to address cardiovascular disease has led to a steady decline in mortality and morbidity caused by cardiovascular disorders in developed countries[200]. Nevertheless, these disorders remain the leading cause of death worldwide, accounting for 17.8 million deaths in 2017 and for an expected 22.2 million deaths by 2030, and it is expected that these diseases will continue to constitute a significant cause of death in developing nations in the next decades, according to reports by the World Health Organization[201,202]. Cardiovascular disorders not only greatly diminish the quality of life of patients, but they also pose a significant burden on the economy, with an estimated annual cost of 210 billion euros in the European Union and 296 billion euros in the United States[201,203].

As such, there is high demand for novel approaches to produce cardiac cells, regenerate heart tissue and study cardiac pathophysiology. And core-shell microcapsules provide a versatile platform that can be directed toward these applications. For example, the use of coaxial ES to encapsulate ESCs in liquid core alginate microcapsules has been pursued as a scalable, cost-effective and highly tunable approach to produce cardiomyocytes for cardiac transplantation[70,141,204]. After 7 days, ESCs formed cellular aggregates with dimensions comparable to those of previously used methods, while requiring a much lower number of initial cells[70]. Furthermore, this approach allowed cells to maintain a greater degree of pluripotency than previous approaches while potentially allowing the single step production of millions of capsules per day, providing a sustainable source of embryoid bodies for tissue regeneration. Differentiation of ESCs into the cardiac cell line can be achieved by applying

bone morphogenic protein 4 (BMP-4) and FGF-2, producing beating aggregates that closely mimic the cellular composition of native cardiac tissue. In a later work, Zhao et al. transplanted the obtained aggregates into the infarcted heart, improving heart function[66]. The aggregates were released from the core-shell microparticles and re-encapsulated without a noticeable influence on cell viability or the integrity of the aggregates, demonstrating their high stability.

Promoting vascularization has also been suggested as a potential therapeutic approach in the treatment of ischemic heart disease, in order to ensure the oxygenation of transplanted cells and tissues. Zhang et al. performed the genetic modification of CHO cells to produce and secrete VEGF, in an attempt to improve vascularization. The cells were delivered to infarcted tissue, in rats, using liquid core APA microcapsules[169]. It was shown that the microcapsules were stable post-implantation and displayed lower immunogenicity when compared to non-encapsulated cells, indicating that the capsules were successfully isolating cells from the immune system. Furthermore, the continuous release of VEGF stimulated angiogenesis and restored cardiac function. The co-encapsulation of MSCs and Schwann cells in liquid core APA microcapsules has also been shown to induce angiogenesis[205]. MSCs secrete a wide variety of growth factors and chemical signals that promote vascularization and the Schwann cells extend the viability of MSCs, while also yielding increased density of newborn capillaries in treated areas.

Table 2.3. Summary of core-shell microcapsule platforms used in myocardial TE. This summary covers the materials used to produce both the core and shell of the capsule, the technique used to generate the capsules and the biological materials encapsulated in each structure.

Shell material	Core structure	Production technique	Encapsulated material	Ref.
Alginate/PLL	Alginate	Electrospray, LbL	CHO cells	169
Alginate/PLL	Alginate	Electrospray, LbL	MSCs, Schwann cells	205
PEGDA	Dextran	Microfluidics	VEGF, PDGF	143
PLL	Alginate	Ionotropic gelation	ESCs	204
Alginate	Sodium carboxymethyl cellulose solution	Microfluidics	ESCs	141
Alginate	Sodium carboxymethyl cellulose solution	Coaxial electrospray	ESCs	66, 70
Silica	GelMA	Microfluidics, sol-gel	Cardiac progenitor cells	47

2.4.4. 3D cell culture

In vitro cell culture has commonly relied on 2D plastic substrates, which cannot fully recreate the microenvironment and cell interactions present within native tissues. This has become a widely recognized limitation of *in vitro* models used in the study of diseases and drug screening[206]. Biomimetic 3D platforms can emulate the architecture and properties of living tissues more accurately, providing efficient platforms to model cell behavior. By altering the composition of the core, it is possible to tailor the stiffness of the materials encapsulated alongside the cells, providing a medium to evaluate the effects of mechanical cues on cell behavior[207]. As previously mentioned, liquid core microcapsules present numerous benefits as *in vitro* cell culture platforms when compared to solid core structures, as they facilitate cell-cell interactions and the self-assembly of cells into more complex structures while preserving cell viability[67].

Core-shell microcapsules thus supply an opportunity to improve cell culture methods, by tailoring their inner microenvironment toward different cell types, which can be accomplished owing to the high tunability and versatility of available production methods. Moreover, it is possible to design microcapsules that allow the compartmentalized encapsulation of different cells[208]. For example, Chen and coworkers produced a "liver in a drop" by designing an encapsulation system in which hepatocytes are incorporated in the liquid core of the capsule while fibroblasts were embedded in the alginate shell[209]. This structure keeps the two cell types separated, in order to preserve their specific functions, while still allowing adequate cell-cell interactions to occur, resulting in a promising *in vitro* model for liver function.

While the structure of the microcapsules can be modulated to adjust interactions between encapsulated cells, it is also possible to construct systems that promote interactions with cells on the outside of the capsules. For example, Correia et al. co-encapsulated osteoblastic cells and PCL microparticles in liquefied core microcapsules coated in a multilayered membrane of alginate, PLL and chitosan and enveloped in an outer layer of RGD-functionalized alginate[115]. When transferred to a 2D cell bed of fibroblasts and human umbilical vein endothelial cells (HUVECs), the RGD domains in the outer surface of the microcapsules promoted cell attachment to the outer surface of the membrane, and allowed the aggregation of cell-coated microcapsules, producing constructs with complex hierarchical structures. In a follow-up work, it was shown that adjusting the composition of the outer layer of the

microcapsule shell can promote the modulation of surrounding macrophages toward a pro-regenerative behavior, an effect which is enhanced through the encapsulation of cells that can communicate with macrophages through paracrine signaling[210]. This demonstrates that the properties of microcapsules can be tailored in order to guide native cells toward desired phenotypes.

These 3D cell culture systems also hold great promise in the modeling of diseases for high-throughput assays. The design of robust tumor models for drug screening is an ongoing challenge in oncogenic research[211]. Core-shell microcapsules have been explored as suitable platforms for the formation of cell spheroids, which can represent accurate models for cell-cell interactions and diffusion of nutrients and drugs in tumors[212]. The possibility of encapsulating cells in separate compartments enables an effective recreation of the tumor microenvironment[211]. Furthermore, microcapsules can provide physicochemical and mechanical cues that can direct gene expression and cell function in order to study different aspects of tumor growth[213,214]. Alessandri et al., for example, designed an elastic capsule-based platform that can be used to evaluate the force exerted by expanding multicellular spheroids, simulating the pressure exerted by growing tumors on surrounding tissues, while also providing insight into the influence of mechanical cues on tumor progression[214]. This system was even able to induce the formation of spheroids in recalcitrant cell lines.

Bioencapsulation in liquefied core capsules has been proposed as a timely and cost-effective procedure to enrich cancer stem-like cells (CSCs), a rare subpopulation of cells highly involved in the initiation, expansion, metastasis and resistance of tumors[215]. Core-shell microcapsules have also been successfully used as modular units in the bottom-up assembly of vascularized constructs[207]. Cancer cells were suspended in a collagen I solution and encapsulated in alginate microcapsules, generating avascular microtumors. To produce a vascularized structure, the microcapsules were incorporated in a collagen I gel alongside ASCs and HUVECs, resulting in a 3D capillary network surrounding the microtumors. When compared to 2D-cultured cells, the vascularized construct was shown to be more

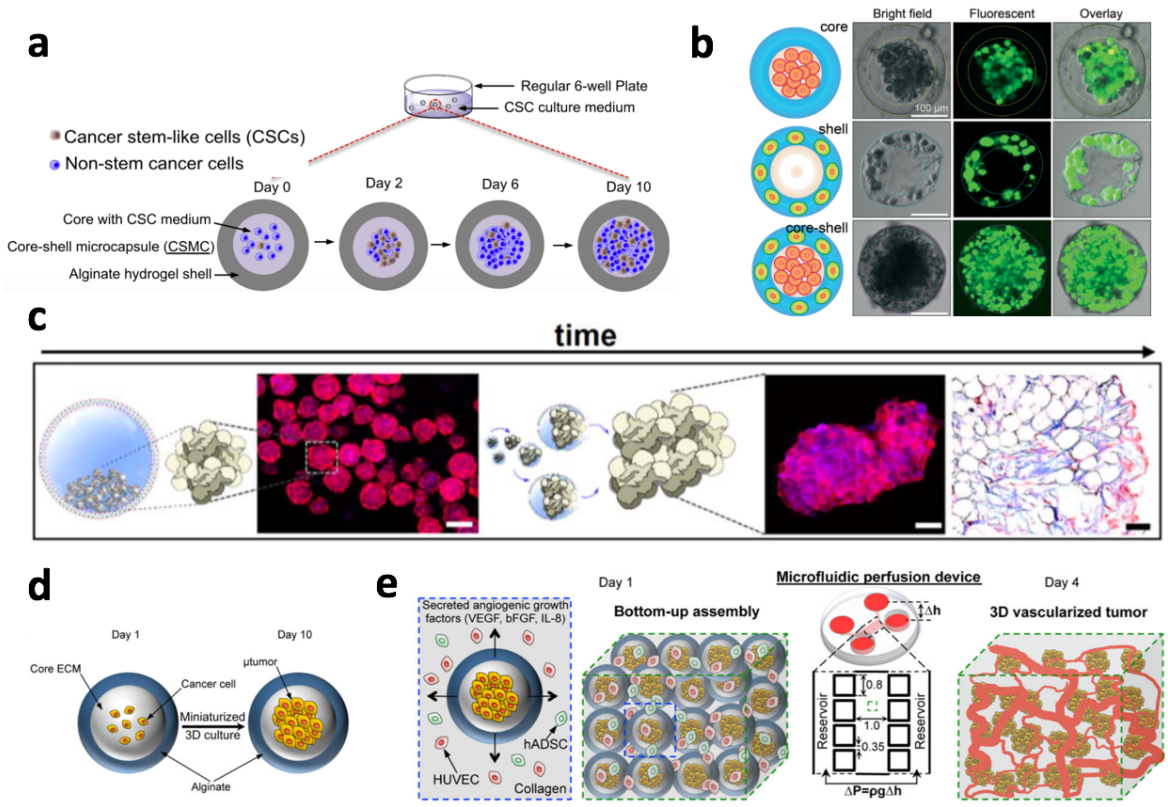

Fig. 2.2. Outline of biomedical applications of microcapsules addressed in this document. (a) 3D platforms for the culture, proliferation and differentiation of cells, with potential for the enrichment of rare cell subpopulations[215]. (b) Development of compartmentalized platforms for a more accurate recreation of *in vivo* tissue architecture[209]. (c) Assembly of complex structures, such as microtissues and spheroids through the self-assembly and aggregation of cells within the capsules. This can be aided by seeding cells alongside surfaces that permit cell attachment, such as microparticles. Scale bars represent 50 µm[117]. (d) Development of robust disease models to evaluate the effects of mechanical cues on cell behavior and the efficacy of drug candidates. (e) Production of functional units for the modular assembly of larger constructs, and even vascularized structures[207].

tumorigenic and more resistant to anti-cancer drugs, providing a robust tumor model for drug testing. Thus, core-shell capsules represent an important breakthrough in the development of 3D culture systems for the study of diseases and potential treatment options. Future developments in this field will require the development of capsule-based systems that can better emulate human tissues, which will require a careful selection of appropriate core and shell components. One possibility under consideration is the incorporation of human derived hydrogels, which would minimize the use of xenogeneic materials, thus creating structures that are more faithful to the composition of human ECM[216,217].

Table 2.4. Core-shell microcapsule platforms employed in tumor models. This summary covers the materials used to produce the capsules, the technique used in their generation and the encapsulated cells.

Shell material	Core structure	Production technique	Encapsulated material	Ref.
Alginate	Sorbitol solution	Microfluidics	CT26, HeLa and S180 cells	[213]
Alginate/PLL	Alginate	Electrospray/LbL	HT-29 cells	[212]
Alginate	Sodium carboxymethyl cellulose solution	Coaxial electrospray	Prostate CSCs	[214]
Alginate	Alginate	Microfluidics	MCF-7 cells	[211]
Alginate	Collagen + alginate + Matrigel®	Microfluidics	MCF-7 cells	[137]
Alginate	Collagen I, Collagen I + Alginate	Microfluidics	MCF-7 cells	[207]
Alginate	Cell culture medium	Microfluidics	MCF-7 cells (core) Human Mammary Fibroblasts (shell)	[210]

2.5. Conclusions and future directions

A wide variety of materials and techniques have been harnessed to produce core-shell microcapsules, generating versatile platforms that can be precisely fine-tuned in terms of their composition, mechanical properties and 3D structure, in order to recreate different physiological niches. These systems have already been implemented in tumor modeling, bone, pancreatic and heart tissue engineering, as well as lung[218], cartilage[113] and hepatic[138,209] tissue engineering. At present, the application of core-shell microcapsules in a clinical setting still presents significant challenges, due to factors such as a lack of appropriate vascularization of the constructs *in vivo*, reduced scalability of production techniques and insufficient long-term stability of encapsulated materials. Further research into these platforms will continue to tackle these issues. Recent studies have also focused on the development of long-term strategies for the storage and preservation of encapsulated structures, a requirement for wide application of these platforms at a clinical level[74].

While originally conceived as a platform for cell immunoisolation, recent works on microcapsules have also attempted to move away from this framework, shifting the focus from hiding transplanted cells from the immune system, and instead toward cooperation with immune cells by guiding them toward a pro-regenerative phenotype[219]. Through careful selection of the biomaterials used to produce the outer shell, as well as the encapsulation of

cells that can interact with immune cells through paracrine signaling, it has been shown that capsule-based systems can be used as immunomodulatory platforms for tissue regeneration[210]. Immunomodulatory systems that promote a pro-regenerative phenotype could provide an invaluable tool to mitigate the damage caused by disorders in which adverse inflammatory processes play a significant role, such as myocardial infarction[220].

As bioencapsulation technologies advance, it is envisioned that these platforms will become a vital tool in biomedical research, with possible applications at all stages of the value chain, from the design of effective disease models for pre-clinical studies, to the generation of large amounts of cells and tissues for clinical application, to the development of novel systems for cell transplantation, delivery of drugs and release of paracrine factors.

2.6. References

1. Jawad H, Ali NN, Lyon AR, Chen QZ, Harding SE, Boccaccini AR. Myocardial tissue engineering: a review. *J Tissue Eng Regen Med*. 2007;1(5):327-342. doi:10.1002/term.46

2. Eng G, Lee BW, Radisic M, Vunjak-Novakovic G. Cardiac Tissue Engineering. In: *Principles of Tissue Engineering*. Elsevier; 2014:771-792. doi:10.1016/B978-0-12-398358-9.00038-0

3. Daar AS, Greenwood HL. A proposed definition of regenerative medicine. *J Tissue Eng Regen Med*. 2007;1(3):179-184. doi:10.1002/term.20

4. Mao AS, Mooney DJ. Regenerative medicine: Current therapies and future directions. *Proc Natl Acad Sci USA*. 2015;112(47):14452-14459. doi:10.1073/pnas.1508520112

5. Bikram M, Fouletier-Dilling C, Hipp JA, et al. Endochondral Bone Formation from Hydrogel Carriers Loaded with BMP2-transduced Cells. *Ann Biomed Eng*. 2007;35(5):796-807. doi:10.1007/s10439-007-9263-4

6. Luo C, Fang H, Zhou M, et al. Biomimetic open porous structured core-shell microtissue with enhanced mechanical properties for bottom-up bone tissue engineering. *Theranostics*. 2019;9(16):4663-4677. doi:10.7150/thno.34464

7. Kim S, Cho AN, Min S, Kim S, Cho SW. Organoids for Advanced Therapeutics and Disease Models. *Adv Therap*. 2019;2(1):1800087. doi:10.1002/adtp.201800087

8. Mazza G, Al-Akkad W, Rombouts K, Pinzani M. Liver tissue engineering: From implantable tissue to whole organ engineering. *Hepatol Commun*. 2018;2(2):131-141. doi:10.1002/hep4.1136

9. Bakry AM, Abbas S, Ali B, et al. Microencapsulation of Oils: A Comprehensive Review of Benefits, Techniques, and Applications. *Compr Rev Food Sci Food Saf*. 2016;15(1):143-182. doi:10.1111/1541-4337.12179

10. Yin J, Qiu S, Shi B, et al. Controlled release of FGF-2 and BMP-2 in tissue engineered periosteum promotes bone repair in rats. *Biomed Mater*. 2018;13(2):025001. doi:10.1088/1748-605X/aa93c0

11. Singh MN, Hemant KSY, Ram M, Shivakumar HG. Microencapsulation: a promising technique for controlled drug delivery. *Res Farm Sci*. 2010;5(2):65-77.

12. Mohan A, Rajendran SRCK, He QS, Bazinet L, Udenigwe CC. Encapsulation of food protein hydrolysates and peptides: a review. *RSC Adv*. 2015;5(97):79270-79278. doi:10.1039/C5RA13419F

13. Yao M, Xie J, Du H, McClements DJ, Xiao H, Li L. Progress in microencapsulation of probiotics: A review. *Compr Rev Food Sci Food Saf*. 2020;19(2):857-874. doi:10.1111/1541-4337.12532

14. Kang A, Park J, Ju J, Jeong GS, Lee SH. Cell encapsulation via microtechnologies. *Biomaterials*. 2014;35(9):2651-2663. doi:10.1016/j.biomaterials.2013.12.073

15. Chang TMS. Semipermeable Microcapsules. *Science*. 1964;146(3643):524-525. doi:10.1126/science.146.3643.524

16. Yang CH, Wang CY, Grumezescu AM, et al. Core-shell structure microcapsules with dual pH-responsive drug release function: General. *Electrophoresis*. 2014;35(18):2673-2680. doi:10.1002/elps.201400210

17. Orive G, Gascón AR, Hernández RM, Igartua M, Luis Pedraz J. Cell microencapsulation technology for biomedical purposes: novel insights and challenges. *Trends Pharmacol Sci*. 2003;24(5):207-210. doi:10.1016/S0165-6147(03)00073-7

18. Majewski RL, Zhang W, Ma X, Cui Z, Ren W, Markel DC. Bioencapsulation technologies in tissue engineering. *J Appl Biomater Func*. 2016;14(4):0-0. doi:10.5301/jabfm.5000299

19. Jenjob R, Phakkeeree T, Crespy D. Core–shell particles for drug-delivery, bioimaging, sensing, and tissue engineering. *Biomater Sci*. 2020;8(10):2756-2770. doi:10.1039/C9BM01872G

20. Freiberg S, Zhu XX. Polymer microspheres for controlled drug release. *Int J Pharm*. 2004;282(1-2):1-18. doi:10.1016/j.ijpharm.2004.04.013

21. Lee KY, Mooney DJ. Alginate: Properties and biomedical applications. *Prog Polym Sci*. 2012;37(1):106-126. doi:10.1016/j.progpolymsci.2011.06.003

22. Majid QA, Fricker ATR, Gregory DA, et al. Natural Biomaterials for Cardiac Tissue Engineering: A Highly Biocompatible Solution. *Front Cardiovasc Med*. 2020;7:554597. doi:10.3389/fcvm.2020.554597

23. Venugopal JR, Prabhakaran MP, Mukherjee S, Ravichandran R, Dan K, Ramakrishna S. Biomaterial strategies for alleviation of myocardial infarction. *J R Soc Interface*. 2012;9(66):1-19. doi:10.1098/rsif.2011.0301

24. Cattelan G, Guerrero Gerbolés A, Foresti R, et al. Alginate Formulations: Current Developments in the Race for Hydrogel-Based Cardiac Regeneration. *Front Bioeng Biotechnol*. 2020;8:414. doi:10.3389/fbioe.2020.00414

25. Wang X. Advanced Polymers for Three-Dimensional (3D) Organ Bioprinting. *Micromachines*. 2019;10(12):814. doi:10.3390/mi10120814

26. Simó G, Fernández-Fernández E, Vila-Crespo J, Ruipérez V, Rodríguez-Nogales JM. Research progress in coating techniques of alginate gel polymer for cell encapsulation. *Carbohydr Polym*. 2017;170:1-14. doi:10.1016/j.carbpol.2017.04.013

27. Bremond N, Santanach-Carreras E, Chu LY, Bibette J. Formation of liquid-core capsules having a thin hydrogel membrane: liquid pearls. *Soft Matter*. 2010;6(11):2484. doi:10.1039/b923783f

28. Abang S, Chan ES, Poncelet D. Effects of process variables on the encapsulation of oil in ca-alginate capsules using an inverse gelation technique. *J Microencapsul*. 2012;29(5):417-428. doi:10.3109/02652048.2012.655331

29. Ben Messaoud G, Sánchez-González L, Probst L, Desobry S. Influence of internal composition on physicochemical properties of alginate aqueous-core capsules. *J Colloid Interface Sci*. 2016;469:120-128. doi:10.1016/j.jcis.2016.02.018

30. Correia CR, Pirraco RP, Cerqueira MT, Marques AP, Reis RL, Mano JF. Semipermeable Capsules Wrapping a Multifunctional and Self-regulated Co-culture Microenvironment for Osteogenic Differentiation. *Sci Rep*. 2016;6(1):21883. doi:10.1038/srep21883

31. Wang X, Wang W, Ma J, Guo X, Yu X, Ma X. Proliferation and Differentiation of Mouse Embryonic Stem Cells in APA Microcapsule: A Model for Studying the Interaction

between Stem Cells and Their Niche. *Biotechnol Prog*. 2006;22(3):791-800. doi:10.1021/bp050386n

32. Lim F, Sun A. Microencapsulated islets as bioartificial endocrine pancreas. *Science*. 1980;210(4472):908-910. doi:10.1126/science.6776628

33. Soon-Shiong P, Heintz RE, Merideth N, et al. Insulin independence in a type 1 diabetic patient after encapsulated islet transplantation. *Lancet*. 1994;343(8903):950-951. doi:10.1016/S0140-6736(94)90067-1

34. Ashimova A, Yegorov S, Negmetzhanov B, Hortelano G. Cell Encapsulation Within Alginate Microcapsules: Immunological Challenges and Outlook. *Front Bioeng Biotechnol*. 2019;7:380. doi:10.3389/fbioe.2019.00380

35. Tam SK, Dusseault J, Polizu S, Ménard M, Hallé JP, Yahia L. Impact of residual contamination on the biofunctional properties of purified alginates used for cell encapsulation. *Biomaterials*. 2006;27(8):1296-1305. doi:10.1016/j.biomaterials.2005.08.027

36. Morra M, Cassineli C. Non-fouling properties of polysaccharide-coated surfaces. *J Biomater Sci Polym Ed*. 1999;10(10):1107-1124. doi:10.1163/156856299X00711

37. Alsberg E, Anderson KW, Albeiruti A, Franceschi RT, Mooney DJ. Cell-interactive Alginate Hydrogels for Bone Tissue Engineering. *J Dent Res*. 2001;80(11):2025-2029. doi:10.1177/00220345010800111501

38. Dhoot NO, Tobias CA, Fischer I, Wheatley MA. Peptide-modified alginate surfaces as a growth permissive substrate for neurite outgrowth. *J Biomed Mater Res*. 2004;71A(2):191-200. doi:10.1002/jbm.a.30103

39. Wang H, Liu H, Liu H, Su W, Chen W, Qin J. One-Step Generation of Core–Shell Gelatin Methacrylate (GelMA) Microgels Using a Droplet Microfluidic System. *Adv Mater Technol*. 2019;4(6):1800632. doi:10.1002/admt.201800632

40. Li Y, Yan D, Fu F, et al. Composite core-shell microparticles from microfluidics for synergistic drug delivery. *Sci China Mater*. 2017;60(6):543-553. doi:10.1007/s40843-016-5151-6

41. Lima AC, Custódio CA, Alvarez-Lorenzo C, Mano JF. Biomimetic Methodology to Produce Polymeric Multilayered Particles for Biotechnological and Biomedical Applications. *Small*. 2013;9(15):2487-2492. doi:10.1002/smll.201202147

42. Shin SR, Zihlmann C, Akbari M, et al. Reduced Graphene Oxide-GelMA Hybrid Hydrogels as Scaffolds for Cardiac Tissue Engineering. *Small*. 2016;12(27):3677-3689. doi:10.1002/smll.201600178

43. Navaei A, Saini H, Christenson W, Sullivan RT, Ros R, Nikkhah M. Gold nanorod-incorporated gelatin-based conductive hydrogels for engineering cardiac tissue constructs. *Acta Biomater*. 2016;41:133-146. doi:10.1016/j.actbio.2016.05.027

44. Xiao S, Zhao T, Wang J, et al. Gelatin Methacrylate (GelMA)-Based Hydrogels for Cell Transplantation: an Effective Strategy for Tissue Engineering. *Stem Cell Rev and Rep*. 2019;15(5):664-679. doi:10.1007/s12015-019-09893-4

45. Yue K, Trujillo-de Santiago G, Alvarez MM, Tamayol A, Annabi N, Khademhosseini A. Synthesis, properties, and biomedical applications of gelatin methacryloyl (GelMA) hydrogels. *Biomaterials*. 2015;73:254-271. doi:10.1016/j.biomaterials.2015.08.045

46. Gomes MC, Costa DCS, Oliveira CS, Mano JF. Design of Protein-Based Liquefied Cell-Laden Capsules with Bioinspired Adhesion for Tissue Engineering. *Adv Healthcare Mater*. 2021;10(19):2100782. doi:10.1002/adhm.202100782

47. Cha C, Oh J, Kim K, et al. Microfluidics-Assisted Fabrication of Gelatin-Silica Core–Shell Microgels for Injectable Tissue Constructs. *Biomacromolecules*. 2014;15(1):283-290. doi:10.1021/bm401533y

48. Wu C, Fan W, Gelinsky M, et al. *In situ* preparation and protein delivery of silicate–alginate composite microspheres with core-shell structure. *J R Soc Interface*. 2011;8(65):1804-1814. doi:10.1098/rsif.2011.0201

49. Cellesi F, Weber W, Fussenegger M, Hubbell JA, Tirelli N. Towards a fully synthetic substitute of alginate: Optimization of a thermal gelation/chemical cross-linking scheme ("tandem" gelation) for the production of beads and liquid-core capsules. *Biotechnol Bioeng*. 2004;88(6):740-749. doi:10.1002/bit.20264

50. Cruise GM, Hegre OD, Lamberti FV, et al. In Vitro and in Vivo Performance of Porcine Islets Encapsulated in Interfacially Photopolymerized Poly(Ethylene Glycol) Diacrylate Membranes. *Cell Transplant*. 1999;8(3):293-306. doi:10.1177/096368979900800310

51. Koh WG, Revzin A, Pishko MV. Poly(ethylene glycol) Hydrogel Microstructures Encapsulating Living Cells. *Langmuir*. 2002;18(7):2459-2462. doi:10.1021/la0115740

52. Lin CC, Metters AT, Anseth KS. Functional PEG–peptide hydrogels to modulate local inflammation inducedby the pro-inflammatory cytokine TNFα. *Biomaterials*. 2009;30(28):4907-4914. doi:10.1016/j.biomaterials.2009.05.083

53. Zhu J. Bioactive modification of poly(ethylene glycol) hydrogels for tissue engineering. *Biomaterials*. 2010;31(17):4639-4656. doi:10.1016/j.biomaterials.2010.02.044

54. Rinker TE, Philbrick BD, Temenoff JS. Core-shell microparticles for protein sequestration and controlled release of a protein-laden core. *Acta Biomater*. 2017;56:91-101. doi:10.1016/j.actbio.2016.12.042

55. Watanabe T, Motohiro I, Ono T. Microfluidic Formation of Hydrogel Microcapsules with a Single Aqueous Core by Spontaneous Cross-Linking in Aqueous Two-Phase System Droplets. *Langmuir*. 2019;35(6):2358-2367. doi:10.1021/acs.langmuir.8b04169

56. Kastania G, Campbell J, Mitford J, Volodkin D. Polyelectrolyte Multilayer Capsule (PEMC)-Based Scaffolds for Tissue Engineering. *Micromachines*. 2020;11(9):797. doi:10.3390/mi11090797

57. Shenoy DB, Antipov AA, Sukhorukov GB, Möhwald H. Layer-by-Layer Engineering of Biocompatible, Decomposable Core−Shell Structures. *Biomacromolecules*. 2003;4(2):265-272. doi:10.1021/bm025661y

58. Facca S, Cortez C, Mendoza-Palomares C, et al. Active multilayered capsules for in vivo bone formation. *Proc Natl Acad Sci USA*. 2010;107(8):3406-3411. doi:10.1073/pnas.0908531107

59. Petrov AI, Volodkin DV, Sukhorukov GB. Protein-Calcium Carbonate Coprecipitation: A Tool for Protein Encapsulation. *Biotechnol Progress*. 2008;21(3):918-925. doi:10.1021/bp0495825

60. Ma M, Chiu A, Sahay G, et al. Core-Shell Hydrogel Microcapsules for Improved Islets Encapsulation. *Adv Healthc Mater*. 2013;2(5):667-672. doi:10.1002/adhm.201200341

61. Hernández RM, Orive G, Murua A, Pedraz JL. Microcapsules and microcarriers for in situ cell delivery. *Adv Drug Deliv Rev*. 2010;62(7-8):711-730. doi:10.1016/j.addr.2010.02.004

62. Mohamed MGA, Ambhorkar P, Samanipour R, Yang A, Ghafoor A, Kim K. Microfluidics-based fabrication of cell-laden microgels. *Biomicrofluidics*. 2020;14(2):021501. doi:10.1063/1.5134060

63. Lu YC, Fu DJ, An D, et al. Scalable Production and Cryostorage of Organoids Using Core-Shell Decoupled Hydrogel Capsules. *Adv Biosys*. 2017;1(12):1700165. doi:10.1002/adbi.201700165

64. Agarwal P, Choi JK, Huang H, et al. A Biomimetic Core-Shell Platform for Miniaturized 3D Cell and Tissue Engineering. *Part Part Syst Charact*. 2015;32(8):809-816. doi:10.1002/ppsc.201500025

65. Chaimov D, Baruch L, Krishtul S, Meivar-levy I, Ferber S, Machluf M. Innovative encapsulation platform based on pancreatic extracellular matrix achieve substantial insulin delivery. *J Control Release*. 2017;257:91-101. doi:10.1016/j.jconrel.2016.07.045

66. Zhao S, Xu Z, Wang H, et al. Bioengineering of injectable encapsulated aggregates of pluripotent stem cells for therapy of myocardial infarction. *Nat Commun*. 2016;7(1):13306. doi:10.1038/ncomms13306

67. Nguyen DK, Son YM, Lee NE. Hydrogel Encapsulation of Cells in Core-Shell Microcapsules for Cell Delivery. *Adv Healthc Mater*. 2015;4(10):1537-1544. doi:10.1002/adhm.201500133

68. Costa NL, Sher P, Mano JF. Liquefied Capsules Coated with Multilayered Polyelectrolyte Films for Cell Immobilization. *Adv Eng Mater*. 2011;13(6):B218-B224. doi:10.1002/adem.201080138

69. Qayyum AS, Jain E, Kolar G, Kim Y, Sell SA, Zustiak SP. Design of electrohydrodynamic sprayed polyethylene glycol hydrogel microspheres for cell encapsulation. *Biofabrication*. 2017;9(2):025019. doi:10.1088/1758-5090/aa703c

70. Zhao S, Agarwal P, Rao W, et al. Coaxial electrospray of liquid core–hydrogel shell microcapsules for encapsulation and miniaturized 3D culture of pluripotent stem cells. *Integr Biol*. 2014;6(9):874-884. doi:10.1039/c4ib00100a

71. Yang XL, Ju XJ, Mu XT, et al. Core–Shell Chitosan Microcapsules for Programmed Sequential Drug Release. *ACS Appl Mater Interfaces*. 2016;8(16):10524-10534. doi:10.1021/acsami.6b01277

72. Guarnido IL, Routh AF, Mantle MD, Serrano MF, Marr PC. Ionic Liquid Microcapsules: Formation and Application of Polystyrene Microcapsules with Ionic Liquid Cores. *ACS Sustainable Chem Eng*. 2019;7(2):1870-1874. doi:10.1021/acssuschemeng.8b05478

73. Barron C, He JQ. Alginate-based microcapsules generated with the coaxial electrospray method for clinical application. *J Biomater Sci Polym Ed*. 2017;28(13):1245-1255. doi:10.1080/09205063.2017.1318030

74. Gryshkov O, Mutsenko V, Tarusin D, et al. Coaxial Alginate Hydrogels: From Self-Assembled 3D Cellular Constructs to Long-Term Storage. *Int J Mol Sci*. 2021;22(6):3096. doi:10.3390/ijms22063096

75. Park J, Choe G, Oh S, Lee JY. *In Situ* Formation of Proangiogenic Mesenchymal Stem Cell Spheroids in Hyaluronic Acid/Alginate Core–Shell Microcapsules. *ACS Biomater Sci Eng*. 2020;6(12):6938-6948. doi:10.1021/acsbiomaterials.0c01489

76. Rodriguez S, Lau H, Corrales N, et al. Characterization of chelator-mediated recovery of pancreatic islets from barium-stabilized alginate microcapsules. *Xenotransplantation*. 2020;27(1). doi:10.1111/xen.12554

77. Young AT, White OC, Daniele MA. Rheological Properties of Coordinated Physical Gelation and Chemical Crosslinking in Gelatin Methacryloyl (GelMA) Hydrogels. *Macromol Biosci*. 2020;20(12):2000183. doi:10.1002/mabi.202000183

78. Sakai S, Ito S, Kawakami K. Calcium alginate microcapsules with spherical liquid cores templated by gelatin microparticles for mass production of multicellular spheroids. *Acta Biomater*. 2010;6(8):3132-3137. doi:10.1016/j.actbio.2010.02.003

79. Chiarugi P, Giannoni E. Anoikis: A necessary death program for anchorage-dependent cells. *Biochem Pharmacol*. 2008;76(11):1352-1364. doi:10.1016/j.bcp.2008.07.023

80. Merten OW. Advances in cell culture: anchorage dependence. *Phil Trans R Soc B*. 2015;370(1661):20140040. doi:10.1098/rstb.2014.0040

81. Stoker M, O'Neill C, Berryman S, Waxman V. Anchorage and growth regulation in normal and virus-transformed cells. *Int J Cancer*. 1968;3(5):683-693. doi:10.1002/ijc.2910030517

82. Correia CR, Sher P, Reis RL, Mano JF. Liquified chitosan–alginate multilayer capsules incorporating poly(L -lactic acid) microparticles as cell carriers. *Soft Matter*. 2013;9(7):2125-2130. doi:10.1039/C2SM26784E

83. Correia CR, Reis RL, Mano JF. Multilayered Hierarchical Capsules Providing Cell Adhesion Sites. *Biomacromolecules*. 2013;14(3):743-751. doi:10.1021/bm301833z

84. Van Wezel AL. Growth of Cell-strains and Primary Cells on Micro-carriers in Homogeneous Culture. *Nature*. 1967;216(5110):64-65. doi:10.1038/216064a0

85. Park JH, Pérez RA, Jin GZ, Choi SJ, Kim HW, Wall IB. Microcarriers Designed for Cell Culture and Tissue Engineering of Bone. *Tissue Eng Part B Rev*. 2013;19(2):172-190. doi:10.1089/ten.teb.2012.0432

86. Martin Y, Eldardiri M, Lawrence-Watt DJ, Sharpe JR. Microcarriers and Their Potential in Tissue Regeneration. *Tissue Eng Part B Rev*. 2011;17(1):71-80. doi:10.1089/ten.teb.2010.0559

87. Wang Y, Yuan X, Yu K, et al. Fabrication of nanofibrous microcarriers mimicking extracellular matrix for functional microtissue formation and cartilage regeneration. *Biomaterials*. 2018;171:118-132. doi:10.1016/j.biomaterials.2018.04.033

88. Tharmalingam T, Sunley K, Spearman M, Butler M. Enhanced Production of Human Recombinant Proteins from CHO cells Grown to High Densities in Macroporous Microcarriers. *Mol Biotechnol*. 2011;49(3):263-276. doi:10.1007/s12033-011-9401-y

89. Gallo–Ramírez LE, Nikolay A, Genzel Y, Reichl U. Bioreactor concepts for cell culture-based viral vaccine production. *Expert Review of Vaccines*. 2015;14(9):1181-1195. doi:10.1586/14760584.2015.1067144

90. Rourou S, van der Ark A, Majoul S, Trabelsi K, van der Velden T, Kallel H. A novel animal-component-free medium for rabies virus production in Vero cells grown on Cytodex 1 microcarriers in a stirred bioreactor. *Appl Microbiol Biotechnol*. 2009;85(1):53-63. doi:10.1007/s00253-009-2064-y

91. Genzel Y, Fischer M, Reichl U. Serum-free influenza virus production avoiding washing steps and medium exchange in large-scale microcarrier culture. *Vaccine*. 2006;24(16):3261-3272. doi:10.1016/j.vaccine.2006.01.019

92. Bodiou V, Moutsatsou P, Post MJ. Microcarriers for Upscaling Cultured Meat Production. *Front Nutr*. 2020;7:10. doi:10.3389/fnut.2020.00010

93. Tavassoli H, Alhosseini SN, Tay A, Chan PPY, Weng Oh SK, Warkiani ME. Large-scale production of stem cells utilizing microcarriers: A biomaterials engineering perspective from academic research to commercialized products. *Biomaterials*. 2018;181:333-346. doi:10.1016/j.biomaterials.2018.07.016

94. Meuwly F, Loviat F, Ruffieux PA, Bernard AR, Kadouri A, von Stockar U. Oxygen supply for CHO cells immobilized on a packed-bed of Fibra-Cel® disks. *Biotechnol Bioeng*. 2006;93(4):791-800. doi:10.1002/bit.20766

95. Oh SKW, Chen AK, Mok Y, et al. Long-term microcarrier suspension cultures of human embryonic stem cells. *Stem Cell Res*. 2009;2(3):219-230. doi:10.1016/j.scr.2009.02.005

96. Zhou Z, Wu W, Fang J, Yin J. Polymer-based porous microcarriers as cell delivery systems for applications in bone and cartilage tissue engineering. *Int Mater Rev*. 2021;66(2):77-113. doi:10.1080/09506608.2020.1724705

97. Shi X, Sun L, Jiang J, Zhang X, Ding W, Gan Z. Biodegradable Polymeric Microcarriers with Controllable Porous Structure for Tissue Engineering. *Macromol Biosci*. 2009;9(12):1211-1218. doi:10.1002/mabi.200900224

98. Nilsson K, Buzsaky F, Mosbach K. Growth of Anchorage–Dependent Cells on Macroporous Microcarriers. *Nat Biotechnol*. 1986;4(11):989-990. doi:10.1038/nbt1186-989

99. Leong W, Wang DA. Cell-laden Polymeric Microspheres for Biomedical Applications. *Trends Biotechnol*. 2015;33(11):653-666. doi:10.1016/j.tibtech.2015.09.003

100. Loh QL, Choong C. Three-Dimensional Scaffolds for Tissue Engineering Applications: Role of Porosity and Pore Size. *Tissue Eng Part B Rev*. 2013;19(6):485-502. doi:10.1089/ten.teb.2012.0437

101. Ornelas-González A, González-González M, Rito-Palomares M. Microcarrier-based stem cell bioprocessing: GMP-grade culture challenges and future trends for regenerative medicine. *Crit Rev Biotechnol*. Published online March 17, 2021. Accessed December 7, 2021. https://www.tandfonline.com/doi/full/10.1080/07388551.2021.1898328

102. Newland B, Ehret F, Hoppe F, et al. Macroporous heparin-based microcarriers allow long-term 3D culture and differentiation of neural precursor cells. *Biomaterials*. 2020;230:119540. doi:10.1016/j.biomaterials.2019.119540

103. Bjørge IM, Choi IS, Correia CR, Mano JF. Nanogrooved microdiscs for bottom-up modulation of osteogenic differentiation. *Nanoscale*. 2019;11(35):16214-16221. doi:10.1039/C9NR06267J

104. Guedes JC, Park JH, Lakhkar NJ, Kim HW, Knowles JC, Wall IB. TiO_2 -doped phosphate glass microcarriers: A stable bioactive substrate for expansion of adherent mammalian cells. *J Biomater Appl*. 2013;28(1):3-11. doi:10.1177/0885328212459093

105. Sopyan I, Mel M, Ramesh S, Khalid KA. Porous hydroxyapatite for artificial bone applications. *Science and Technology of Advanced Materials*. 2007;8(1-2):116-123. doi:10.1016/j.stam.2006.11.017

106. Frauenschuh S, Reichmann E, Ibold Y, Goetz PM, Sittinger M, Ringe J. A Microcarrier-Based Cultivation System for Expansion of Primary Mesenchymal Stem Cells. *Biotechnol Prog*. 2007;23(1):187-193. doi:10.1021/bp060155w

107. Serra M, Brito C, Leite SB, et al. Stirred bioreactors for the expansion of adult pancreatic stem cells. *Ann Anat*. 2009;191(1):104-115. doi:10.1016/j.aanat.2008.09.005

108. Takahashi I, Sato K, Mera H, Wakitani S, Takagi M. Effects of agitation rate on aggregation during beads-to-beads subcultivation of microcarrier culture of human mesenchymal stem cells. *Cytotechnology*. 2017;69(3):503-509. doi:10.1007/s10616-016-9999-5

109. Mizukami A, Fernandes-Platzgummer A, Carmelo JG, et al. Stirred tank bioreactor culture combined with serum-/xenogeneic-free culture medium enables an efficient expansion of umbilical cord-derived mesenchymal stem/stromal cells. *Biotechnol J*. 2016;11(8):1048-1059. doi:10.1002/biot.201500532

110. Zhao D, Yu S, Sun B, Gao S, Guo S, Zhao K. Biomedical Applications of Chitosan and Its Derivative Nanoparticles. *Polymers*. 2018;10(4):462. doi:10.3390/polym10040462

111. Dias CS, Custódio CA, Antunes GC, Telo da Gama MM, Mano JF, Araújo NAM. Modeling of Cell-Mediated Self-Assembled Colloidal Scaffolds. *ACS Appl Mater Interfaces*. 2020;12(43):48321-48328. doi:10.1021/acsami.0c13457

112. Shekaran A, Lam A, Sim E, et al. Biodegradable ECM-coated PCL microcarriers support scalable human early MSC expansion and in vivo bone formation. *Cytotherapy*. 2016;18(10):1332-1344. doi:10.1016/j.jcyt.2016.06.016

113. Correia CR, Gil S, Reis RL, Mano JF. A Closed Chondromimetic Environment within Magnetic-Responsive Liquified Capsules Encapsulating Stem Cells and Collagen II/TGF-β3 Microparticles. *Adv Healthcare Mater*. 2016;5(11):1346-1355. doi:10.1002/adhm.201600034

114. Correia CR, Santos TC, Pirraco RP, et al. In vivo osteogenic differentiation of stem cells inside compartmentalized capsules loaded with co-cultured endothelial cells. *Acta Biomater*. 2017;53:483-494. doi:10.1016/j.actbio.2017.02.007

115. Correia CR, Bjørge IM, Zeng J, Matsusaki M, Mano JF. Liquefied Microcapsules as Dual-Microcarriers for 3D+3D Bottom-Up Tissue Engineering. *Adv Healthcare Mater*. 2019;8(22):1901221. doi:10.1002/adhm.201901221

116. Nadine S, Patrício SG, Barrias CC, et al. Geometrically Controlled Liquefied Capsules for Modular Tissue Engineering Strategies. *Adv Biosys*. 2020;4(11):2000127. doi:10.1002/adbi.202000127

117. Nadine S, Patrício SG, Correia CR, Mano JF. Dynamic microfactories co-encapsulating osteoblastic and adipose-derived stromal cells for the biofabrication of bone units. *Biofabrication*. 2019;12(1):015005. doi:10.1088/1758-5090/ab3e16

118. McEver RP, Zhu C. Rolling Cell Adhesion. *Annu Rev Cell Dev Biol*. 2010;26(1):363-396. doi:10.1146/annurev.cellbio.042308.113238

119. Metwally S, Stachewicz U. Surface potential and charges impact on cell responses on biomaterials interfaces for medical applications. *Mater Sci Eng C*. 2019;104:109883. doi:10.1016/j.msec.2019.109883

120. Silva Couto P, Rotondi MC, Bersenev A, et al. Expansion of human mesenchymal stem/stromal cells (hMSCs) in bioreactors using microcarriers: lessons learnt and what the future holds. *Biotechnology Advances*. 2020;45:107636. doi:10.1016/j.biotechadv.2020.107636

121. Lecina M, Ting S, Choo A, Reuveny S, Oh S. Scalable Platform for Human Embryonic Stem Cell Differentiation to Cardiomyocytes in Suspended Microcarrier Cultures. *Tissue Eng Part C Methods*. 2010;16(6):1609-1619. doi:10.1089/ten.tec.2010.0104

122. Samsudin N, Hashim YZHY, Arifin MA, et al. Optimization of ultraviolet ozone treatment process for improvement of polycaprolactone (PCL) microcarrier performance. *Cytotechnology*. 2017;69(4):601-616. doi:10.1007/s10616-017-0071-x

123. van der Flier A, Sonnenberg A. Function and interactions of integrins. *Cell Tissue Res*. 2001;305(3):285-298. doi:10.1007/s004410100417

124. Zhao J, Santino F, Giacomini D, Gentilucci L. Integrin-Targeting Peptides for the Design of Functional Cell-Responsive Biomaterials. *Biomedicines*. 2020;8(9):307. doi:10.3390/biomedicines8090307

125. Xu Y, Guan J. Biomaterial property-controlled stem cell fates for cardiac regeneration. *Bioact Mater*. 2016;1(1):18-28. doi:10.1016/j.bioactmat.2016.03.002

126. Karimi F, O'Connor AJ, Qiao GG, Heath DE. Integrin Clustering Matters: A Review of Biomaterials Functionalized with Multivalent Integrin-Binding Ligands to Improve Cell Adhesion, Migration, Differentiation, Angiogenesis, and Biomedical Device Integration. *Adv Healthcare Mater*. 2018;7(12):1701324. doi:10.1002/adhm.201701324

127. Custódio CA, Cerqueira MT, Marques AP, Reis RL, Mano JF. Cell selective chitosan microparticles as injectable cell carriers for tissue regeneration. *Biomaterials*. 2015;43:23-31. doi:10.1016/j.biomaterials.2014.11.047

128. Ma J zhong, Liu Y hong, Bao Y, Liu J li, Zhang J. Research advances in polymer emulsion based on "core–shell" structure particle design. *Advances in Colloid and Interface Science*. 2013;197-198:118-131. doi:10.1016/j.cis.2013.04.006

129. Costa AMS, Mano JF. Solvent-Free Strategy Yields Size and Shape-Uniform Capsules. *J Am Chem Soc*. 2017;139(3):1057-1060. doi:10.1021/jacs.6b11925

130. Damiati S, Kompella U, Damiati S, Kodzius R. Microfluidic Devices for Drug Delivery Systems and Drug Screening. *Genes*. 2018;9(2):103. doi:10.3390/genes9020103

131. Barata D, van Blitterswijk C, Habibovic P. High-throughput screening approaches and combinatorial development of biomaterials using microfluidics. *Acta Biomater*. 2016;34:1-20. doi:10.1016/j.actbio.2015.09.009

132. Ma J, Wang Y, Liu J. Biomaterials Meet Microfluidics: From Synthesis Technologies to Biological Applications. *Micromachines*. 2017;8(8):255. doi:10.3390/mi8080255

133. Dendukuri D, Doyle PS. The Synthesis and Assembly of Polymeric Microparticles Using Microfluidics. *Adv Mater*. 2009;21(41):4071-4086. doi:10.1002/adma.200803386

134. Li W, Zhang L, Ge X, et al. Microfluidic fabrication of microparticles for biomedical applications. *Chem Soc Rev*. 2018;47(15):5646-5683. doi:10.1039/C7CS00263G

135. Alessandri K, Feyeux M, Gurchenkov B, et al. A 3D printed microfluidic device for production of functionalized hydrogel microcapsules for culture and differentiation of human Neuronal Stem Cells (hNSC). *Lab Chip*. 2016;16(9):1593-1604. doi:10.1039/C6LC00133E

136. Kim C, Chung S, Kim YE, et al. Generation of core-shell microcapsules with three-dimensional focusing device for efficient formation of cell spheroid. *Lab Chip*. 2011;11(2):246-252. doi:10.1039/C0LC00036A

137. Yu L, Grist SM, Nasseri SS, et al. Core-shell hydrogel beads with extracellular matrix for tumor spheroid formation. *Biomicrofluidics*. 2015;9(2):024118. doi:10.1063/1.4918754

138. Siltanen C, Diakatou M, Lowen J, et al. One step fabrication of hydrogel microcapsules with hollow core for assembly and cultivation of hepatocyte spheroids. *Acta Biomater*. 2017;50:428-436. doi:10.1016/j.actbio.2017.01.010

139. Zhu H, Nawar S, Werner JG, et al. Hydrogel micromotors with catalyst-containing liquid core and shell. *J Phys: Condens Matter*. 2019;31(21):214004. doi:10.1088/1361-648X/ab0822

140. Mastiani M, Seo S, Mosavati B, Kim M. High-Throughput Aqueous Two-Phase System Droplet Generation by Oil-Free Passive Microfluidics. *ACS Omega*. 2018;3(8):9296-9302. doi:10.1021/acsomega.8b01768

141. Agarwal P, Zhao S, Bielecki P, et al. One-step microfluidic generation of pre-hatching embryo-like core–shell microcapsules for miniaturized 3D culture of pluripotent stem cells. *Lab Chip*. 2013;13(23):4525. doi:10.1039/c3lc50678a

142. Jeyhani M, Thevakumaran R, Abbasi N, Hwang DK, Tsai SSH. Microfluidic Generation of All-Aqueous Double and Triple Emulsions. *Small*. 2020;16(7):1906565. doi:10.1002/smll.201906565

143. Dinh ND, Kukumberg M, Nguyen AT, et al. Functional reservoir microcapsules generated *via* microfluidic fabrication for long-term cardiovascular therapeutics. *Lab Chip*. 2020;20(15):2756-2764. doi:10.1039/D0LC00296H

144. Zhu K, Yu Y, Cheng Y, Tian C, Zhao G, Zhao Y. All-Aqueous-Phase Microfluidics for Cell Encapsulation. *ACS Appl Mater Interfaces*. 2019;11(5):4826-4832. doi:10.1021/acsami.8b19234

145. He T, Jokerst JV. Structured micro/nano materials synthesized *via* electrospray: a review. *Biomater Sci*. 2020;8(20):5555-5573. doi:10.1039/D0BM01313G

146. Wang M, Zhao Q. Electrospinning and Electrospray for Biomedical Applications. In: *Encyclopedia of Biomedical Engineering*. Elsevier; 2019:330-344. doi:10.1016/B978-0-12-801238-3.11028-1

147. Morais AÍS, Vieira EG, Afewerki S, et al. Fabrication of Polymeric Microparticles by Electrospray: The Impact of Experimental Parameters. *J Funct Biomater*. 2020;11(1):4. doi:10.3390/jfb11010004

148. Nguyen DN, Clasen C, Van den Mooter G. Pharmaceutical Applications of Electrospraying. *J Pharm Sci*. 2016;105(9):2601-2620. doi:10.1016/j.xphs.2016.04.024

149. Correia CR, Ghasemzadeh-Hasankolaei M, Mano JF. Cell encapsulation in liquified compartments: Protocol optimization and challenges. Hamad-Schifferli K, ed. *PLoS ONE*. 2019;14(6):e0218045. doi:10.1371/journal.pone.0218045

150. Chang MW, Stride E, Edirisinghe M. A New Method for the Preparation of Monoporous Hollow Microspheres. *Langmuir*. 2010;26(7):5115-5121. doi:10.1021/la903592s

151. Moghaddam MK, Mortazavi SM, Khayamian T. Preparation of calcium alginate microcapsules containing n-nonadecane by a melt coaxial electrospray method. *J Electrostat*. 2015;73:56-64. doi:10.1016/j.elstat.2014.10.013

152. Zhang L, Huang J, Si T, Xu RX. Coaxial electrospray of microparticles and nanoparticles for biomedical applications. *Expert Rev Med Devices*. 2012;9(6):595-612. doi:10.1586/erd.12.58

153. Boda SK, Li X, Xie J. Electrospraying an enabling technology for pharmaceutical and biomedical applications: A review. *J Aerosol Sci*. 2018;125:164-181. doi:10.1016/j.jaerosci.2018.04.002

154. Xie J, Jiang J, Davoodi P, Srinivasan MP, Wang CH. Electrohydrodynamic atomization: A two-decade effort to produce and process micro-/nanoparticulate materials. *Chem Eng Sci*. 2015;125:32-57. doi:10.1016/j.ces.2014.08.061

155. Vilabril S, Nadine S, Neves CMSS, et al. One-Step All-Aqueous Interfacial Assembly of Robust Membranes for Long-Term Encapsulation and Culture of Adherent Stem/Stromal Cells. *Adv Healthcare Mater*. 2021;10(10):2100266. doi:10.1002/adhm.202100266

156. Kim W, Kim SS. Multishell Encapsulation Using a Triple Coaxial Electrospray System. *Anal Chem*. 2010;82(11):4644-4647. doi:10.1021/ac100278c

157. Im DJ, Noh J, Yi NW, Park J, Kang IS. Influences of electric field on living cells in a charged water-in-oil droplet under electrophoretic actuation. *Biomicrofluidics*. 2011;5(4):044112. doi:10.1063/1.3665222

158. Strand BL, Gåserød O, Kulseng B, Espevik T, Skjåk-Bræk G. Alginate-polylysine-alginate microcapsules: effect of size reduction on capsule properties. *J Microencapsul*. 2002;19(5):615-630. doi:10.1080/02652040210144243

159. Koch S, Schwinger C, Kressler J, Heinzen Ch, Rainov NG. Alginate encapsulation of genetically engineered mammalian cells: Comparison of production devices, methods and microcapsule characteristics. *J Microencapsul*. 2003;20(3):303-316. doi:10.3109/02652040309178071

160. Yan WC, Tong YW, Wang CH. Coaxial electrohydrodynamic atomization toward large scale production of core-shell structured microparticles. *AIChE J*. 2017;63(12):5303-5319. doi:10.1002/aic.15821

161. Oliveira MB, Hatami J, Mano JF. Coating Strategies Using Layer-by-layer Deposition for Cell Encapsulation. *Chem Asian J*. 2016;11(12):1753-1764. doi:10.1002/asia.201600145

162. Liu T, Wang Y, Zhong W, et al. Biomedical Applications of Layer-by-Layer Self-Assembly for Cell Encapsulation: Current Status and Future Perspectives. *Adv Healthcare Mater*. 2019;8(1):1800939. doi:10.1002/adhm.201800939

163. Zhang P, Bookstaver M, Jewell C. Engineering Cell Surfaces with Polyelectrolyte Materials for Translational Applications. *Polymers*. 2017;9(12):40. doi:10.3390/polym9020040

164. Yow HN, Routh AF. Formation of liquid core–polymer shell microcapsules. *Soft Matter*. 2006;2(11):940-949. doi:10.1039/B606965G

165. Paul A, Ge Y, Prakash S, Shum-Tim D. Microencapsulated stem cells for tissue repairing: implications in cell-based myocardial therapy. *Regen Med*. 2009;4(5):733-745. doi:10.2217/rme.09.43

166. Ding HF, Liu R, Li BG, Lou JR, Dai KR, Tang TT. Biologic effect and immunoisolating behavior of BMP-2 gene-transfected bone marrow-derived mesenchymal stem cells in APA microcapsules. *Biochem Biophys Res Commun*. 2007;362(4):923-927. doi:10.1016/j.bbrc.2007.08.094

167. O'Shea GM, Goosen MFA, Sun AM. Prolonged survival of transplanted islets of Langerhans encapsulated in a biocompatible membrane. *Biochim Biophys Acta Mol Cell Res*. 1984;804(1):133-136. doi:10.1016/0167-4889(84)90107-1

168. Teng Y, Wang Y, Li S, et al. Treatment of Acute Hepatic Failure in Mice by Transplantation of Mixed Microencapsulation of Rat Hepatocytes and Transgenic Human Fetal Liver Stromal Cells. *Tissue Eng Part C Methods*. 2010;16(5):1125-1134. doi:10.1089/ten.tec.2009.0374

169. Zhang H, Zhu SJ, Wang W, Wei YJ, Hu SS. Transplantation of microencapsulated genetically modified xenogeneic cells augments angiogenesis and improves heart function. *Gene Ther*. 2008;15(1):40-48. doi:10.1038/sj.gt.3303049

170. Strand BL, Ryan TL, In't Veld P, et al. Poly-L-Lysine induces fibrosis on alginate microcapsules via the induction of cytokines. *Cell Transplant*. 2001;10(3):263-275.

171. Duvivier-Kali VF, Omer A, Parent RJ, O'Neil JJ, Weir GC. Complete Protection of Islets Against Allorejection and Autoimmunity by a Simple Barium-Alginate Membrane. *Diabetes*. 2001;50(8):1698-1705. doi:10.2337/diabetes.50.8.1698

172. Van Raamsdonk JM, Cornelius RM, Brash JL, Chang PL. Deterioration of polyamino acid-coated alginate microcapsules in vivo. *J Biomater Sci Polym Ed*. 2002;13(8):863-884. doi:10.1163/156856202320401933

173. Zhang W, Zhao S, Rao W, et al. A novel core–shell microcapsule for encapsulation and 3D culture of embryonic stem cells. *J Mater Chem B*. 2013;1(7):1002-1009. doi:10.1039/C2TB00058J

174. Luca G, Calafiore R, Basta G, et al. Improved function of rat islets upon co-microencapsulation with Sertoli's cells in alginate/poly-L-ornithine. *AAPS PharmSciTech*. 2001;2(3):48-54. doi:10.1208/pt020315

175. Lu MZ, Lan HL, Wang FF, Chang SJ, Wang YJ. Cell encapsulation with alginate and alpha-phenoxycinnamylidene-acetylated poly(allylamine). *Biotechnol Bioeng*. 2000;70(5):479-483. doi:10.1002/1097-0290(20001205)70:5<479::aid-bit1>3.0.co;2-e

176. Spasojevic M, Bhujbal S, Paredes G, Haan BJ, Schouten AJ, Vos P. Considerations in binding diblock copolymers on hydrophilic alginate beads for providing an immunoprotective membrane. *J Biomed Mater Res*. 2014;102(6):1887-1896. doi:10.1002/jbm.a.34863

177. Krishnan R, Alexander M, Robles L, Foster CE, Lakey JRT. Islet and Stem Cell Encapsulation for Clinical Transplantation. *Rev Diabet Stud*. 2014;11(1):84-101. doi:10.1900/RDS.2014.11.84

178. Mobasseri M, Shirmohammadi M, Amiri T, Vahed N, Hosseini Fard H, Ghojazadeh M. Prevalence and incidence of type 1 diabetes in the world: a systematic review and meta-analysis. *Health Promot Perspect*. 2020;10(2):98-115. doi:10.34172/hpp.2020.18

179. Norris JM, Johnson RK, Stene LC. Type 1 diabetes—early life origins and changing epidemiology. *Lancet Diabetes Endocrinol*. 2020;8(3):226-238. doi:10.1016/S2213-8587(19)30412-7

180. Yang HK, Ham DS, Park HS, et al. Long-term Efficacy and Biocompatibility of Encapsulated Islet Transplantation With Chitosan-Coated Alginate Capsules in Mice and Canine Models of Diabetes: *Transplantation*. 2016;100(2):334-343. doi:10.1097/TP.0000000000000927

181. Opara EC, Mirmalek-Sani SH, Khanna O, Moya ML, Brey EM. Design of a bioartificial pancreas. *J Investig Med*. 2010;58(7):831-837. doi:10.231/JIM.0b013e3181ed3807

182. Wang T, Lacík I, Brissová M, et al. An encapsulation system for the immunoisolation of pancreatic islets. *Nat Biotechnol*. 1997;15(4):358-362. doi:10.1038/nbt0497-358

183. Davis NE, Beenken-Rothkopf LN, Mirsoian A, et al. Enhanced function of pancreatic islets co-encapsulated with ECM proteins and mesenchymal stromal cells in a silk hydrogel. *Biomaterials*. 2012;33(28):6691-6697. doi:10.1016/j.biomaterials.2012.06.015

184. Kerby A, Jones ES, Jones PM, King AJ. Co-transplantation of islets with mesenchymal stem cells in microcapsules demonstrates graft outcome can be improved in an isolated-graft model of islet transplantation in mice. *Cytotherapy*. 2013;15(2):192-200. doi:10.1016/j.jcyt.2012.10.018

185. Cañibano-Hernández A, Saenz del Burgo L, Espona-Noguera A, et al. Hyaluronic acid enhances cell survival of encapsulated insulin-producing cells in alginate-based microcapsules. *Int J Pharm*. 2019;557:192-198. doi:10.1016/j.ijpharm.2018.12.062

186. Safley SA, Kenyon NS, Berman DM, et al. Microencapsulated adult porcine islets transplanted intraperitoneally in streptozotocin-diabetic non-human primates. *Xenotransplantation*. 2018;25(6):e12450. doi:10.1111/xen.12450

187. Lee S, Park H, Yang Y, et al. Improvement of islet function and survival by integration of perfluorodecalin into microcapsules *in vivo* and *in vitro*. *J Tissue Eng Regen Med*. 2018;12(4):e2110-e2122. doi:10.1002/term.2643

188. Agarwal T, Kazemi S, Costantini M, et al. Oxygen releasing materials: Towards addressing the hypoxia-related issues in tissue engineering. *Mater Sci Eng C*. 2021;122:111896. doi:10.1016/j.msec.2021.111896

189. Pareta R, McQuilling JP, Sittadjody S, et al. Long-Term Function of Islets Encapsulated in a Redesigned Alginate Microcapsule Construct in Omentum Pouches of Immune-Competent Diabetic Rats: *Pancreas*. 2014;43(4):605-613. doi:10.1097/MPA.0000000000000107

190. Richardson TP, Peters MC, Ennett AB, Mooney DJ. Polymeric system for dual growth factor delivery. *Nat Biotechnol*. 2001;19(11):1029-1034. doi:10.1038/nbt1101-1029

191. Yin N, Han Y, Xu H, et al. VEGF-conjugated alginate hydrogel prompt angiogenesis and improve pancreatic islet engraftment and function in type 1 diabetes. *Mater Sci Eng C*. 2016;59:958-964. doi:10.1016/j.msec.2015.11.009

192. McQuilling JP, Arenas-Herrera J, Childers C, et al. New Alginate Microcapsule System for Angiogenic Protein Delivery and Immunoisolation of Islets for Transplantation in the Rat Omentum Pouch. *Transplant Proc*. 2011;43(9):3262-3264. doi:10.1016/j.transproceed.2011.10.030

193. He W, Goodkind D, Kowal P. *An Aging World: 2015*. U.S. Census Bureau; 2016. https://www.census.gov/content/dam/Census/library/publications/2016/demo/p95-16-1.pdf

194. Campana V, Milano G, Pagano E, et al. Bone substitutes in orthopaedic surgery: from basic science to clinical practice. *J Mater Sci: Mater Med*. 2014;25(10):2445-2461. doi:10.1007/s10856-014-5240-2

195. Haugen HJ, Lyngstadaas SP, Rossi F, Perale G. Bone grafts: which is the ideal biomaterial? *J Clin Periodontol*. 2019;46:92-102. doi:10.1111/jcpe.13058

196. Amini AR, Laurencin CT, Nukavarapu SP. Bone tissue engineering: recent advances and challenges. *Crit Rev Biomed Eng*. 2012;40(5):363-408. doi:10.1615/critrevbiomedeng.v40.i5.10

197. Salgado AJ, Coutinho OP, Reis RL. Bone Tissue Engineering: State of the Art and Future Trends. *Macromol Biosci*. 2004;4(8):743-765. doi:10.1002/mabi.200400026

198. Tang D, Tare RS, Yang LY, Williams DF, Ou KL, Oreffo ROC. Biofabrication of bone tissue: approaches, challenges and translation for bone regeneration. *Biomaterials*. 2016;83:363-382. doi:10.1016/j.biomaterials.2016.01.024

199. Kumar Meena L, Rather H, Kedaria D, Vasita R. Polymeric microgels for bone tissue engineering applications – a review. *Int J Polym Mater*. 2020;69(6):381-397. doi:10.1080/00914037.2019.1570512

200. Daviglus ML, Lloyd-Jones DM, Pirzada A. Preventing Cardiovascular Disease in the 21st Century: Therapeutic and Preventive Implications of Current Evidence. *Am J Cardiovasc Drugs*. 2006;6(2):87-101. doi:10.2165/00129784-200606020-00003

201. Virani SS, Alonso A, Benjamin EJ, et al. Heart Disease and Stroke Statistics—2020 Update: A Report From the American Heart Association. *Circulation*. 2020;141(9). doi:10.1161/CIR.0000000000000757

202. Oliveira GBF, Avezum A, Roever L. Cardiovascular Disease Burden: Evolving Knowledge of Risk Factors in Myocardial Infarction and Stroke through Population-Based Research and Perspectives in Global Prevention. *Front Cardiovasc Med*. 2015;2. doi:10.3389/fcvm.2015.00032

203. Wilkins E, Wilson L, Wickramasinghe K, et al. *European Cardiovascular Disease Statistics 2017*.; 2017.

204. Jing D, Parikh A, Tzanakakis ES. Cardiac Cell Generation from Encapsulated Embryonic Stem Cells in Static and Scalable Culture Systems. *Cell Transplant*. 2010;19(11):1397-1412. doi:10.3727/096368910X513955

205. Wang Y, Zhang G, Hou Y, et al. Transplantation of microencapsulated Schwann cells and mesenchymal stem cells augment angiogenesis and improve heart function. *Mol Cell Biochem*. 2012;366(1-2):139-147. doi:10.1007/s11010-012-1291-1

206. Duval K, Grover H, Han LH, et al. Modeling Physiological Events in 2D vs. 3D Cell Culture. *Physiology*. 2017;32(4):266-277. doi:10.1152/physiol.00036.2016

207. Agarwal P, Wang H, Sun M, et al. Microfluidics Enabled Bottom-Up Engineering of 3D Vascularized Tumor for Drug Discovery. *ACS Nano*. 2017;11(7):6691-6702. doi:10.1021/acsnano.7b00824

208. Lu YC, Song W, An D, et al. Designing compartmentalized hydrogel microparticles for cell encapsulation and scalable 3D cell culture. *J Mater Chem B*. 2015;3(3):353-360. doi:10.1039/C4TB01735H

209. Chen Q, Utech S, Chen D, Prodanovic R, Lin JM, Weitz DA. Controlled assembly of heterotypic cells in a core–shell scaffold: organ in a droplet. *Lab Chip*. 2016;16(8):1346-1349. doi:10.1039/C6LC00231E

210. Nadine S, Correia CR, Mano JF. An Immunomodulatory Miniaturized 3D Screening Platform Using Liquefied Capsules. *Adv Healthcare Mater*. 2021;10(10):2001993. doi:10.1002/adhm.202001993

211. Sun Q, Tan SH, Chen Q, et al. Microfluidic Formation of Coculture Tumor Spheroids with Stromal Cells As a Novel 3D Tumor Model for Drug Testing. *ACS Biomater Sci Eng*. 2018;4(12):4425-4433. doi:10.1021/acsbiomaterials.8b00904

212. Yu L, Ni C, Grist SM, Bayly C, Cheung KC. Alginate core-shell beads for simplified three-dimensional tumor spheroid culture and drug screening. *Biomed Microdevices*. 2015;17(2):33. doi:10.1007/s10544-014-9918-5

213. Saberianpour S, Rezaie Nezhad Zamani A, Karimi A, et al. Hollow Alginate-Poly-L-Lysine-Alginate Microspheres Promoted an Epithelial-Mesenchymal Transition in Human Colon Adenocarcinoma Cells. *Adv Pharm Bull*. 2019;10(1):141-145. doi:10.15171/apb.2020.019

214. Alessandri K, Sarangi BR, Gurchenkov VV, et al. Cellular capsules as a tool for multicellular spheroid production and for investigating the mechanics of tumor progression in vitro. *Proc Natl Acad Sci USA*. 2013;110(37):14843-14848. doi:10.1073/pnas.1309482110

215. Rao W, Zhao S, Yu J, Lu X, Zynger DL, He X. Enhanced enrichment of prostate cancer stem-like cells with miniaturized 3D culture in liquid core-hydrogel shell microcapsules. *Biomaterials*. 2014;35(27):7762-7773. doi:10.1016/j.biomaterials.2014.06.011

216. Monteiro CF, Santos SC, Custódio CA, Mano JF. Human Platelet Lysates-Based Hydrogels: A Novel Personalized 3D Platform for Spheroid Invasion Assessment. *Adv Sci*. 2020;7(7):1902398. doi:10.1002/advs.201902398

217. Monteiro CF, Custódio CA, Mano JF. Bioengineering a humanized 3D tri-culture osteosarcoma model to assess tumor invasiveness and therapy response. *Acta Biomater*. Published online July 2021:S1742706121004724. doi:10.1016/j.actbio.2021.07.034

218. Zhang WJ, Lin QX, Zhang Y, et al. The reconstruction of lung alveolus-like structure in collagen-matrigel/microcapsules scaffolds in vitro. *J Cell Mol Med*. 2011;15(9):1878-1886. doi:10.1111/j.1582-4934.2010.01189.x

219. Correia CR, Nadine S, Mano JF. Cell Encapsulation Systems Toward Modular Tissue Regeneration: From Immunoisolation to Multifunctional Devices. *Adv Funct Mater*. 2020;30(26):1908061. doi:10.1002/adfm.201908061

220. Saparov A, Ogay V, Nurgozhin T, et al. Role of the immune system in cardiac tissue damage and repair following myocardial infarction. *Inflamm Res*. 2017;66(9):739-751. doi:10.1007/s00011-017-1060-4

CHAPTER 3

Experimental Section

Chapter 3 – Experimental Section

3.1. Materials

Low viscosity (Sigma-Aldrich, viscosity 5.0-40.0 cP (1%, 25°C)) and medium viscosity (Sigma-Aldrich, viscosity ≥2000 cP (2%, 25°C)) alginate, extracted from brown algae (*Macrocystis pyrifera*), was incorporated into the shell solution in these experiments. Human platelet lysate (STEMCELL Technologies Inc., Vancouver, Canada) from peripheral blood was purchased to produce methacrylated platelet lysates, used in the core solution. Calcium chloride (anhydrous, ≥96.0% purity), EDTA (anhydrous, ≥98.5% purity) and phosphate buffer saline (PBS) tablets were bought from Sigma-Aldrich (MI, USA). Sodium dodecyl sulphate (SDS, 99% purity) was purchased from NZYTech (Lisbon, Portugal). Calcein AM dissolved in dimethyl sulfoxide (DMSO, 1 mg/mL), propidium iodide dissolved in ultrapure water (1 mg/mL) and 4',6-diamidino-2-phenylindole (DAPI) dissolved in ultrapure water (1 mg/mL) were purchased from Thermo Fisher Scientific and phalloidin (Flash Phalloidin™ Red 594, 300U) was purchased from BioLegend.

3.2. Methods

3.2.1. Synthesis of Methacryloyl Platelet Lysate

Methacryloyl platelet lysate was prepared according to a previously published procedure[1]. Briefly, human platelet lysate was thawed at 37 ºC and reacted with methacrylic anhydride containing 2000 ppm of topanol A, 94% (Sigma-Aldrich, USA) in a 100:1 ratio to produce low-degree modification PLMA (PLMA100)). The reaction mixture was kept at room temperature with constant stirring for 4 h. pH was kept between 6 and 8 by using a sodium hydroxide solution (NaOH, 5 M). The PLMA was then purified by dialysis with a 3.5K MWCO, 35 mm dry I.D. SnakeSkin™ dialysis membrane (Thermo Fisher Scientific, USA) against deionized water for 24 h. The solution was then sterilized through a Sartolab™ P20 0.2 µm filter (Sartorius, Germany), frozen with liquid nitrogen, lyophilized in a freeze-dryer (LyoQuest Plus Eco, Telstar, Spain) operating under vacuum at a temperature of –60°C, and stored at 4 ºC until further use.

3.2.2. Generation of PLMA/Alginate core-shell microcapsules

Microcapsules were produced using an electrospray system (Spraybase, Ireland). A coaxial needle (outer nozzle – 20 G; inner nozzle – 26 G) was used to generate PLMA/alginate core-

shell microcapsules. PLMA was dissolved in a 1% (w/v) solution of 2-hydroxy-4'-(2-hydroxyethoxy)-2-methylpropriophenone (Sigma-Aldrich, USA) in PBS to a final concentration of 15% (w/v) of PLMA. This solution was connected to the inner nozzle, while an alginate solution was connected to the outer nozzle. Low viscosity and medium viscosity variants of alginate were used. A 2.5% (w/v) solution of low viscosity alginate was prepared in PBS, as well as 1% (w/v) and 2% (w/v) solutions of medium viscosity alginate. Crosslinking of the outer alginate layer was accomplished by collecting the droplets in 6 mL of a 0.1 M $CaCl_2$ bath with low stirring (300 rpm). Flow rates were controlled using a programmable dual drive syringe pump (Pump 33 DDS, Harvard Apparatus, USA). 10 and 1 mL capacity plastic syringes (Soft-Ject^{TM}, HSW, Germany) were connected to the outer and inner tubes, respectively, using silicone tubing. To produce an electric field, a high-voltage power supply (LNC 30000-2, Heinzinger, Germany) was used. The resulting capsules were observed through a Primo Star optical microscope (Zeiss, Germany) and photographs were taken using an EOS 1200D digital camera (Canon, Japan). Photographs were processed using ImageJ (NIH, USA) software. The diameter of both capsules and cores was calculated as an average of the largest diameter and its lowest perpendicular diameter. The aspect ratio of the capsules and respective cores was calculated by dividing their largest diameter by the lowest perpendicular diameter. At least 20 microcapsules were used in image analysis for each set of parameters. The measurements are expressed as mean ± standard deviation. Additionally, the effect of adding a surfactant to the shell solution on the properties of the microcapsules was evaluated. In this case, a 1% (w/v) solution of medium viscosity alginate containing 0.5 mM of SDS was prepared and placed under magnetic stirring for 5h. A 0.5 mM SDS solution was also prepared and used to produce a 0.1 M $CaCl_2$ collecting bath. This solution was filtered through a 0.2 µm cellulose acetate syringe filter (VWR, Pennsylvania, USA).

3.2.3. Preparation of PLMA microsponges

PLMA/alginate microcapsules were produced through electrohydrodynamic atomization in short intervals, transferred to Petri dishes and immediately placed under a UV lamp (OmniCure S2000, Excelitas Technologies Corp., USA) placed at a height of 10 cm, and subjected to 3 min of UV radiation while employing a radiation intensity of 3 W/cm^2 and using a collimator. The resulting matrix-core microcapsules were collected, the $CaCl_2$

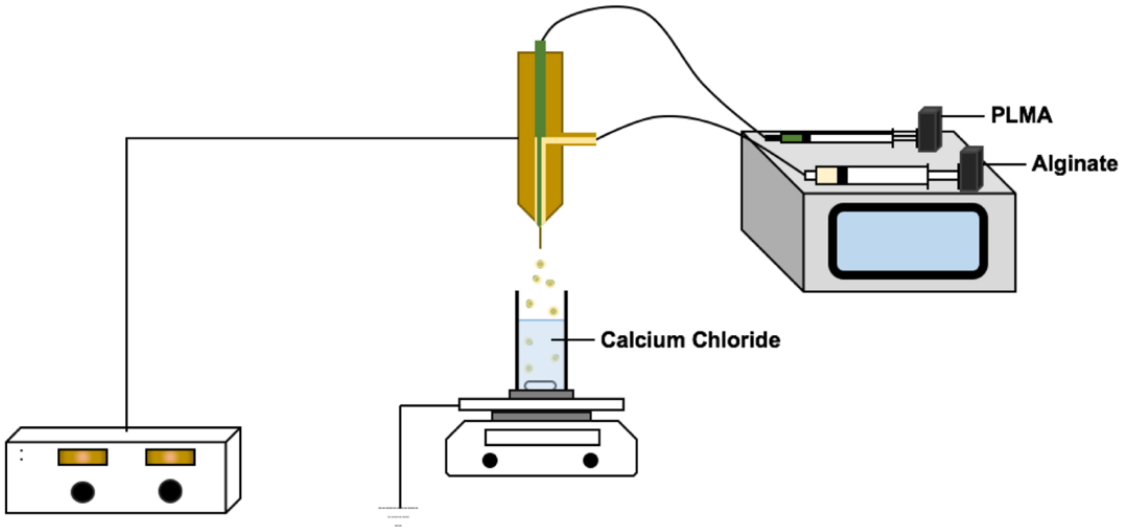

Fig. 3.1. Experimental setup for the coaxial ES equipment used in the production of the initial liquid PLMA core/alginate shell microcapsules.

solution was removed and the microcapsules were washed with a 0.2 M solution of EDTA (pH 7.0, Sigma-Aldrich, USA) for 15 min to remove the alginate shell. EDTA solution was added at a ratio of 1 mL/ 500 µL of microcapsules. The microparticles were then centrifuged at 1000 xg for 5 min at room temperature. After removing the supernatant, EDTA solution was once again added and the microparticles were subjected to a second centrifugation at 1000 xg for 5 min at room temperature. The EDTA was removed, the microparticles were resuspended in distilled water and placed in Mr. Frosty® (Nalgene, Nalge Nunc International, USA) containers, which were stored at -80 °C overnight. The frozen microspheres were then transferred to a freeze-dryer and lyophilized overnight. The resulting microsponges were stored at room temperature for future use.

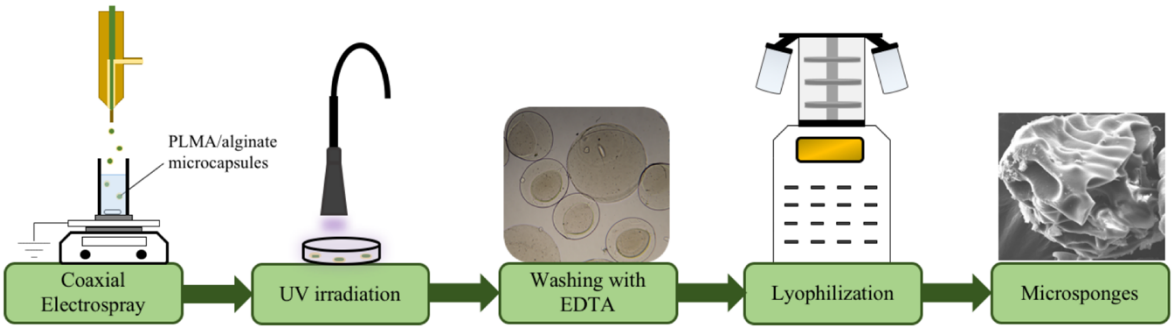

Fig. 3.2. Schematic representation of the workflow employed in microsponge production. Coaxial ES is employed to produce microcapsules, which are immediately subjected to irradiation to crosslink the PLMA and washed with EDTA to remove the shell. PLMA microsponges are obtained after lyophilization.

3.2.4. Cell culture

3.2.4.1. H9c2 (2-1) rat cardiac myoblasts cell culture

H9c2 (2-1) rat cardiac myoblast cells were purchased from Sigma-Aldrich (MA, USA). The cells were grown in high glucose Dulbecco's modified medium (DMEM) supplemented with 10% fetal bovine serum (FBS, Gibco®, Thermo Fisher Scientific) and 1% antibiotic-antimycotic (Gibco®, Thermo Fisher Scientific, containing penicillin, streptomycin and amphotericin B). The cells were cultured in plastic tissue culture flasks, placed in an incubator at 37°C in a humidified atmosphere with 5% CO_2. Upon reaching 70-80% confluence, the cells were trypsinized with TrypLE™ Express Enzyme (Gibco®, Thermo Fisher Scientific) at 37 °C for 5 min, centrifuged at 130 xg for 5 min, counted and re-seeded in a fresh culture flask.

3.2.4.2. Human umbilical vein endothelial cell culture

Human umbilical vein endothelial cells (HUVECs) had previously been isolated from the umbilical cord vein by our group using a well-established procedure[3]. They were grown in M-199 growth medium initially supplemented with 20% fetal bovine serum (FBS, Gibco®, Thermo Fisher Scientific), 1% GlutaMAX™ (Gibco®, Thermo Fisher Scientific) and 1% antibiotic-antimycotic, and further supplemented with sodium heparin (PanReac AppliChem, Barcelona, Spain) and endothelial cell growth supplement (Sigma-Aldrich), extracted from bovine neural tissue. The cells were cultured in plastic flasks and placed in an incubator at 37°C in a humidified atmosphere with 5% CO_2. Upon reaching approximately 80% confluence, cells were enzymatically detached through incubation with trypsin (Gibco®, Thermo Fisher Scientific) at 37 °C for 5 min, followed by centrifugation at 300 xg for 5 min.

3.2.4.3. Human adipose tissue-derived stem cell culture

Human adipose tissue-derived stem cells (hASCs) had previously been isolated from human lipoaspirates by our group through a well-established procedure[2]. Cells were cultured in T75 plastic flasks using α-MEM medium (Gibco®, ThermoFisher Scientific), supplemented with 10% fetal bovine serum (FBS, Gibco®, ThermoFisher Scientific) and 1% antibiotic-antimycotic. The flasks were placed in an incubator at 37°C in a humidified atmosphere with 5% CO_2. Upon reaching approximately 80% confluence, cells were enzymatically detached

through incubation with trypsin (Gibco®, ThermoFisher Scientific) at 37 °C for 5 min, followed by centrifugation at 300 xg for 5 min.

3.2.5. Cell seeding on microsponges

Approximately 250 microsponges were pre-weighed and sterilized through 30 min of UV exposure. They were then transferred to µ-Slide 8-well coverslips (Ibidi, Germany) and resuspended in the appropriate cell culture medium. Cells were then seeded in the microsponge suspension, and the coverslips were placed at 37°C in a humidified atmosphere with 5% CO_2. Medium changes were performed every 2-3 days. H9c2 and hASCs monocultures were seeded on the microsponges at initial cell densities of 50, 100 and 150 cells/microsponge. HUVECs were seeded at an initial cell density of 150 cells/microsponge. H9c2 cells and HUVECs were also co-cultured at a 4:1 ratio (total cell density of 150 cells/microsponge) on the microsponges. In this case, the cell culture medium was a 4:1 mixture of high glucose DMEM and M199 medium. H9c2 cells were also seeded at 50 cells/microsponge on microsponges pre-treated with human platelet lysate (hPL). In this case, hPL was diluted ten-fold in PBS. The microsponges were then transferred to µ-Slide 8-well coverslips and incubated with diluted hPL for 30 min. The hPL was then removed and cell culture medium was added, followed by cell seeding.

3.2.6. Live-Dead assays

To assess the viability of cells seeded on the microsponges, live-dead fluorescence assays were performed. At pre-determined time points, samples were washed 2–3 times with PBS and incubated with 300 µL of calcein AM (Thermo Fisher Scientific, USA) diluted 1:500 in PBS (final concentration: 2 µg/mL) and propidium iodide (Thermo Fisher Scientific, USA) diluted 1:1000 in PBS (final concentration: 1 µg/mL) for 15 min at 37 °C in a humidified atmosphere with 5% CO_2, while protected from light. After washing 2–3 times with PBS, the samples were resuspended in PBS and visualized by fluorescence microscopy (Axio Imager 2, Zeiss, Germany).

3.2.7. Cell morphology analysis

Analysis of cell morphology was performed 14 days after seeding cells on microsponges, through DAPI/phalloidin staining. The cell-laden PLMA microsponges were collected and

fixed at room temperature by incubating the samples in 300 µl of a 4% formaldehyde solution (Sigma-Aldrich, USA) in PBS for at least 2h. Samples were incubated at room temperature in 300 µL of a solution of phalloidin (Flash Phalloidin Red 594, Biolegend, USA) diluted 1:40 in PBS for 45 min and protected from light. The samples were then washed with PBS and incubated in 300 µL of a solution of DAPI (Thermo Fisher Scientific, USA) diluted 1:1000 in PBS for 5 min. After washing with PBS, the constructs were observed using a fluorescence microscope (Axio Imager 2, Zeiss, Germany).

3.2.8. Quantification of cell proliferation

Cell proliferation was evaluated through DNA quantification using a Quant-iT PicoGreen dsDNA kit (Thermo Fisher Scientific, USA). Approximately 500 microsponges were pre-weighed and sterilized before cell seeding, which was performed on 24-well plates for suspension cell culture (Sarstedt, Germany). At pre-determined time points, the cell-laden microsponges were washed with PBS, resuspended in ultrapure water and frozen at -80 ºC. The samples were thawed at 37 ºC and placed in an ultrasound bath for 15 min to disrupt the cells. DNA standards of concentration between 0 and 2 µg/mL were prepared. The samples and standards were incubated for 10 min with PicoGreen reagent diluted by following the manufacturer's instructions. Fluorescence was measured using an excitation wavelength of 480 nm and an emission wavelength of 528 nm (Microplate Reader–Synergy HTX with luminescence, fluorescence and absorbance, Biotek, USA).

3.2.9. Scanning Electron Microscopy (SEM)

SEM was performed in order to assess the morphology and porosity of the microsponges, as well as analyze the structure of the resulting cell-laden constructs. Biological samples were fixed at room temperature in a 4% formaldehyde solution in PBS buffer (pH 7.4) for at least 1h and were then washed twice in PBS (pH 7.4). All samples were dehydrated in water/ethanol mixtures of 25%, 50%, 75%, 95% and 100% ethanol for 1h each. Dehydration in 100% ethanol was performed twice. The samples were then dried in a critical point dryer. The samples were then mounted on aluminum stubs using double-sided tape, sputtered with carbon and visualized by SEM (Hitachi SU-70, Japan). Pore measurement was performed through analysis with ImageJ software.

3.2.10. Statistical analysis

Statistical significance was evaluated using one-way ANOVA with Tukey's post-hoc comparison of the means using GraphPad Prism (Version 8.4.2) software at the significance level of 0.05.

3.3. References

1. Santos SC, Custódio CA, Mano JF. Photopolymerizable Platelet Lysate Hydrogels for Customizable 3D Cell Culture Platforms. *Adv Healthcare Mater*. 2018;7(23):1800849. doi:10.1002/adhm.201800849

2. Zuk PA, Zhu M, Ashjian P, et al. Human Adipose Tissue Is a Source of Multipotent Stem Cells. Raff M, ed. *Mol Biol Cell*. 2002;13(12):4279-4295. doi:10.1091/mbc.e02-02-0105

3. Silva AS, Santos LF, Mendes MC, Mano JF. Multi-layer pre-vascularized magnetic cell sheets for bone regeneration. *Biomaterials*. 2020;231:119664. doi:10.1016/j.biomaterials.2019.119664

CHAPTER 4

Preparation of porous microsponges for the assembly of humanized cardiac microtissues by coaxial electrospray

Chapter 4 – Preparation of porous microsponges for the assembly of humanized cardiac microtissues by coaxial electrospray

Abstract

Human platelet lysate (hPL) has increasingly been incorporated in biomaterial scaffolds and cell culture media as a source of proteins and growth factors. Herein, hPL was chemically modified with photocrosslinkable moieties to produce PLMA, which was encapsulated within alginate microcapsules using coaxial electrospray technology. This system was thoroughly studied in order to determine the effect of production parameters on the properties of the microcapsules. An optimized procedure was used to prepare PLMA microsponges, a tentative base material in the bottom-up assembly of microtissues. The resulting microsponges displayed the ability to support the attachment of different cell lines and promote the assembly of cell-laden three dimensional constructs.

Keywords: Microtissues; Coaxial electrospray; Core-shell capsules; Microsponges; Methacryloyl platelet lysate; Bottom-up assembly

4.1. Introduction

Early tissue engineering and regenerative medicine (TERM) approaches focused on top-down strategies, in which cells were seeded on pre-formed bulk scaffolds. These strategies, however, have displayed limited ability to recreate the properties and architecture of living tissues accurately[1]. More recent approaches have focused on bottom-up methods in which small cell-laden units are used as building blocks in the production of microtissues and other complex 3D structures by modular assembly[2]. The preparation of microtissues can encompass the development of scaffold-free structures such as cell spheroids[3] or cell sheets[4], as well as cell encapsulation and the microfabrication of cell-laden particulate materials[5]. Bottom-up approaches provide greater control over the composition and architecture of bioengineered tissues, producing 3D structures that are able to reproduce cell behavior more faithfully than typical 2D platforms[6]. This facilitates functional integration of the resulting tissues after transplantation, while also producing robust *in vitro* models of disease[7].

Cardiac microtissues that recreate the native microenvironment of heart tissue can provide valuable insight into the pathophysiology of heart disease and potential therapeutic options.

These microtissues have been used to research the effect of mechanical cues on cardiomyocyte behavior[8]; to model different aspects of cardiac disease, such as fibrosis[9], formation of scar tissue[10] and arrhythmia[11]; and to perform cardiotoxicity assays to evaluate the safety of potential drug candidates and environmental pollutants[12–14].

In vivo, cells are surrounded by a complex mixture of macromolecules that comprise the extracellular matrix (ECM), which provides mechanical and biochemical cues that aid in cell differentiation and organization[15,16]. A high fidelity model of heart tissue requires the recreation of the ECM, through the selection and application of suitable biomaterials. Human platelet lysate (hPL) is a remarkable resource that has been incorporated in biomaterial scaffolds for tissue engineering, and which has increasingly been used as a substitute for animal-derived serums in cell culture in order to produce xeno-free formulations for the culture of human cells[17–19]. It is an easily accessible material, which can potentially be used in the development of autologous therapeutic approaches, minimizing risk of rejection and providing a pathway toward the development of personalized medicine approaches. Furthermore, hPL contains a rich cocktail of bioactive molecules that promote tissue regeneration, angiogenesis and immunomodulation, including cytokines, chemokines, microRNAs, growth factors and proteins with recognition sites for cell adhesion[20–22].

Regarding the regeneration of cardiac tissue, hPL has been shown to improve the proliferation and survival of cardiac cells[23,24]. hPL can also be used to produce hydrogels of human origin, which have been shown to promote vasculogenesis and support the formation of a vascular network[25]. Additionally, the injection of platelet-derived gels has been shown to alleviate some of the damage caused by myocardial infarction and improve heart function[26]. However, the poor mechanical properties of gels derived from platelet lysate can render them unsuitable for application in cardiac tissue. Recently, the modification of hPL with photocrosslinkable moieties has been reported, generating methacryloyl platelet lysate (PLMA)[27], a biomaterial that can be photocrosslinked through UV irradiation, producing hydrogels with improved mechanical properties. Additionally, the photopolymerization of PLMA requires low irradiation times and radiation intensities, making it a suitable material for cell encapsulation. PLMA has already been successfully implemented in the development of 3D osteosarcoma models for the high-throughput screening of potential drug candidates[28,29].

In this work, the production of microcapsules with liquid PLMA cores using coaxial electrospray technology was attempted, in order to generate novel platforms for the development and culture of cardiac microtissues. The shell of the microcapsules was produced from alginate, a commonly used biomaterial in the encapsulation of cardiac microtissues[30]. Here, the resulting microcapsules were used as a sacrificial template in the production of porous, human-derived microcarriers, herein referred as PLMA microsponges. These microsponges promoted the short-term attachment of cardiomyoblasts, endothelial cells and stem cells, while displaying the ability to aggregate into larger constructs. It is thus believed that these microsponges display potential as building blocks for the bottom-up assembly of microtissues that can promote the regeneration of heart tissue.

4.2. Experimental Section

4.2.1. Materials

Low viscosity (viscosity 5.0-40.0 cP (1%, 25°C)) and medium viscosity (viscosity ≥2000 cP (2%, 25°C)) alginate were purchased from Sigma-Aldrich (MI, USA). Human platelet lysate (hPL, STEMCELL Technologies Inc., Vancouver, Canada) was purchased to produce PLMA. Calcium chloride (anhydrous, ≥96.0% purity), EDTA (anhydrous, ≥98.5% purity) and phosphate buffer saline (PBS) tablets were bought from Sigma-Aldrich (MI, USA). Sodium dodecyl sulphate (SDS, 99% purity) was purchased from NZYTech (Lisbon, Portugal). Calcein AM dissolved in DMSO (1 mg/mL), propidium iodide dissolved in ultrapure water (1 mg/mL) and DAPI dissolved in ultrapure water (1 mg/mL) were purchased from Thermo Fisher Scientific and phalloidin (Flash Phalloidin™ Red 594, 300U) was purchased from BioLegend (CA, USA).

4.2.2. Methods

4.2.2.1. Synthesis of Methacryloyl Platelet Lysate

Methacryloyl platelet lysate (PLMA) was prepared according to a previously published procedure[27]. Briefly, human platelet lysate was thawed at 37 ºC and reacted with methacrylic anhydride (Sigma-Aldrich, USA) in a 100:1 ratio. The reaction mixture was kept at room temperature with constant stirring for 4 h. pH was kept between 6 and 8. The PLMA was then purified by dialysis with a 3.5K MWCO, 35 mm dry I.D. SnakeSkin™ dialysis membrane (Thermo Fisher Scientific, USA) against deionized water for 24 h. The solution

was then sterilized through a Sartolab^{TM} P20 0.2 µm filter (Sartorius, Germany), frozen with liquid nitrogen, lyophilized in a freeze-dryer (LyoQuest Plus Eco, Telstar, Spain) operating under vacuum at a temperature of –60°C, and stored at 4 ºC until further use.

4.2.2.2. Generation of PLMA/Alginate core-shell microcapsules

Microcapsules were produced using an electrospray system (Spraybase, Ireland). A coaxial needle (outer nozzle – 20 G; inner nozzle – 26 G) was used to generate PLMA/alginate core-shell microcapsules. PLMA was dissolved in a 1% (w/v) solution of 2-hydroxy-4'-(2-hydroxyethoxy)-2-methylpropriophenone (Sigma-Aldrich, USA) in PBS to a final concentration of 15% (w/v) of PLMA. This solution was connected to the inner nozzle, while an alginate solution was connected to the outer nozzle. Low viscosity and medium viscosity variants of alginate were used. The droplets were collected in a 0.1 M $CaCl_2$ bath with low stirring. Flow rates were controlled using a programmable dual drive syringe pump (Pump 33 DDS, Harvard Apparatus, USA). To produce an electric field, a high-voltage power supply (LNC 30000-2, Heinzinger, Germany) was used. The resulting capsules were observed through a Primo Star optical microscope (Zeiss, Germany) and photographs were taken using an EOS 1200D digital camera (Canon, Japan). Photographs were processed using ImageJ (NIH, USA) software. The diameter of both capsules and cores was calculated as an average of the largest diameter and its lowest perpendicular diameter. The aspect ratio of the capsules and respective cores was calculated by dividing their largest diameter by the lowest perpendicular diameter. At least 20 microcapsules were used in image analysis for each set of parameters. The measurements are expressed as mean ± standard deviation. The effect of adding a surfactant to the shell solution on the properties of the microcapsules was evaluated. In this case, a 1% (w/v) solution of medium viscosity alginate containing 0.5 mM of SDS was prepared. A 0.5 mM SDS solution was also prepared and used to produce a 0.1 M $CaCl_2$ collecting bath. This solution was filtered through a 0.2 µm cellulose acetate syringe filter (VWR, Pennsylvania, USA).

4.2.2.3. Preparation of PLMA microsponges

PLMA/alginate microcapsules were subjected to 3 min of irradiation under a UV lamp (OmniCure S2000, Excelitas Technologies Corp., USA) placed at a height of 10 cm, employing a radiation intensity of 3 W/cm^2 while using a collimator. The resulting

microcapsules were collected and washed with a 0.2 M solution of EDTA (pH 7.0, Sigma-Aldrich, USA) for 15 min. The particles were then centrifuged at 1000 xg for 5 min at room temperature. After removing the supernatant, the microparticles were once again washed with the EDTA solution and subjected to a second centrifugation at 1000 xg for 5 min at room temperature. The EDTA was removed and the microparticles were resuspended in distilled water and placed in Mr. Frosty® (Nalgene, Nalge Nunc International, USA) containers, which were stored at -80 °C overnight. The frozen microspheres were then transferred to a freeze-dryer and lyophilized overnight. The resulting microsponges were stored at room temperature for future use.

4.2.2.4. Cell culture

4.2.2.4.1. H9c2 (2-1) rat cardiac myoblasts cell culture

H9c2 (2-1) rat cardiac myoblast cells were purchased from Sigma-Aldrich (MA, USA). The cells were grown in high glucose Dulbecco's modified medium (DMEM) supplemented with 10% fetal bovine serum (FBS, Gibco®, Thermo Fisher Scientific) and 1% antibiotic-antimycotic. The cells were cultured in plastic tissue culture flasks, placed in an incubator at 37°C in a humidified atmosphere with 5% CO_2.

4.2.2.4.2. Human umbilical vein endothelial cell culture

Human umbilical vein endothelial cells (HUVECs) had previously been isolated from the umbilical cord vein by our group using a well-established procedure[31]. They were grown in M-199 growth medium initially supplemented with 20% fetal bovine serum (FBS, Gibco®, Thermo Fisher Scientific), 1% GlutaMAX™ (Gibco®, Thermo Fisher Scientific) and 1% antibiotic-antimycotic, and further supplemented with sodium heparin (PanReac AppliChem, Barcelona, Spain) and endothelial cell growth supplement (Sigma-Aldrich), extracted from bovine neural tissue. The cells were cultured in plastic flasks and placed in an incubator at 37°C in a humidified atmosphere with 5% CO_2.

4.2.2.4.3. Human adipose tissue-derived stem cell culture

Human adipose tissue-derived stem cells (hASCs) had previously been isolated from human lipoaspirates by our group through a well-established procedure[32]. Cells were cultured in T75 plastic flasks using α-MEM medium (Gibco®, ThermoFisher Scientific),

supplemented with 10% fetal bovine serum (FBS, Gibco®, ThermoFisher Scientific) and 1% antibiotic-antimycotic. The flasks were placed in an incubator at 37°C in a humidified atmosphere with 5% CO_2.

4.2.2.5. Cell culture on microsponges

Microsponges were pre-weighed and sterilized by 30 min of UV exposure. They were then transferred to µ-Slide 8-well coverslips (Ibidi, Germany) and resuspended in cell culture medium. Cells were then seeded onto the microsponges, and the coverslips were placed at 37°C in a humidified atmosphere with 5% CO_2. Medium changes were performed every 2-3 days. hASCs, H9c2 cells and HUVECs were seeded onto the microsponges in monoculture. Additionally, H9c2 cells and HUVECs were co-cultured onto the microsponges. In some assays, the microsponges were pre-coated with PL before seeding. In this case, the microsponges were first resuspended in hPL 10-fold diluted in PBS for 30 min. The hPL was then removed, cell culture medium was added and cells were seeded.

4.2.2.6. Live-Dead assays

To assess the viability of cells seeded on the microsponges, live-dead fluorescence assays were performed. Samples were washed 2–3 times with PBS and stained with calcein (Thermo Fisher Scientific, USA) diluted 1:500 in PBS and propidium iodide (Thermo Fisher Scientific diluted 1:1000 in PBS for 15 min and protected from light. After washing 2–3 times with PBS, the samples were resuspended in PBS and visualized by fluorescence microscopy (Axio Imager 2, Zeiss, Germany).

4.2.2.7. Cell morphology analysis

Analysis of cell morphology was performed 14 days after seeding cells on microsponges, through DAPI/phalloidin staining. The cell-laden PLMA microsponges were fixed using a 4% formaldehyde solution (Sigma-Aldrich, USA) in PBS for at least 2h. Samples were incubated at room temperature in a solution of phalloidin (Flash Phalloidin Red 594, Biolegend, USA) diluted 1:40 in PBS for 45 min. The samples were then washed with PBS and incubated in a solution of DAPI (Thermo Fisher Scientific, USA) diluted 1:1000 in PBS for 5 min. After washing with PBS, the constructs were observed using a fluorescence microscope (Axio Imager 2, Zeiss, Germany).

4.2.2.8. Quantification of cell proliferation

Cell proliferation was evaluated through DNA quantification using a Quant-iT PicoGreen dsDNA kit (Thermo Fisher Scientific, USA). At pre-determined time points, the cell-laden microsponges were washed with PBS, resuspended in ultrapure water and frozen at -80 ºC. In order to perform the DNA quantification assay, the samples were thawed at 37 ºC and placed in an ultrasound bath for 15 min to disrupt the cells. DNA standards of concentration between 0 and 2 µg/mL were prepared. The samples and standards were incubated with the PicoGreen reagent for 10 min in the dark. Fluorescence was measured using an excitation wavelength of 480 nm and an emission wavelength of 528 nm (Microplate Reader–Synergy HTX with luminescence, fluorescence and absorbance, Biotek, USA).

4.2.2.9. Scanning Electron Microscopy

Scanning Electron Microscopy (SEM) was performed in order to assess the morphology and porosity of the microsponges, as well as analyze the structure of the cell-laden constructs. Biological samples were fixed in a 4% formaldehyde solution in PBS buffer (pH 7.4) for at least 1 h and were then washed twice in PBS (pH 7.4). All samples were dehydrated in water/ethanol mixtures of 25%, 50%, 75%, 95% and 100% ethanol for 1h each. Dehydration in 100% ethanol was performed twice. The samples were then dried in a critical point dryer, mounted on aluminum stubs, sputtered with carbon and visualized by SEM (Hitachi SU-70, Japan). Pore measurement was performed through analysis with ImageJ software.

4.2.2.10. Statistical analysis

Statistical significance was evaluated using one-way ANOVA with Tukey's post-hoc comparison of the means using GraphPad Prism (Version 8.4.2) software at the significance level of 0.05.

4.3. Results and discussion

4.3.1. Influence of production parameters on microcapsule properties

Coaxial electrospray is a microfabrication technique that depends on many parameters, including the properties of both core and shell solutions, their respective flow rates and the strength of the applied electric field. By modifying these parameters, it is possible to

modulate the properties of the obtained capsules, such as their dimensions and morphology. To ensure adequate cell proliferation, the dimensions of the microsponges should approximate those of previously reported microcarriers (diameters in the 100–500 μm range)[33] in order to ensure appropriate diffusion of oxygen and nutrients throughout their inner architecture. Deviations from spherical morphology were evaluated by measuring the aspect ratio of the capsules and respective cores. To optimize this system, the influence of different parameters on the characteristics of the PLMA/alginate core-shell microcapsules was evaluated, including alginate concentration, applied voltage, tip to collector distance, solution flow rate and the addition of a surfactant to the shell solution. A complete description of the average dimensions of the microcapsules for each parameter has been provided in Supplementary Table S4.1-3.

4.3.1.1. Alginate solution

The concentration and viscosity of the core and shell solutions have a significant influence on the morphology of the capsules. Commercially available alginate can differ in its molecular weight, mannuronic acid/gulluronic acid ratio and viscosity. Both low viscosity and medium viscosity alginates were used in this experiment. A low viscosity alginate solution was prepared at a 2.5% (w/v) concentration, while medium viscosity alginate solutions were prepared at 1 and 2% (w/v) concentrations. Low viscosity alginate was only able to produce amorphous particles or capsules with tear-like shape (Figure 4.1A). By switching to a medium viscosity alginate solution, it was possible to obtain round capsules (Figure 4.1B). In order to produce spherical capsules, the 1% alginate solution is preferred, as higher concentrations produced capsules with an elongated morphology (Figure 4.1C).

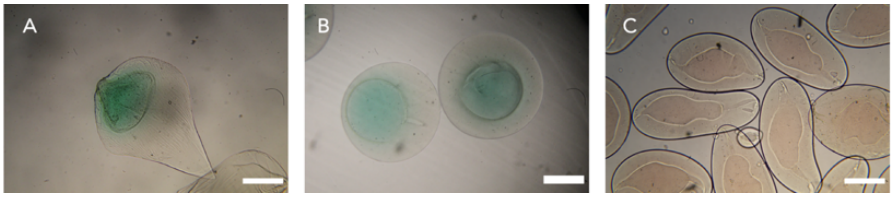

Fig. 4.1. Influence of alginate concentration and viscosity on capsule morphology. Solutions used in the generation of microcapsules were (A) a 2.5% (w/v) solution of low viscosity alginate; (B) a 1% (w/v) solution of medium viscosity alginate; (C) a 2% (w/v) solution of medium viscosity alginate. Other production parameters include an alginate flow rate of 40 mL/h, PLMA flow rate of 5 mL/h, applied voltage of 14 kV, TTC distance of 7 cm and the use of magnetic stirring with a speed of 300 rpm. Commercial food coloring was added to the PLMA solution to facilitate visualization of the cores. Scale bars represent 500 μm.

4.3.1.2. Influence of the strength of the applied electrical field

In electrospray, an electric field is applied in order to produce a spray of charged droplets with reduced dimensions. The strength of the electrical field depends on the applied voltage and the distance between the tip of the coaxial nozzle and the collector (TTC distance). The effect of the applied voltage has been displayed on Figure 4.2.

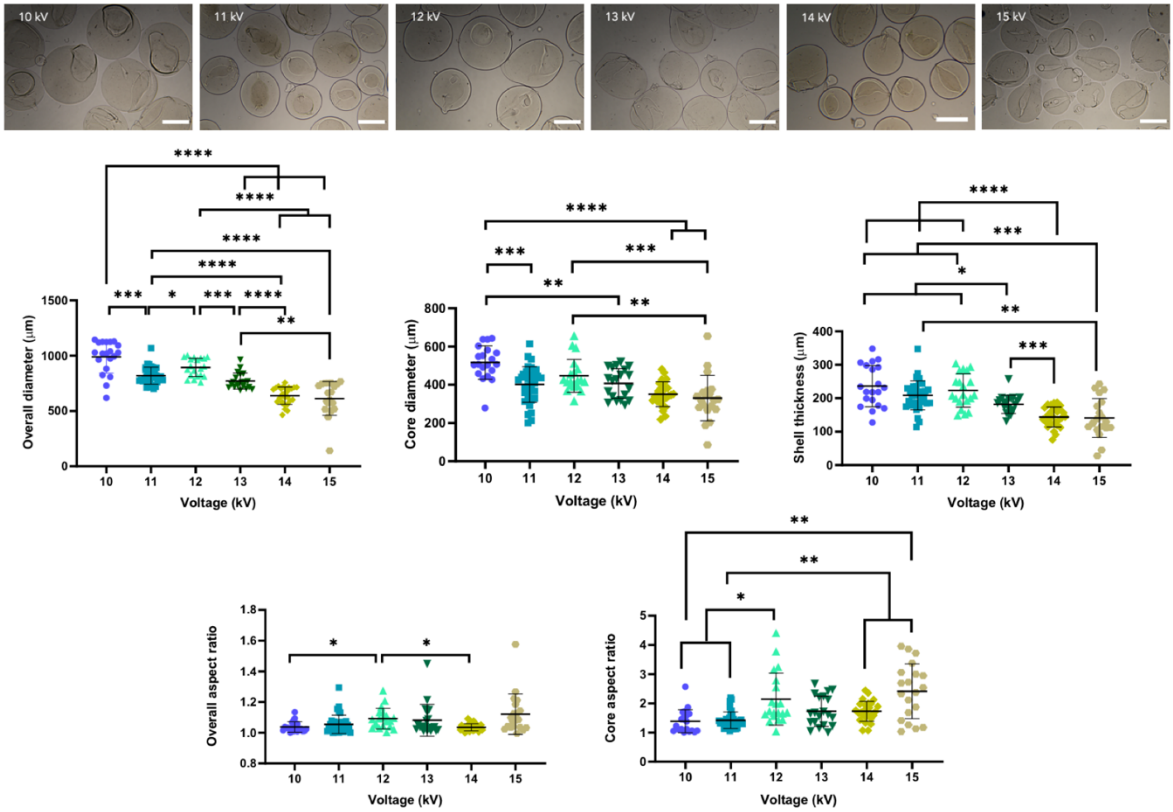

Fig. 4.2. Influence of applied voltage on the properties of microcapsule cores. The diameter and aspect ratio of the cores was evaluated using ImageJ software. Significant differences are marked with $^{*}p<0.05$, $^{**}p<0.01$, $^{***}p<0.001$ and $^{****}p<0.0001$. Other production parameters include an alginate flow rate of 15 mL/h, PLMA flow rate of 1 mL/h, TTC distance of 5 cm and the use of magnetic stirring with a speed of 300 rpm. Scale bars represent 500 µm.

The average total diameter of the capsules ranged from 989 ± 147 µm at 10 kV to 613 ± 153 µm at 15 kV, while the diameter of the cores ranged from 517 ± 87 µm to 330 ± 119 µm, respectively. In general, a reduction in core diameter, capsule diameter and shell thickness can be observed as the applied voltage increases. On the other hand, the aspect ratio of the cores ranged from 1.39 ± 0.40 to 2.41 ± 0.94, indicating that higher voltages compromise the morphology of the microcapsules. In fact, voltages of 12 kV or above produced

microcapsules with non-spherical cores. While the capsules with the lowest core diameter were obtained at 15 kV, the dimensions of the cores presented high variability, their morphology was not spherical, and many capsules were damaged. As such, it would not be suitable to employ applied voltages of 15 kV or above to produce PLMA/alginate core-shell capsules.

The effect of the TTC distance on the microcapsule characteristics has been shown on Figure 4.3. At a TTC distance of 4 cm, the production process was unstable, leading to the production of enlarged microcapsules in which PLMA cores were not visible, indicating that encapsulation of the PLMA may have been unsuccessful. When the TTC distance was increased to 5, 6 and 7 cm, the diameter of the obtained capsules was 819 ± 76 cm, 828 ± 106 and 838 ± 108 µm. Similarly, core dimensions were 402 ± 93, 463 ± 98 and 478 ± 76 µm, respectively, with aspect ratios of 1.42 ± 0.28, 1.54 ± 0.54 and 1.44 ± 0.33.

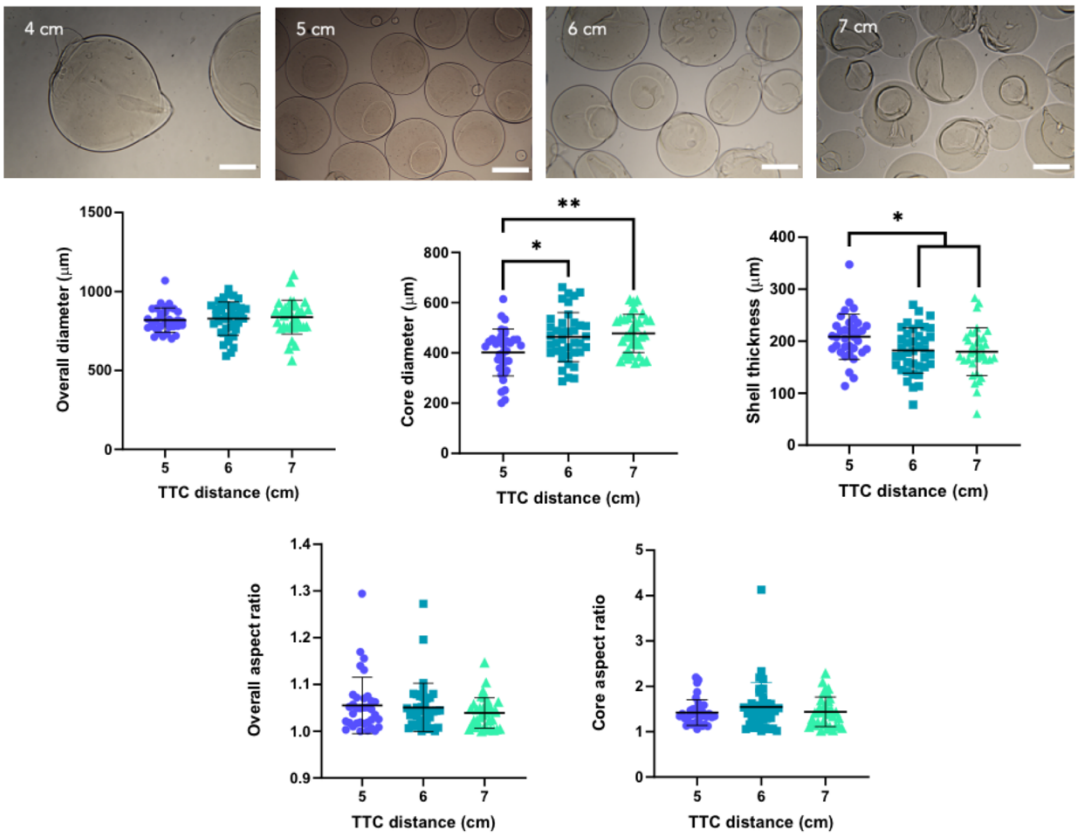

Fig. 4.3. Influence of TTC distance on the properties of microcapsule cores. The diameter and aspect ratio of the cores was evaluated using ImageJ software. Significant differences are marked with $^{*}p<0.05$, $^{**}p<0.01$, $^{***}p<0.001$ and $^{****}p<0.0001$. Other production parameters include an alginate flow rate of 15 mL/h, PLMA flow rate of 1 mL/h, applied voltage of 11 kV and the use of magnetic stirring with a speed of 300 rpm. Scale bars represent 500 µm.

Analyzing these values, it appears that TTC distance has only a slight influence on capsule properties. Nevertheless, a as the TTC distance decreases, the dimensions of the core are also reduced.

As the TTC distance decreases, the strength of the applied electrical field increases. As such, these experiments have shown that it is possible to produce smaller microcapsules with lower core diameter by increasing the strength of the electric field, either by increasing the applied voltage or decreasing the TTC distance, which is in accordance with previous reports[34].

4.3.1.3. Influence of core and shell solution flow rates

In coaxial electrospray, the flow rate of both the core and shell solutions, as well as the ratio between them, are all parameters that play a vital role in determining the characteristics of the microcapsules. Initially, the influence of the alginate solution flow rate:PLMA solution flow rate ratio was investigated (Figure 4.4).

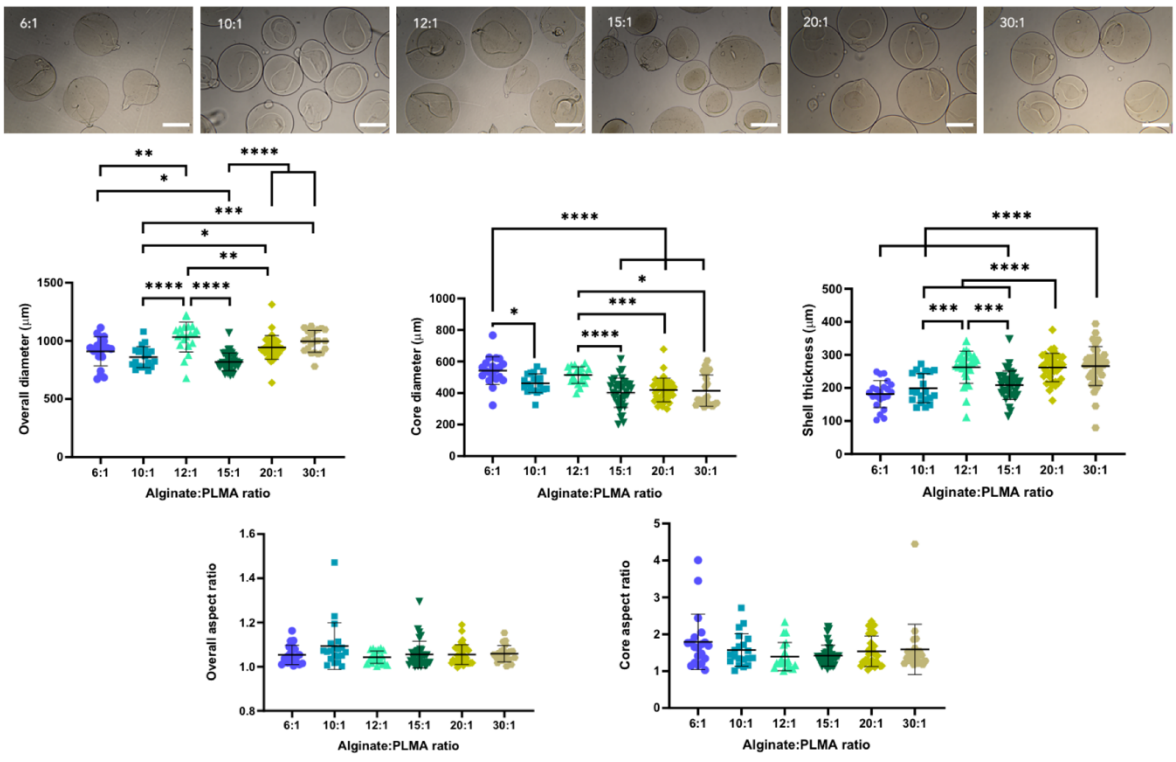

Fig. 4.4. Influence of the ratio between the flow rate of the alginate solution (in mL/h) and the flow rate of the PLMA solution (in mL/h) on the properties of microcapsule cores. The diameter and aspect ratio of the cores was evaluated using ImageJ software. Significant differences are marked with $^{*}p<0.05$, $^{**}p<0.01$, $^{***}p<0.001$ and $^{****}p<0.0001$. Other production parameters include an applied voltage of 11 kV, TTC distance of 5 cm and the use of magnetic stirring with a speed of 300 rpm. Scale bars represent 500 µm.

The PLMA flow rate was kept constant at 1 mL/h while the alginate flow rate was allowed to change, producing different flow rate ratios. Six different ratios were tested, 6:1, 10:1, 12:1, 15:1, 20:1 and 30:1, which produced capsules with diameters of 907 ± 121, 860 ± 90, 1043 ± 115, 819 ± 76, 943 ± 102 and 946 ± 110 µm, respectively. These values show that the ratio between the flow rates appears to have only a slight effect on the diameter of the capsules, which is in accordance with previously reported results[35]. Regarding the dimensions of the cores, the average diameters ranged between 544 ± 88, when the ratio between flow rates was 6:1, to 402 ± 93, when the flow rate was 15:1. Flow rate ratios of 15:1 and above produced capsules with reduced core diameter, which is also in accordance with previous studies[35]. A flow rate ratio of 15:1 produced microcapsules with average core diameters approaching 400 µm, which falls under the size range of commercially available microcarriers. As such, this ratio was selected for further studies on the influence of the flow rate, which has been shown in Figure 4.5.

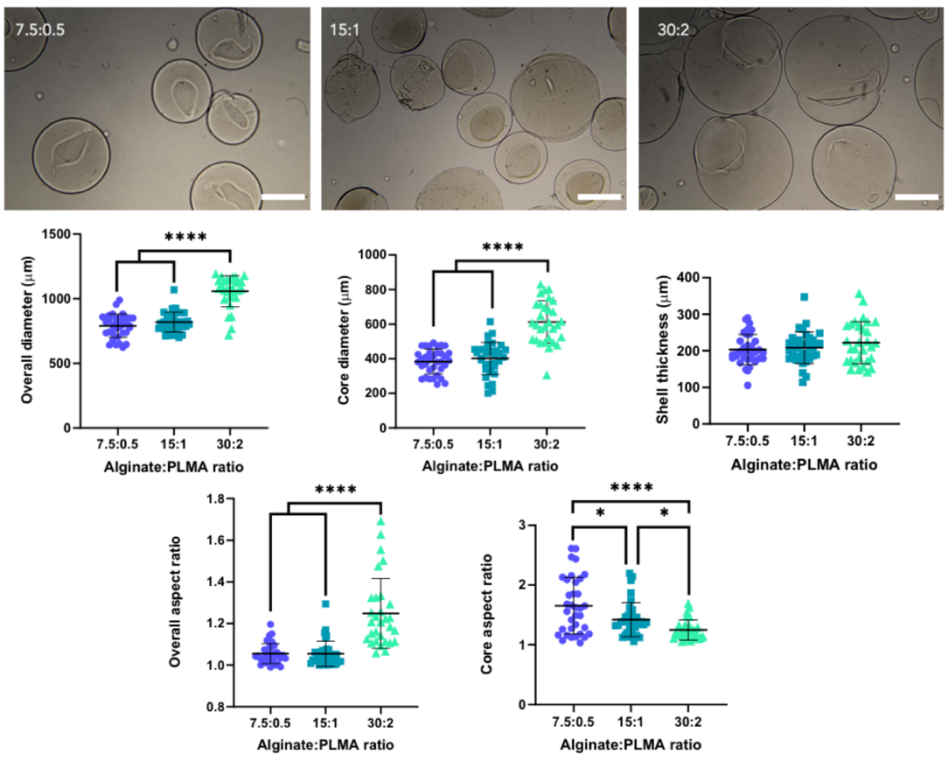

Fig. 4.5. Influence of the solution flow rates (in mL/h) on the properties of microcapsule cores. The diameter and aspect ratio of the cores was evaluated using ImageJ software. Other production parameters include an applied voltage of 11 kV, TTC distance of 5 cm and the use of magnetic stirring with a speed of 300 rpm. Significant differences are marked with $^{*}p<0.05$, $^{**}p<0.01$, $^{***}p<0.001$ and $^{****}p<0.0001$. Scale bars represent 500 µm.

Decreasing both flow rates to a 7.5:0.5 ratio lowered the average diameter of the microcapsules to 790 ± 89, while increasing the flow rates to a ratio of 30:2 also increased the average diameter of the microcapsules to 1058 ± 120. The microcapsules contain liquid PLMA cores with average diameters of 384 ± 71, 402 ± 93 and 613 ± 123 μm, as well as aspect ratios of 1.65 ± 0.47, 1.42 ± 0.28 and 1.25 ± 0.17, indicating that there is a trade-off between lower core dimensions and lower aspect ratio. While a flow rate ratio of 7.5:0.5 produced a slight decrease on average core diameter when compared to the flow rate ratio of 15:1, the cores were elongated and presented a tear-like morphology, and were thus deemed less suitable for microsponge production or cell encapsulation.

4.3.1.4. Influence of the addition of a surfactant

The addition of a surfactant, such as sodium dodecyl sulfate (SDS), to an alginate solution has previously been reported to allow the generation of capsules with thin shells for the encapsulation of different liquids[36]. This is of vital importance in cell encapsulation, as the prevalence of hypoxic conditions within capsules has been cited as a critical factor in the failure of capsule-based systems for clinical application[34,37]. When studying the influence of the other parameters, the average thickness of the shell often exceeded 200 μm, which has been reported as the maximum distance between blood vessels and cells that guarantees proper diffusion of nutrients and oxygen[38]. Voltages above 14 kV were able to produce capsules with shell thickness approaching 140 μm, however, high voltages also result in deformation of the core morphology and could compromise cell viability. The incorporation of a reduced concentration of surfactant in both the alginate solution and collection bath should thus decrease shell thickness without compromising cell proliferation within the capsules[39].

By incorporating 0.5 mM of SDS within the alginate solution and 0.5 mM of SDS in the $CaCl_2$ bath, it was possible to obtain capsules with thin shells, whose average thickness does not exceed 100 μm, displayed in Figure 4.6.

The microcapsules displayed an average shell thickness of 86 ± 17 μm, much lower than what could be achieved without a surfactant. The microcapsules also presented a spherical shape, with quasi-spherical cores, as evidenced by an aspect ratio of 1.06 ± 0.05 for the microcapsules and 1.27 ± 0.15 for the cores, thus preserving the morphology of the capsules. While this reduction in shell thickness is not necessarily relevant for the purposes of

microsponge production, it paves the way toward the future encapsulation of cells and other cellular constructs within the microcapsules.

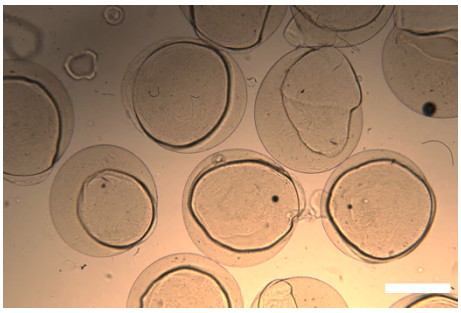

Fig. 4.6. Microcapsules produced after the addition of SDS to the alginate and $CaCl_2$ solutions. Production parameters were an alginate flow rate of 8 mL/h, PLMA flow rate of 1.5 mL/h, applied voltage of 12 kV, TTC distance of 7 cm and the use of magnetic stirring with a speed of 200 rpm. Scale bar represents 500 µm.

4.3.2. Production of PLMA microsponges

To obtain the microsponges, a photoinitiator was included in the PLMA solution in order to allow the photopolymerization reaction to occur. Microcapsules were subjected to UV irradiation immediately after preparation, in order to minimize diffusion of the photoinitiator toward the surrounding $CaCl_2$ bath. After irradiation, the $CaCl_2$ solution was removed, and the capsules were incubated in a solution of EDTA, a chelating agent that removes the Ca^{2+} ions, resulting in dissolution of the alginate shells. The EDTA solution and the alginate were removed after centrifugation, and the resulting PLMA microspheres were collected in distilled water, frozen to -80°C at a rate of 1°C/min and freeze-dried in order to produce a porous structure. The purpose of producing this porous structure is to maximize the available surface area for cell proliferation in order to produce a minimalist scaffold that supports cell growth and the bottom-up assembly of microtissues[40,41].

Different sets of parameters were used to produce the initial microcapsules. The size distributions of the final microsponges have been presented in Figure 4.7. As expected, the production parameters influence the final dimensions of the microsponges just as they influence the core dimensions of the initial microcapsules. Increasing the applied voltage results in a reduction of the dimensions of both the microcapsules and the resulting microsponges. By contrast, increasing the flow rate of the PLMA solution results in an increase of the microsponge dimensions, while increasing the flow rate of the alginate solution restrains the dimensions of the PLMA core, thus resulting in smaller microsponges.

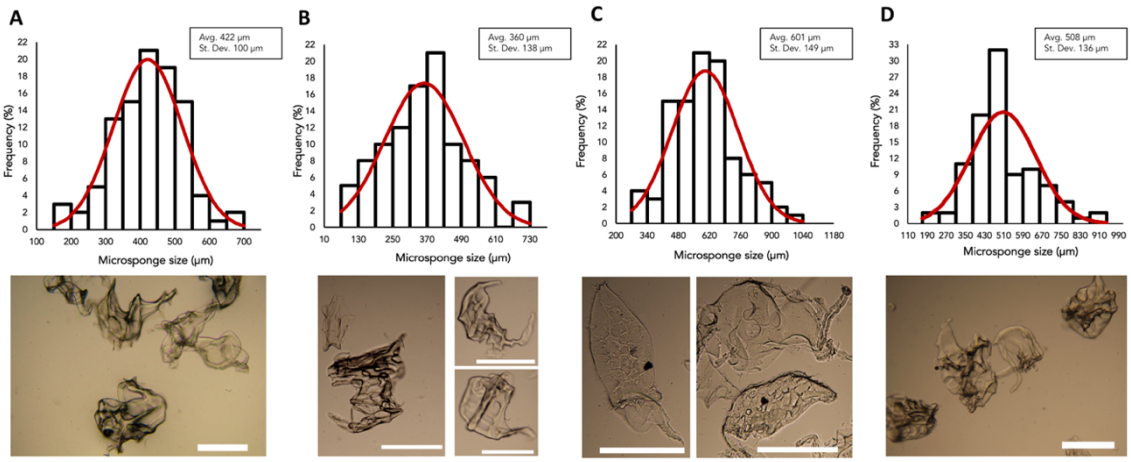

Fig. 4.7. Representative size distribution of PLMA microsponges (n=100) produced using respective alginate solution flow rates, PLMA solution flow rates and applied voltages of (A) 15 mL/h, 1 mL/h and 11 kV; (B) 15 mL/h, 1 mL/h and 14 kV; (C) 15 mL/h, 2 mL/h and 11 kV; (D) 30 mL/h, 2mL/h and 11 kV. A TTC distance of 5 cm was used in the production of all microsponges. For each set of conditions, the average size of the microsponges, respective standard deviation and images of the microsponges have been displayed. Scale bars represent 500 µm.

By increasing the flow rate of both solutions while maintaining a constant ratio, a slight increase in the dimensions of the microsponges is observed, resembling the results previously reported for the microcapsules. These results demonstrate that it is possible to tailor the average diameter of the microsponges by altering the conditions used to produce them. An alginate flow rate of 15 mL/h, a PLMA flow rate of 1 mL/h and an applied voltage of 11 kV were selected as the default parameters for further characterization. These microsponges present a diameter of 422 ± 100 µm, and an approximate average pore diameter of 30 µm, which was determined through the analysis of SEM images (Figure 4.8). The microsponges were then seeded with clinically relevant cell lines, in order to assess their capabilities as scaffolds in tissue engineering applications.

4.3.3. Cell growth and attachment on PLMA microsponges

4.3.3.1. Seeding cardiac cells on PLMA microsponges

Cardiomyocytes occupy a majority of cardiac tissue volume, accounting for 30% of an adult heart's cell population[42]. The H9c2 cell line, obtained from embryonic left ventricular rat heart tissue, has commonly been used as a model for cardiomyocyte behavior, as it presents similarities with primary cardiomyocytes[43,44]. As an immortalized cell line, H9c2 cells present high proliferative ability, in contrast with cardiomyocytes, which facilitates their use

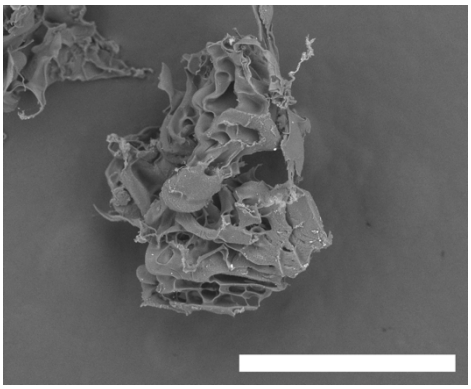

Fig. 4.8. Photograph of a microsponge obtained through scanning electron microscopy (SEM). Scale bar represents 500 μm.

in cell assays. As such, H9c2 (2-1) cells were seeded onto the PLMA microsponges. The proteins present hPL possess chemical moieties that favor cell adhesion[27]. As such, PLMA microsponges should be able to sustain cell attachment without any additional treatment. However, it was considered that the production process could impair the ability of cells to attach to the microsponges, mainly due to the use of alginate as a shell material. Unlike PLMA, alginate does not possess sites that allow cell recognition and because of this, residual alginate on the surface of the microsponges could compromise cell attachment[45].

As such, to evaluate whether cell adhesion is impacted by the production method, some microsponges were pre-coated with hPL before cell seeding, in order to produce a positive control. Cardiac myoblasts were seeded onto the microsponges at cell densities of 50, 100 and 150 cells/microsponge. Fluorescence microscopy images of the microsponges seeded with cells are shown in Figure 4.9. The cells were stained with Calcein AM and Propidium Iodide.

After 2 days of cell culture on the microsponges, it could be observed that attachment of the cardiac myoblasts was not improved by performing a pre-treatment with hPL. This indicates that the production method reported in this work does not hamper the ability of cells to recognize cell adhesion motifs on the surface of the microsponges. Throughout the experiments, it could be observed that microsponges in the wells were aggregated into larger constructs. By day 2, it could be observed that macroscopic PLMA aggregates were present in the culture wells and the resulting constructs were maintained throughout the duration of the experiments.

Cell viability appeared to be maintained for at least 7 days. However, by day 14 cell viability appeared to be greatly reduced if the initial cell seeding density was lower than 150

cells/microsponge. In order to examine the morphology of adhered cells, the microsponges were stained with DAPI/Phalloidin (Figure 4.9B).

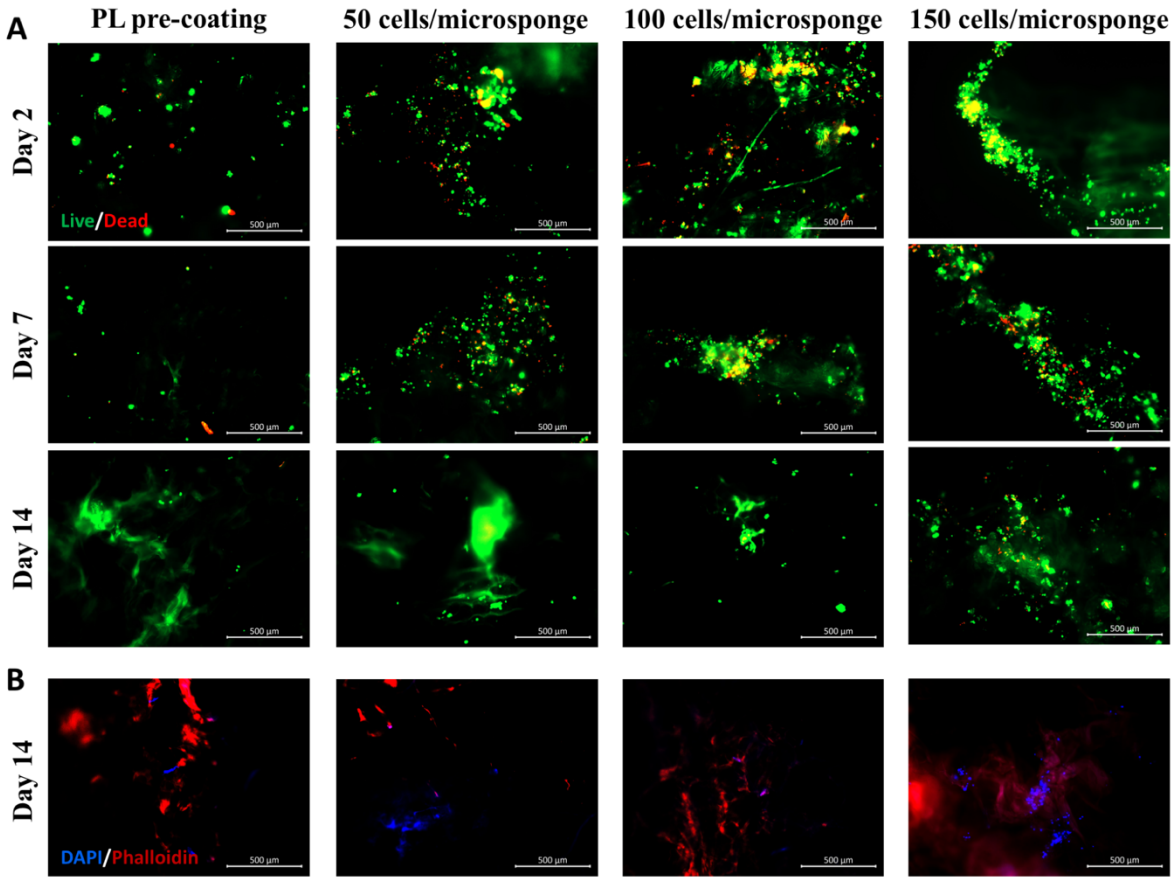

Fig. 4.9. Representative fluorescence images of H9c2 cells seeded on microsponges after A) live/dead staining at 2,7 and 14 days of culture. B) DAPI/phalloidin staining at 14 days of culture. Cardiac myoblasts were seeded at initial densities of 50, 100 and 150 cells/microsponge. H9c2 cells were also seeded at a density of 50 cells/microsponge on microsponges subjected to a pre-treatment with hPL.

Evaluation of the cell morphology at lower cell seeding densities could not produce conclusive results, due to the reduced number of observable cells and the intense background fluorescence that results from the autofluorescence of PLMA. When the initial cell seeding density is 150 cells/microsponge, cells appear to maintain a rounded morphology, even though they continue to adhere to the microsponges. The presence of H9c2 cells on the microsponges was then evaluated through SEM (Figure 4.10), which also confirmed that cells maintain a rounded morphology and preferably form clusters on the surface of the microsponges.

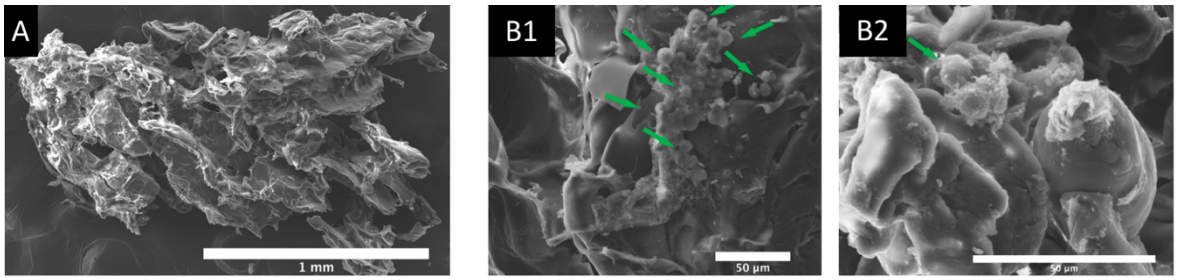

Fig. 4.10. SEM images of cell-laden PLMA constructs. (A) Full view of a PLMA construct after 7 days of cell culture. (B) Close-up view of PLMA constructs seeded with H9c2 cells at an initial density of 150 cells/microsponge after (B1) 2 days of cell culture; (B2) 14 days of cell culture. Scale bars represent 50 µm. Green arrows point toward small clusters of H9c2 cells.

While cardiomyocytes occupy a majority of cardiac volume, non-myocytes largely outnumber cardiomyocytes[42]. As such, an appropriate model for cardiac tissue should consider the inclusion of other cell types. Endothelial cells comprise the predominant non-myocyte cell line in the heart. Moreover, proper oxygenation of the assembled constructs will require the promotion of vascularization through angiogenesis, which will necessitate the migration and organization of endothelial cells. As such, in a preliminary assay, HUVECs were seeded onto microsponges in monoculture for 6 days, however, low cell attachment was observed (Figure 4.11).

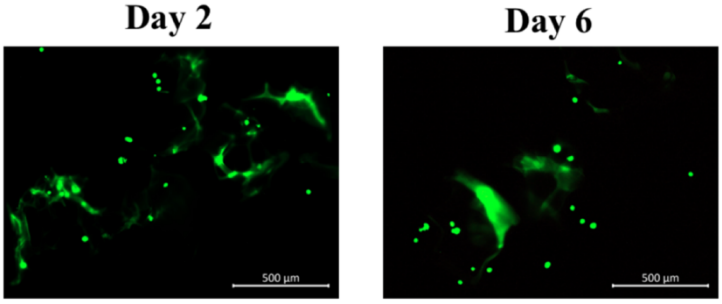

Fig. 4.11. Representative fluorescence microscopy images of microsponges seeded with HUVECs in monoculture (150 cells/microsponge).

Additionally, HUVECs failed to promote the aggregation of PLMA microsponges into constructs. In an attempt to improve cell adhesion through heterotypic cell-cell interactions, HUVECs were co-cultured with H9c2 cells at a 4:1 ratio of H9c2 cells to HUVECs (Figure 4.12). The cells were seeded at a total cell density of 150 cells/microsponge.

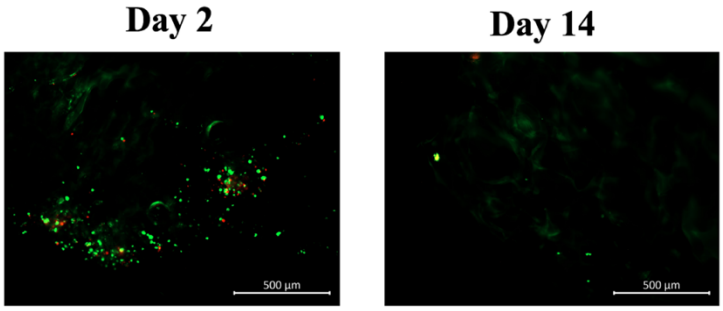

Fig. 4.12. Representative fluorescence images of a co-culture of H9c2 cells and HUVECs seeded onto PLMA microsponges at a 4:1 ratio after 2 and 14 days of culture.

Similar to H9c2 monoculture, the co-culture of H9c2 cells and HUVECs resulted in observable cell attachment by day 2, and constructs resulting from the aggregation of the microsponges were present in the culture wells, however, by day 14 the number of attached cells had greatly diminished. Similar results were obtained in preliminary assays in which HUVECs were seeded in greater number than H9c2 cells (Figure S4.1).

The results obtained in both monoculture and co-culture assays also appear to be confirmed by preliminary DNA quantification assays (Figure 4.13), which show that DNA concentration declines throughout the length of the experiments, except when H9c2 cells were seeded in monoculture at an initial cell density of 50 cells/microsponge, in which an increase in DNA concentration over time was observed. However, a single experiment was performed, and as such, further confirmation is required. Additionally, the DNA concentrations determined in these assays were low, and as such, cell proliferation assays should be repeated with a greater number of microsponges and cells in order to ensure the statistical validity of the results.

In some experiments with H9c2 cells, at early stages of cell culture (day 2-3), contractions appeared to be observed in the assembled constructs. Although it has been previously reported that H9c2 cells do not beat[44], it has also been stated that they are capable of experiencing contraction and relaxation[46], which could explain this observation. This could indicate that PLMA microsponges may become a suitable platform for the development of cardiac models to study the effect of drug candidates on the beating rate of cardiac tissue.

It was also observed that cells were not evenly distributed throughout the surface of the microsponges. Cells tended to aggregate closely on the edges of the constructs, resulting in areas with high cell density and other areas with little to no cells. As such, the formation of cell-cell contacts may be required to ensure long-term cell attachment to the constructs.

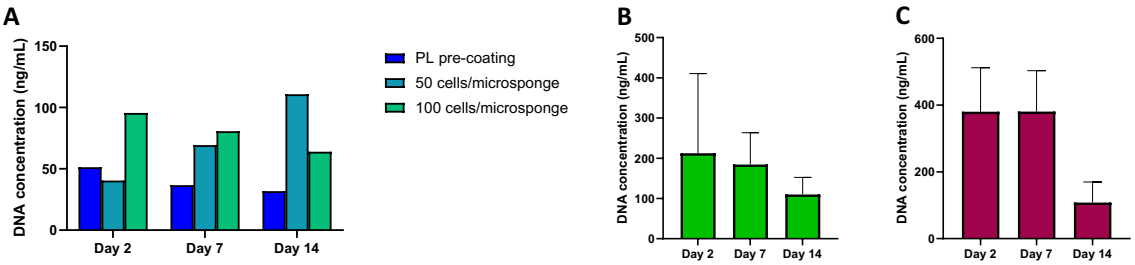

Fig. 4.13. Evaluation of cell proliferation by DNA quantification assays at 2, 7 and 14 days of culture. (A) H9c2 cell seeding on microsponges pre-coated with PL at a cell density of 50 cells/microsponge and on microsponges without any pre-treatment at cell densities of 50 and 100 cells/microsponge. A single experiment was performed. (B) H9c2 cell seeding on microsponges at a cell density of 150 cells/microsponge. Three independent experiments were performed. (C) Seeding a co-culture of H9c2 cells:HUVECs (4:1) onto microsponges. Three independent experiments were performed.

Indeed, direct cell-cell contact has been reported to be essential to maintain cell viability, orientation and function in muscle tissue, as well as ensure mechanical and electrical coupling between cells[47]. As such, the depletion of H9c2 cells after 14 days of culture may be caused due to an insufficient quantity of cells attached to the microsponges to ensure cell-cell interactions. As such, it may be relevant to compare the cell density employed in this work with the literature. For example, ESC-derived α-MHC^{+} cardiomyocytes have been previously seeded on CultiSpher-S, a commercially available protein-derived macroporous, by Akasha et al[48]. The cells were seeded at a density of 250 cells/microcarrier, much higher than the cell seeding densities we report here. Furthermore, the size of CultiSpher-S microcarriers ranges between 130 and 380 µm, which is below the average diameter of the PLMA microsponges used here (422 µm). This may indicate that the ratio of cell density/surface area is even greater than initially suggested.

Moreover, it could be observed that throughout all cell experiments, cells had also adhered to the surfaces of the wells, even though the coverslips were uncoated and should only allow weak cell adhesion. The attachment of cells to the microsponges could thus be impaired by the competing attachment of cells to the surface of the wells. If necessary, this problem could be minimized by using ultra-low adhesion well-plates, a common procedure in previously reported studies of cell-laden microcarriers[49–51]. A more homogeneous distribution of cells throughout the microsponges could also be ensured by placing the coverslips on a microplate

stirrer. As such, in order to provide meaningful conclusions, further studies should be conducted to optimize cell culture conditions. Additionally, in future co-culture experiments, procedures that allow the visual differentiation between HUVECs and H9c2 cells should be included, such as the use of lipophilic dyes or immunocytochemistry assays.

4.3.3.2. Seeding stem cells on PLMA microsponges

Mesenchymal stem cells are frequently employed in TERM approaches due to their beneficial properties. These self-renewing and highly proliferative cells can differentiate into a wide variety of different cell lines, including osteocytes, adipocytes, chondrocytes, myocytes, fibroblasts and potentially even neural cells and cardiomyocytes[52–55]. Furthermore, these cells have also been shown to produce and secrete a diverse cocktail of pro-regenerative chemical signals that aid in tissue recovery[56]. MSCs can be obtained from different sources, including bone marrow, umbilical cord blood and adipose tissue[57]. Human adipose-derived stem cells (ASCs) are an easily accessible resource that can be obtained by a simple liposuction procedure, which offers little to no risk to the patients[58]. As such, microsponges seeded with ASCs could eventually provide an opportunity toward personalized tissue engineering therapies. To evaluate cell attachment on the microsponges, ASCs were seeded onto the surface of the microsponges at different cell densities (Figure 4.14).

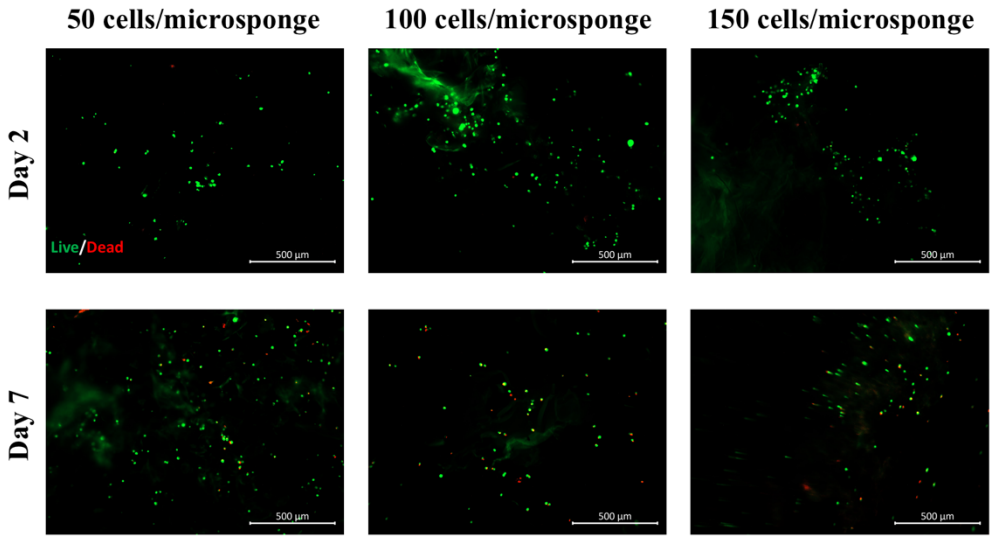

Fig. 4.14. Representative fluorescence images of hASCs seeded on microsponges after live/dead staining at 2 and 7 days of culture. hASCs were seeded at initial densities of 50, 100 and 150 cells/microsponge.

By day 2, cells had attached to the microsponges regardless of the initial cell density, and some of the microsponges had aggregated into constructs, similar to the results previously reported for H9c2 cells. By day 7, the cells remained attached to the microsponges, however, few cells were adhered to the PLMA-microsponge constructs. Instead, they preferably adhered to individual microsponges and smaller microsponge fragments. The presence of these fragments may indicate that the ASCs are degrading the microsponges, although this should be confirmed with additional studies. hPL contains a wide variety of proteins in its composition, and as such, the degradation of the microsponges could provide cells with nutrients and essential growth factors for cell proliferation. This could even allow the cells to grow in serum-free cell culture medium, which could be useful to achieve xeno-free cell culture systems. In future assays, ASCs could be seeded onto the surface of microsponges resuspended in serum-free media, in order to determine whether the components of PLMA are able to sustain cell proliferation even in the absence of additional supplementation. Additionally, protein quantification assays should be performed to evaluate the release profiles of the microsponges.

On the other hand, if a certain application of the microsponges requires their integrity to be maintained, it may be possible to delay the degradation by producing microsponges with denser polymer networks, which can be accomplished by employing higher concentrations of PLMA, or by producing PLMA with a greater number of methacryloyl moieties. The PLMA used in this work, previously described as PLMA100[27], possesses a low substitution degree of 14%. By increasing the ratio between methacrylic anhydride and hPL, PLMA with higher substitution rates will be obtained, permitting the preparation of sturdier hydrogels, with a greater number of crosslinks.

4.4. Conclusions

In this work, a procedure to encapsulate photopolymerizable human platelet lysate in alginate microcapsules through coaxial electrospray has been developed and optimized.

It has been demonstrated that the morphology and dimensions of the microcapsules and their cores can be tailored toward different applications by adjusting the composition of the alginate solution and production parameters. We succeeded in crosslinking the PLMA core of the microcapsules and were able to employ these microcapsules in the preparation of porous PLMA microsponges.

The resulting microsponges were able to sustain the attachment of ASCs and H9c2 cells without any further functionalization of their surface. Cell-laden microsponge constructs were observed in the coverslips, a promising prospect in the application of PLMA microsponges in bottom-up assembly of cardiac microtissues. Further studies may be required to determine optimal cell seeding density, and evaluate long-term cell proliferation and viability on the surface of the constructs.

4.5. References

1. Nichol JW, Khademhosseini A. Modular tissue engineering: engineering biological tissues from the bottom up. *Soft Matter*. 2009;5(7):1312. doi:10.1039/b814285h

2. Schon BS, Hooper GJ, Woodfield TBF. Modular Tissue Assembly Strategies for Biofabrication of Engineered Cartilage. *Ann Biomed Eng*. 2017;45(1):100-114. doi:10.1007/s10439-016-1609-3

3. Lee GH, Lee JS, Wang X, Hoon Lee S. Bottom-Up Engineering of Well-Defined 3D Microtissues Using Microplatforms and Biomedical Applications. *Adv Healthcare Mater*. 2016;5(1):56-74. doi:10.1002/adhm.201500107

4. Sakaguchi K, Shimizu T, Okano T. Construction of three-dimensional vascularized cardiac tissue with cell sheet engineering. *J Control Release*. 2015;205:83-88. doi:10.1016/j.jconrel.2014.12.016

5. Leferink AM, Tibbe MP, Bossink EGBM, et al. Shape-defined solid micro-objects from poly(d,l-lactic acid) as cell-supportive counterparts in bottom-up tissue engineering. *Mater Today Bio*. 2019;4:100025. doi:10.1016/j.mtbio.2019.100025

6. Kelm JM, Ehler E, Nielsen LK, Schlatter S, Perriard JC, Fussenegger M. Design of Artificial Myocardial Microtissues. *Tissue Eng*. 2004;10(1-2):201-214. doi:10.1089/107632704322791853

7. Elbert DL. Bottom-up tissue engineering. *Curr Opin Biotechnol*. 2011;22(5):674-680. doi:10.1016/j.copbio.2011.04.001

8. Wang C, Koo S, Park M, et al. Maladaptive Contractility of 3D Human Cardiac Microtissues to Mechanical Nonuniformity. *Adv Healthcare Mater*. 2020;9(8):1901373. doi:10.1002/adhm.201901373

9. Lee MO, Jung KB, Jo SJ, et al. Modelling cardiac fibrosis using three-dimensional cardiac microtissues derived from human embryonic stem cells. *J Biol Eng*. 2019;13(1):15. doi:10.1186/s13036-019-0139-6

10. Occhetta P, Isu G, Lemme M, et al. A three-dimensional *in vitro* dynamic micro-tissue model of cardiac scar formation. *Integr Biol*. 2018;10(3):174-183. doi:10.1039/C7IB00199A

11. Williams K, Liang T, Massé S, et al. A 3-D human model of complex cardiac arrhythmias. *Acta Biomater*. Published online March 2021:S1742706121001458. doi:10.1016/j.actbio.2021.03.004

12. Polonchuk L, Chabria M, Badi L, et al. Cardiac spheroids as promising in vitro models to study the human heart microenvironment. *Sci Rep*. 2017;7(1):7005. doi:10.1038/s41598-017-06385-8

13. Archer CR, Sargeant R, Basak J, Pilling J, Barnes JR, Pointon A. Characterization and Validation of a Human 3D Cardiac Microtissue for the Assessment of Changes in Cardiac Pathology. *Sci Rep*. 2018;8(1):10160. doi:10.1038/s41598-018-28393-y

14. Kofron CM, Kim TY, Munarin F, et al. A predictive in vitro risk assessment platform for pro-arrhythmic toxicity using human 3D cardiac microtissues. *Sci Rep*. 2021;11(1):10228. doi:10.1038/s41598-021-89478-9

15. Zhong X, Rescorla FJ. Cell surface adhesion molecules and adhesion-initiated signaling: Understanding of anoikis resistance mechanisms and therapeutic opportunities. *Cell Signal*. 2012;24(2):393-401. doi:10.1016/j.cellsig.2011.10.005

16. Jansen KA, Atherton P, Ballestrem C. Mechanotransduction at the cell-matrix interface. *Semin Cell Dev Biol*. 2017;71:75-83. doi:10.1016/j.semcdb.2017.07.027

17. Chen FM, Liu X. Advancing biomaterials of human origin for tissue engineering. *Prog Polym Sci*. 2016;53:86-168. doi:10.1016/j.progpolymsci.2015.02.004

18. Chen MS, Wang TJ, Lin HC, Burnouf T. Four types of human platelet lysate, including one virally inactivated by solvent-detergent, can be used to propagate Wharton jelly mesenchymal stromal cells. *N Biotechnol*. 2019;49:151-160. doi:10.1016/j.nbt.2018.11.003

19. Barro L, Burnouf PA, Chou ML, et al. Human platelet lysates for human cell propagation. *Platelets*. 2021;32(2):152-162. doi:10.1080/09537104.2020.1849602

20. Hemeda H, Giebel B, Wagner W. Evaluation of human platelet lysate versus fetal bovine serum for culture of mesenchymal stromal cells. *Cytotherapy*. 2014;16(2):170-180. doi:10.1016/j.jcyt.2013.11.004

21. Zamani M, Yaghoubi Y, Movassaghpour A, et al. Novel therapeutic approaches in utilizing platelet lysate in regenerative medicine: Are we ready for clinical use? *J Cell Physiol*. 2019;234(10):17172-17186. doi:10.1002/jcp.28496

22. Santos SCN da S, Sigurjonsson ÓE, Custódio C de A, Mano JFC da L. Blood Plasma Derivatives for Tissue Engineering and Regenerative Medicine Therapies. *Tissue Eng Part B Rev*. 2018;24(6):454-462. doi:10.1089/ten.teb.2018.0008

23. Saporito F, Baugh LM, Rossi S, et al. In Situ Gelling Scaffolds Loaded with Platelet Growth Factors to Improve Cardiomyocyte Survival after Ischemia. *ACS Biomater Sci Eng*. 2019;5(1):329-338. doi:10.1021/acsbiomaterials.8b01064

24. Saporito F, Sandri G, Bonferoni MC, et al. Electrospun Gelatin–Chondroitin Sulfate Scaffolds Loaded with Platelet Lysate Promote Immature Cardiomyocyte Proliferation. *Polymers*. 2018;10(2):208. doi:10.3390/polym10020208

25. Fortunato TM, Beltrami C, Emanueli C, De Bank PA, Pula G. Platelet lysate gel and endothelial progenitors stimulate microvascular network formation in vitro: tissue engineering implications. *Sci Rep*. 2016;6(1):25326. doi:10.1038/srep25326

26. Cheng K, Malliaras K, Shen D, et al. Intramyocardial Injection of Platelet Gel Promotes Endogenous Repair and Augments Cardiac Function in Rats With Myocardial Infarction. *J Am Coll Cardiol*. 2012;59(3):256-264. doi:10.1016/j.jacc.2011.10.858

27. Santos SC, Custódio CA, Mano JF. Photopolymerizable Platelet Lysate Hydrogels for Customizable 3D Cell Culture Platforms. *Adv Healthcare Mater*. 2018;7(23):1800849. doi:10.1002/adhm.201800849

28. Monteiro CF, Santos SC, Custódio CA, Mano JF. Human Platelet Lysates-Based Hydrogels: A Novel Personalized 3D Platform for Spheroid Invasion Assessment. *Adv Sci*. 2020;7(7):1902398. doi:10.1002/advs.201902398

29. Monteiro CF, Custódio CA, Mano JF. Bioengineering a humanized 3D tri-culture osteosarcoma model to assess tumor invasiveness and therapy response. *Acta Biomater*. Published online July 2021:S1742706121004724. doi:10.1016/j.actbio.2021.07.034

30. Abecasis B, Canhão PGM, Almeida HV, et al. Toward a Microencapsulated 3D hiPSC-Derived in vitro Cardiac Microtissue for Recapitulation of Human Heart Microenvironment Features. *Front Bioeng Biotechnol*. 2020;8:580744. doi:10.3389/fbioe.2020.580744

31. Silva AS, Santos LF, Mendes MC, Mano JF. Multi-layer pre-vascularized magnetic cell sheets for bone regeneration. *Biomaterials*. 2020;231:119664. doi:10.1016/j.biomaterials.2019.119664

32. Zuk PA, Zhu M, Ashjian P, et al. Human Adipose Tissue Is a Source of Multipotent Stem Cells. Raff M, ed. *Mol Biol Cell*. 2002;13(12):4279-4295. doi:10.1091/mbc.e02-02-0105

33. Koh B, Sulaiman N, Fauzi MB, et al. Three dimensional microcarrier system in mesenchymal stem cell culture: a systematic review. *Cell Biosci*. 2020;10(1):75. doi:10.1186/s13578-020-00438-8

34. Park J, Choe G, Oh S, Lee JY. *In Situ* Formation of Proangiogenic Mesenchymal Stem Cell Spheroids in Hyaluronic Acid/Alginate Core–Shell Microcapsules. *ACS Biomater Sci Eng*. 2020;6(12):6938-6948. doi:10.1021/acsbiomaterials.0c01489

35. Gryshkov O, Mutsenko V, Tarusin D, et al. Coaxial Alginate Hydrogels: From Self-Assembled 3D Cellular Constructs to Long-Term Storage. *Int J Mol Sci*. 2021;22(6):3096. doi:10.3390/ijms22063096

36. Bremond N, Santanach-Carreras E, Chu LY, Bibette J. Formation of liquid-core capsules having a thin hydrogel membrane: liquid pearls. *Soft Matter*. 2010;6(11):2484. doi:10.1039/b923783f

37. Safley SA, Kenyon NS, Berman DM, et al. Microencapsulated adult porcine islets transplanted intraperitoneally in streptozotocin-diabetic non-human primates. *Xenotransplantation*. 2018;25(6):e12450. doi:10.1111/xen.12450

38. de Vos P, Faas MM, Strand B, Calafiore R. Alginate-based microcapsules for immunoisolation of pancreatic islets. *Biomaterials*. 2006;27(32):5603-5617. doi:10.1016/j.biomaterials.2006.07.010

39. Doméjean H, de la Motte Saint Pierre M, Funfak A, et al. Controlled production of sub-millimeter liquid core hydrogel capsules for parallelized 3D cell culture. *Lab Chip*. 2017;17(1):110-119. doi:10.1039/C6LC00848H

40. Zhou Z, Wu W, Fang J, Yin J. Polymer-based porous microcarriers as cell delivery systems for applications in bone and cartilage tissue engineering. *Int Mater Rev*. 2021;66(2):77-113. doi:10.1080/09506608.2020.1724705

41. Correia CR, Bjørge IM, Nadine S, Mano JF. Minimalist Tissue Engineering Approaches Using Low Material-Based Bioengineered Systems. *Adv Healthcare Mater*. 2021;10(9):2002110. doi:10.1002/adhm.202002110

42. Pinto AR, Ilinykh A, Ivey MJ, et al. Revisiting Cardiac Cellular Composition. *Circ Res*. 2016;118(3):400-409. doi:10.1161/CIRCRESAHA.115.307778

43. Kuznetsov AV, Javadov S, Sickinger S, Frotschnig S, Grimm M. H9c2 and HL-1 cells demonstrate distinct features of energy metabolism, mitochondrial function and sensitivity to hypoxia-reoxygenation. *Biochim Biophys Acta Mol Cell Res*. 2015;1853(2):276-284. doi:10.1016/j.bbamcr.2014.11.015

44. Watkins SJ, Borthwick GM, Arthur HM. The H9C2 cell line and primary neonatal cardiomyocyte cells show similar hypertrophic responses in vitro. *In Vitro CellDevBiol-Animal*. 2011;47(2):125-131. doi:10.1007/s11626-010-9368-1

45. Neves MI, Moroni L, Barrias CC. Modulating Alginate Hydrogels for Improved Biological Performance as Cellular 3D Microenvironments. *Front Bioeng Biotechnol*. 2020;8:665. doi:10.3389/fbioe.2020.00665

46. Zhou T, Zhou Z, Zhou S, Huang F. Real-time monitoring of contractile properties of H9C2 cardiomyoblasts by using a quartz crystal microbalance. *Anal Methods*. 2016;8(3):488-495. doi:10.1039/C5AY02835C

47. McCain ML, Lee H, Aratyn-Schaus Y, Kleber AG, Parker KK. Cooperative coupling of cell-matrix and cell-cell adhesions in cardiac muscle. *Proc Natl Acad Sci USA*. 2012;109(25):9881-9886. doi:10.1073/pnas.1203007109

48. Akasha AA, Sotiriadou I, Doss MX, et al. Entrapment of Embryonic Stem Cells-Derived Cardiomyocytes in Macroporous Biodegradable Microspheres: Preparation and Characterization. *Cell Physiol Biochem*. 2008;22(5-6):665-672. doi:10.1159/000185550

49. Ting S, Lam A, Tong G, et al. Meticulous optimization of cardiomyocyte yields in a 3-stage continuous integrated agitation bioprocess. *Stem Cell Res*. 2018;31:161-173. doi:10.1016/j.scr.2018.07.020

50. Chen AKL, Chen X, Choo ABH, Reuveny S, Oh SKW. Critical microcarrier properties affecting the expansion of undifferentiated human embryonic stem cells. *Stem Cell Res*. 2011;7(2):97-111. doi:10.1016/j.scr.2011.04.007

51. Lam ATL, Li J, Chen AKL, Birch WR, Reuveny S, Oh SKW. Improved Human Pluripotent Stem Cell Attachment and Spreading on Xeno-Free Laminin-521-Coated Microcarriers Results in Efficient Growth in Agitated Cultures. *BioRes Open Access*. 2015;4(1):242-257. doi:10.1089/biores.2015.0010

52. Steward AJ, Kelly DJ. Mechanical regulation of mesenchymal stem cell differentiation. *J Anat*. 2015;227(6):717-731. doi:10.1111/joa.12243

53. Tondreau T, Lagneaux L, Dejeneffe M, et al. Bone marrow–derived mesenchymal stem cells already express specific neural proteins before any differentiation. *Differentiation*. 2004;72(7):319-326. doi:10.1111/j.1432-0436.2004.07207003.x

54. Guo X, Bai Y, Zhang L, et al. Cardiomyocyte differentiation of mesenchymal stem cells from bone marrow: new regulators and its implications. *Stem Cell Res Ther*. 2018;9(1):44. doi:10.1186/s13287-018-0773-9

55. Floren M, Bonani W, Dharmarajan A, Motta A, Migliaresi C, Tan W. Human mesenchymal stem cells cultured on silk hydrogels with variable stiffness and growth factor differentiate into mature smooth muscle cell phenotype. *Acta Biomaterialia*. 2016;31:156-166. doi:10.1016/j.actbio.2015.11.051

56. Teixeira FG, Carvalho MM, Sousa N, Salgado AJ. Mesenchymal stem cells secretome: a new paradigm for central nervous system regeneration? *Cell Mol Life Sci*. 2013;70(20):3871-3882. doi:10.1007/s00018-013-1290-8

57. Kern S, Eichler H, Stoeve J, Klüter H, Bieback K. Comparative Analysis of Mesenchymal Stem Cells from Bone Marrow, Umbilical Cord Blood, or Adipose Tissue. *Stem Cells*. 2006;24(5):1294-1301. doi:10.1634/stemcells.2005-0342

58. Locke M, Feisst V, Dunbar PR. Concise Review: Human Adipose-Derived Stem Cells: Separating Promise from Clinical Need. *Stem Cells*. 2011;29(3):404-411. doi:10.1002/stem.593

Supplementary Information

Preparation of porous microsponges for the assembly of humanized cardiac microtissues by coaxial electrospray

Table S4.1. Influence of applied voltage on the dimensions of the resulting core-shell microcapsules. Results have been shown as mean ± standard deviation.

Applied Voltage (kV)	Overall diameter (µm)	Overall aspect ratio	Core diameter (µm)	Core aspect ratio	Shell thickness (µm)
10	989 ± 147	1.04 ± 0.03	517 ± 87	1.39 ± 0.40	236 ± 61
11	819 ± 76	1.09 ± 0.05	402 ± 93	1.42 ± 0.28	209 ± 43
12	894 ± 83	1.09 ± 0.07	447 ± 86	2.14 ± 0.89	223 ± 50
13	771 ± 72	1.08 ± 0.10	407 ± 78	1.73 ± 0.52	182 ± 27
14	638 ± 79	1.04 ± 0.02	351 ± 64	1.73 ± 0.34	144 ± 30
15	613 ± 153	1.12 ± 0.13	330 ± 119	2.41 ± 0.94	141 ± 58

Table S4.2. Influence of tip-to-collector distance on the dimensions of the resulting core-shell microcapsules. Results have been shown as mean ± standard deviation.

TTC distance (cm)	Overall diameter (µm)	Overall aspect ratio	Core diameter (µm)	Core aspect ratio	Shell thickness (µm)
5	819 ± 76	1.06 ± 0.06	402 ± 93	1.42 ± 0.28	209 ± 43
6	828 ± 106	1.05 ± 0.05	463 ± 98	1.54 ± 0.54	182 ± 43
7	838 ± 108	1.04 ± 0.03	478 ± 76	1.44 ± 0.33	180 ± 46

Table S4.3. Influence of the ratio between the flow rates of alginate and PLMA on the dimensions of the resulting core-shell microcapsules. Results have been shown as mean ± standard deviation.

Alginate flow rate (mL/h):PLMA flow rate (mL/h)	Overall diameter (µm)	Overall aspect ratio	Core diameter (µm)	Core aspect ratio	Shell thickness (µm)
6:1	907 ± 121	1.05 ± 0.04	544 ± 88	1.83 ± 0.72	181 ± 41
10:1	860 ± 90	1.09 ± 0.11	462± 60	1.57 ± 0.44	199 ± 44
12:1	1043 ± 115	1.04 ± 0.03	518 ± 50	1.38 ± 0.40	263 ± 49
15:1	819 ± 76	1.06 ± 0.06	402 ± 93	1.42 ± 0.28	209 ± 43
20:1	943 ± 102	1.05 ± 0.04	419 ± 75	1.54 ± 0.41	262 ± 43
30:1	946 ± 110	1.06 ± 0.03	414 ± 105	1.58 ± 0.55	266 ± 59
7.5:0.5	790 ± 89	1.06 ± 0.05	384 ± 71	1.65 ± 0.47	203 ± 41
30:2	1058 ± 120	1.05 ± 0.06	613 ± 123	1.25 ± 0.17	222 ± 58

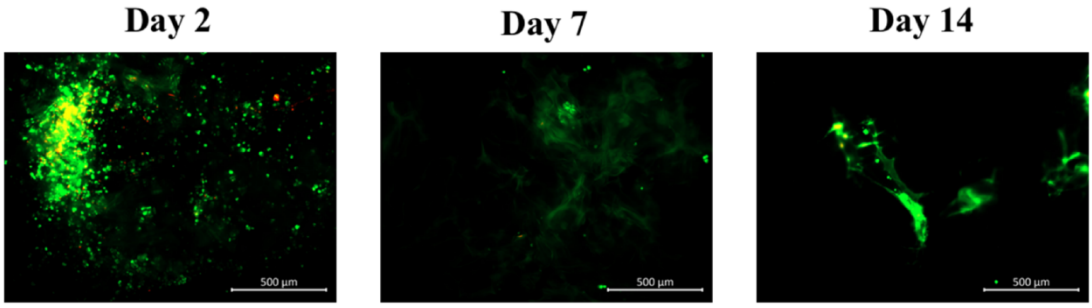

Fig. S4.1. Representative fluorescence microscopy images of a co-culture assay. Microsponges were seeded with H9c2 cells (50 cells/microsponge) and HUVECs (150 cells/microsponge).

CHAPTER 5

General conclusions

Chapter 5 – General Conclusions and Prospects

5.1. Conclusions

Faced with the high incidence, prevalence and mortality of myocardial infarction, the need for new therapeutic options becomes evident. Tissue engineering approaches have increasingly been used to restore cardiac function through the combination of cells, biomaterials and bioactive molecules to produce a diverse array of novel platforms.

Core-shell microcapsules are a particularly versatile and highly-tunable platform that can be used to encapsulate cells and bioactive molecules to promote tissue regeneration. In myocardial tissue engineering, these platforms could potentially be used in large scale cell production and differentiation, in the delivery of cells, drugs and pro-angiogenic growth factors, in the development of cardiac models of disease and in the modulation of the inflammatory processes that occur after MI.

In this work, coaxial electrospray was used to produce porous microcarriers derived from human platelet lysate, aiming for the development of a humanized scaffold for the bottom-up assembly of cardiac microtissues. This procedure was thoroughly studied in order to produce microcapsules with defined characteristics, and it was optimized to produce microcarriers with specific properties. Here, core-shell microcapsules were not used as a finalized structure. Instead, PLMA was encapsulated within microcapsules, producing an intermediary structure that was used in the preparation of PLMA microsponges. It was demonstrated that these scaffolds could support the adhesion of cells, assemble into larger three dimensional structures and could even potentially promote the contraction and relaxation of seeded myocytes.

5.2. Future work

The potential applications of the microsponges we have developed have only begun to be explored. Cell proliferation studies should be repeated and possibly complemented with studies of cell viability, such as 3-(4,5-dimethylthiazol-2-yl)-5-(3-carboxymethoxyphenyl)-2-(4-sulfophenyl)-2H-tetrazolium (MTS) assays, to examine the metabolic ability of cells. Additionally, higher cell seeding densities could also be studied, in order to evaluate the effect on long-term cell attachment and optimize cell culture conditions. Alternate production conditions, including coaxial electrospray parameters and freezing rates, could be used in order to alter the dimensions, morphology and porosity of the microsponges to

produce structures more favorable to cell attachment. The use of cells of human origin, such as cardiomyocytes derived from iPSCs, could also be attempted in order to produce a fully humanized platform for tissue engineering. Furthermore, the use of beating cardiomyocytes could be used to confirm and evaluate the possibility of using PLMA in the development of models of cardiac beating.

The assembly of cell-laden shape-defined constructs for cardiac tissue engineering, the development of injectable approaches toward tissue recovery *in vivo* and the incorporation of microsponges within bioreactors as microcarriers for suspension cell culture are all possibilities for further exploration of the PLMA microsponges developed in this work.

Additionally, it would also be possible to conceive of alternative applications for the PLMA core microcapsules, such as the encapsulation of cells or spheroids within the core of the microcapsules. Due to the photopolymerizable character of PLMA, it may be possible to modulate the stiffness and viscoelastic properties of the core microenvironment by adjusting exposure time and radiation intensity during UV irradiation, producing heart-in-a-capsule models of disease to test the influence of mechanical cues on cell behavior.